SEASONAL SPATIAL ANALYSIS IN DETERMINATION OF FLASH FLOOD AND DROUGHT HAZARD AREAS USING AHP AND GIS: A CASE STUDY OF KAMPONG SPEU PROVINCE IN CAMBODIA

CHHUONVUOCH KOEM

A Thesis Submitted to the Graduate School of Naresuan University
in Partial Fulfillment of the Requirements
for the Master of Science in (Disaster Management - (Plan A Type A2) International Program)
2020

SEASONAL SPATIAL ANALYSIS IN DETERMINATION OF FLASH FLOOD AND DROUGHT HAZARD AREAS USING AHP AND GIS: A CASE STUDY OF KAMPONG SPEU PROVINCE IN CAMBODIA

CHHUONVUOCH KOEM

A Thesis Submitted to the Graduate School of Naresuan University
in Partial Fulfillment of the Requirements
for the Master of Science in (Disaster Management - (Plan A Type A2) International Program)
2020

Thesis entitled "Seasonal Spatial Analysis in Determination of Flash Flood and Drought Hazard Areas Using AHP and GIS:
A Case Study of Kampong Speu Province in Cambodia"

By CHHUONVUOCH KOEM

has been approved by the Graduate School as partial fulfillment of the requirements for the Master of Science in Disaster Management - (Plan A Type A2) International Program of Naresuan University

Oral Defense Committee

.... Chair
(Bhichit Rattakul, Ph.D.)

.... Advisor
(Associate Professor Sarintip Tantanee, Ph.D.)

.... Co Advisor
(Assistant Professor Korakod Nusit, Ph.D.)

.... Internal Examiner
(Charatdao Kongmuang, Ph.D.)

Approved

....
(Professor Paisarn Muneesawang, Ph.D.)

Dean of the Graduate School

Title SEASONAL SPATIAL ANALYSIS IN DETERMINATION OF FLASH FLOOD AND DROUGHT HAZARD AREAS USING AHP AND GIS: A CASE STUDY OF KAMPONG SPEU PROVINCE IN CAMBODIA

Author CHHUONVUOCH KOEM

Advisor Associate Professor Sarintip Tantanee, Ph.D.

Co-Advisor Assistant Professor Korakod Nusit, Ph.D.

Academic Paper Thesis M.S. in Disaster Management - (Plan A Type A2) International Program, Naresuan University, 2020

Keywords Analytical Hierarchy Process, Geographic Information System, Flash Flood, Drought, Bi-hazard, Kampong Speu Province

ABSTRACT

Climate change increases the incidence and magnitude of extreme events, especially, hydro-meteorological events including floods and droughts. Cambodia faces serious floods and droughts almost every year. Hazard mapping is significant for mitigation and prevention approaches. The integration of the Analytical Hierarchy Process (AHP) with Geographic Information System (GIS) and Remote Sensing data expressed the appreciated inquiry method in the current study. The purpose of this study is to map the seasonal spatial distribution of flash flood and drought hazard with the support of the AHP method and GIS techniques of Kampong Speu Province in Cambodia. The hazard maps are separated into two seasons, rainy season and dry season. Ten parameters are used to assess flash flood hazards including rainfall, elevation, slope, soil types, geology, flow direction, stream order, landuse, distance from drainage, and drainage density. Besides, eight parameters such as rainfall, relative humidity, average temperature, maximum temperature, slope, soil types, landuse, and drainage density are used to identify the drought hazard. With the help of AHP and GIS, the flash flood and drought hazards were further used to develop a bi-hazard map over Kampong Speu Province. The results reveal that Aoral, Thpong, Phnum Srouch,

and Samraong Tong Districts are located in very high hazard to the rainy seasonal flash flood with 9.29%, 0.61%, 0.28%, and 0.01% of the total areas, respectively. For the dry seasonal flash flood, the above-mentioned districts are located in very high hazard spatial distribution with 12.68%, 1.48%, 1.10%, and 0.04% of the total areas, respectively. Furthermore, Basedth, Kong Pisei, Odongk, and Samraong Tong Districts are located in very high hazard to rainy seasonal drought with 4.30%, 4.28%, 4.08%, and 2.62% of the total areas, individually. About 4.26%, 4.21%, 2.72%, 1.76%, and 0.7% of the total areas located in Odongk, Kong Pisei, Samraong Tong, Basedth, and Thpong Districts respectively are found in the very high hazard to dry seasonal drought. Bi-hazard areas are identified as very low (12% of the total areas), low (31% of the total areas), moderate (24% of the total areas), high (30% of the total areas), and very high (3% of the total areas). All districts are identified as located in the very high bi-hazard. Thpong District has the largest areas prone to very high bi-hazard with 64.59 km^2 (0.93% of the total areas). The obtained maps create the various dataset and serve as information for comprehensive hazard assessment. It is also reflected as essential information for planners and decision-makers for the future operational flash flood and drought mitigation measures, planning, management, and sustainable development.

ACKNOWLEDGEMENTS

I would never have been able to finish my dissertation without the guidance of all my committee members, help from all lecturers and friends, and support from the scholarship and my family.

First, I would like to show my genuine gratitude to Her Royal Princess Maha Chakri Sarinhorn for providing a full scholarship, which is a priceless opportunity to chase my higher education in Master of Science in Disaster Management at Naresuan University, Thailand.

Foremost, I would like to express my sincere gratitude to my advisor Assoc. Prof. Dr. Sarintip Tantanee and co-advisor Assist. Prof. Dr. Korakod Nusit for the continuous support of my master's study and research, for their patience, motivation, enthusiasm, and immense knowledge. Their guidance helped me in all the time of research and writing of this thesis. I could not have imagined having a better advisor and mentor for my study.

Besides my advisor and co-advisor, I would like to thank the rest of my thesis committee, Dr. Charatdao Kongmuang and Dr. Bhichit Rattakul for their encouragement, insightful comments, and hard questions.

I do not forget to thank all the lecturers both inside the Engineering Faculty and outside, especially those who gave me precious lectures on the subject. Without them, I would not have done my dissertation precisely. I will never forget their motivation and guidance.

I am very thankful to all the faculty staff who always help me with the information, documents, and guidance.

Finally, yet importantly, I would like to thank all of my family and my friends for providing me both emotional and endless financial support, encouragement, and stay by my side throughout these years. My achievement would not be possible without them.

Thank you so much.

CHHUONVUOCH KOEM

TABLE OF CONTENTS

Page

LIST OF TABLES

Page

LIST OF FIGURES

Page

CHAPTER I

INTRODUCTION

Background

Climate change combined with unplanned rapid urbanization, landuse changes, groundwater recharge declination, poor watershed management, and other human development activities increases the frequency and magnitude of extreme events, particularly hydro-meteorological events including floods and droughts (Jha et al., 2012; Nasiri et al., 2016; Tehrany et al., 2015). Floods and droughts cause direct and indirect effects (Li et al., 2013) on lives, environment, ecosystem, transportation, infrastructure, agriculture, cultural heritage, economic, etc. (Yu et al., 2012). Poor people living in floodplain and drought hazard areas, especially in developing countries like Cambodia, are likely vulnerable to floods and droughts due to a lack of mitigation, preparedness, response, coping capacity, and recovery after flood and drought events (IPCC, 2014). Cambodia is a susceptible country to the impacts of climate change. It was listed in the rank of 19 (High Risk) to climate risk index and rank 54 (Medium Risk) to inform risk index, the risk of humanitarian crises and disasters. Most hazard in Cambodia is associated with floods and droughts (UNDRR, 2019). Cambodia faces serious floods and droughts almost every year and caused many damages. It always has seasonal flooding across the low-lying parts, and it mostly occurs between July and October, both flash floods and river floods. While rainfall is important for domestic use, biodiversity, and irrigation, the impacts of uncontrolled flooding disrupt people. Cambodia was hit by the biggest floods in 2000, 2011, and 2013 (NCDM, 2019). Besides floods, droughts are also one of the serious problems. The frequency of drought varies from one province to one province. The most affected provinces by droughts are Kampong Speu, Takeo, and Battambang (CFE-DM, 2017). Based on the National Committee for Disaster Management (NCDM) (2013), floods and drought occurred 3,564 times and 1,343 times in 20 years, respectively (1993-2013). The numbers of the victim of floods were 12,266,757 and droughts were 2,766,217 (NCDM, 2019). Moreover, the frequency of the disaster belongs to flood 72%, drought 16%, and storm

12%. The economic issue is caused by floods at 91% and droughts at 9% (CFE-DM, 2017). It is impossible to prevent and avoid floods and droughts from happening, but it is reasonable to reduce or minimize the effects and losses.

Statement of the Problems

To minimize the impacts, suitable preparation and mitigation measures are needed. The dependable information on the national disaster's spatial distribution comprised a key tool that is required when the stakeholders are trying to reduce the disaster's impacts (Skilodimou et al., 2019). According to People In Need (PIN), the hazard maps in Cambodia are not coherent or standardized and often directed on an ad-hoc based because of the limitation of available data while the information for hazard mapping is existing. The efforts should be directed toward developing standardized and coherent (UNDRR, 2019). Hazard mapping to identify the zones at the risk of floods and droughts is a significant approach for mitigation and prevention (Radwan et al., 2018). Mapping hazard areas will be beneficial to the community or national managers, risk planners, and disaster and emergency responders for implementing effective plans or activities before, during, and after disasters (Elkhrachy, 2015). Since the hazard map is very essential for mitigation and prevention, several studies conducted mapping on the hazard areas, especially along the Mekong River. Hazarika and Bormudoi (2007) focused on the mapping of flood hazards in provinces located along the Mekong River. Ly et al. (2018) mapped the flooding along the lower Mekong Rivers. Try et al. (2019) determined the flood spatial distribution in the Mekong River basin. Additionally, several studies including Danumah et al. (2016), Elkhrachy (2015), Mohamed (2019), Palchaudhuri and Biswas (2016), Radwan et al. (2018), Saowanee (2018), and Stefanidis and Stathis (2013) focused on the single hazard assessment over the multi-hazard assessment duce to the complexity of natural hazard. It will result in mislead management priorities. Focusing on only one hazard might result in increasing the vulnerability to other ignored hazards since one spatial distribution usually is not disturbed by only single hazard, bi-hazard or multi-hazard can occur at the same time or follow continuously (Budimir et al., 2014; Gill & Malamud, 2016; MS Kappes et al., 2010). When bi-hazard or multi-hazard is taken into account, the application of one map for one disaster might become uncontrollable (Skilodimou et al., 2019). The way to solve this problem is to adopt the multi-hazard assessment with the help of GIS techniques, which supports the different types of data analysis (El Morjani Zel et al., 2007; Melanie Kappes et al., 2011; Schmidt et al., 2011). The word bi-hazard refers to two different hazards that happen in one area. Bi-hazard or multi-hazard might seem to be specific, and it does not need a definition. It is however regularly applied in diverse frameworks within the varied types of hazard and community-based disaster risk reduction (Gill & Malamud, 2016). Moreover, it is adopted to define the multi-hazard independent analysis such as floods, droughts, landslides, and earthquakes (Perry, & Lindell, 2008). It is also applied to identify spatial overlap by overlaying hazard layers (Shi et al., 2015). The bi-hazard approach is broadly advocated in the intergovernmental and government. It is however rarely defined. Likewise, analysis of the spatiotemporal variation of flood seasonality has provided important understandings of the principal flood generation mechanisms and their controlled factors (Ye et al., 2017). A central problem of flash flood prediction and the application of inclusive safety procedures was the absence of comprehensive information concerning seasonal variations (Bush, & Cerveny, 2013). Studying the changeability in seasonal flash floods and droughts is crucial not only for a better understanding of hazard timing but also for its temporal change. Thomas Saaty developed the Analytical Hierarchy Process (AHP) in the 1970s. The AHP method was applied to map hazard areas in different places. The AHP method is a dimension pairwise comparison theory, and it depends on the judgment of the experts and relative literature to obtain the priority scales. The AHP method is more effective when combined with GIS. Many studies used AHP and GIS to map flood and drought hazard areas including Danumah et al. (2016), Elkhrachy (2015), Ouma and Tateishi (2014), Siddayao et al. (2014), Mohamed (2019), and Ogato et al. (2020).

Purposes of the Study

The purpose of the study is to assess the seasonal spatial distribution of flash flood and drought hazard areas with the help of the Analytical Hierarchy Process (AHP) and Geographic Information System (GIS) in Kampong Speu Province, Cambodia. Within the main objective, there are three specific objectives as following:

1. To assess and map the spatial distribution of seasonal flash flood hazard areas

2. To assess and map the spatial distribution of seasonal drought hazard areas
3. To generate the bi-hazard map of flash floods and droughts.

Expected outcome

This study has the expected outcome as follows:

1. Get the seasonal maps of flash flood and drought hazard
2. Illustrate the level of flash flood and drought hazard in each district
3. Get the bi-hazard map considering flash flood and drought
4. Produce a database for further research.

Significant of Study

Kampong Speu Province faces the problems of flash floods and droughts almost every year. Floods hit in 2000, 2001, 2002, 2003, 2005, 2006, 2010, 2016, and 2018, which affected 140,644 people, 93,505 people, 60,355 people, 64,102 people, 65,924 people, 45,009 people, 288 people, 2,216 households, and 230 households, respectively (NCDM, 2019; Walters, & Hun, 2018; WorldVision, 2016). In 2002, 2004, 2005, 2006, and 2012, droughts affected 149,175 people, 308,225 people, 681,039 people, 100,592 people, and 1,925 people, respectively (NCDM, 2019). In 2009, 2010, 2011, 2012, and 2013, floods and droughts also caused numerous impacts on agriculture (MAFF, 2013).

AHP method has been proposed to apply for flood hazard mapping in Cambodia (J. Liu et al., 2019). However, there is no such application on research for flash flood hazards in any area. Likewise, a detailed hazard mapping is hardly found in the literature to the limitation of the criteria used (Danumah et al., 2016; Kazakis et al., 2015). This study is very crucial since it supports priority three of the Sendai Framework (2015-2030), “Investing in disaster risk reduction of the resilience.” It suggests all countries support disaster risk judgment, planning, and mapping through rural areas. It also mentions the need for multi-hazard Disaster Risk Reduction (DRR) practice for efficient and effective preventive approaches. Additionally, understanding the disaster risk is a priority in the Sendai Framework, this knowledge can influence the purpose of prevention and mitigation. It impacts on improvement and application of suitable and effective preparedness and responses to disasters (UNISDR, 2015).

Furthermore, the exiting flash flood and drought hazard assessment are still at a very early stage; therefore, hazard assessments need a more precise and formal approach. Consideration of the hazards at the community level is also very essential since it can promote development activities. This study also focuses on the comprehensive information concerning seasonal variation, which is very crucial for understanding the hazard timing and its temporal changes. The study also illustrates the bi-hazard areas over Kampong Speu Province. The main purpose of bi-hazard assessment is to gather in one map of different hazard-related information to covey a composite picture of the natural hazards of impacted spatial distribution. A Bi-hazard map also can enhance the multi-hazard early warning system, preparedness, response, recovery, rehabilitation, and reconstruction (UNISDR, 2015). The information and data can help decision-makers at both local and national level implements rescue campaigns and plan for mitigation, preparedness, and response on time. It is useful in planning better or appropriated flood and drought risk-reduction strategies. Overall, this study can contribute to lessening the contrary floods and drought impacts, save lives, reduce property and economic losses, and inform relevant stakeholders about flash flood and drought hazards areas. Lastly, this study can be used in preparedness, emergency response, and promote sustainable flash flood and drought hazard assessments.

Scope of the Study

The scopes of the study are presented as follows:

1. Area: the chosen study area is Kampong Speu Province in Cambodia. The north of the province borders Pursat and Kampong Chnang Province. It borders Kandal Province to the east, Takeo province to the southeast, Kampong province to the south. It also borders Koh Kong Province to the west.

2. Method: The Analytical Hierarchy Process (AHP) is used to prioritize the influent parameters that influence the flash flood and drought hazards. The score or priority given for each parameter in the AHP method is depended on the literature review. Likewise, the Geographic Information System (GIS) is applied to generate the map, classification, and reclassification of the map to develop the flash flood hazard maps, drought hazard maps, and bi-hazard maps over the study area.

3. Climate data: Rainfall data is obtained from the Tropical Rainfall Measuring Mission (TRMM). Relative humidity and temperature data are obtained from NASA POWER.

4. The study is based on two seasons in Cambodia: Dry season (Nov-Apr) and Rainy season (May-Oct).

5. Result verification: the results are verified with the historical data loss report from the National Committee of Disaster Management (NCDM).

Key Words

Analytical Hierarchy Process, Geographic Information System, Flash Floods, Droughts, Bi-hazard, Kampong Speu Province

CHAPTER II

LITERATURE REVIEW

Flood

Flooding is the flow of water to usually dry areas, and it is one of the most common hazards in the world (Smith, & Petley, 2009). A flood occurs when the water level is increased due to the failure of technical infrastructures or heavy rainfall over the capacity of the storage. The flood worldwide will be increased due to two trends. Firstly, climate change results in increasing the frequency and magnitude of extreme events. Secondly, there is a spot showing the people and economic factors located in the flood risk areas increasing (Ranke, 2016).

1. Flood Types

Three types of floods occur namely river floods, coastal floods, and flash floods. These floods have dissimilar characteristics (Doswell, 2003; Smith, & Petley, 2009).

1.1 River Flood: It results from the water level overtop of the riverbanks both natural and artificial, which can interrupt human life and damage properties. River flood typically unfolds several days or even a month due to its occurrence in which basin. The magnitude of the flood is express in terms of discharge (rapid peak river flow) while the potential of hazard is related more to the flood stage (maximum height). The causes of river floods are related to climatological forces and secondary flood-intensifying conditions. Excessive rainfall is the most common cause of flood (Smith, & Petley, 2009). Because of the large scale and duration of the river flood, the damage may be enormous or can be billions of dollars. The use of flood-prone areas puts lives and properties at the risk. The choice associated with Landuse is continuing challenges.

1.2 Coastal Flood: It happens when the seawater surface abnormally rises, which is caused by the tide and wave in the short-term and long-term process. The short-term process refers to the increase in height due to the storms such as hurricanes and tsunamis created by an earthquake under the sea. However, the long-term is the relative increases in seawater level along the low-lying coasts by changing the incidence in which the sea defenses are overtopped by win-driven waves of storm stages (Smith, & Petley, 2009).

1.3 Flash Flood: Flash flood occurs when the water rises during or within a few hours of heavy rainfall. It occurs in small catchments where the response time of the drainage basin is short. The factors related to the occurrence of flash floods include soil types, terrain gradients, landuse, rainfall, etc. Rainfall produced by the thunderstorms can result in a flash flood. Additionally, a thunderstorm is improbable to create a flash flood, it is needed several thunderstorms. A flash flood is sometimes not the result of thunderstorms, but it can happen due to heavy rainfall (Doswell, 2003). Flash flood is differentiated from general flooding by the timescale. The sympathetic of the local hydrologic geography and persistent observing of the existing meteorological condition is needed for flash floods forecasting. It is a short period event with a quite high peak discharge. The United Nations National Weather Service specifies the timeframes and threat level; flash flood begins within 6 hours or often 3 hours of the causative event. Intense rainfall, failure of a dam, levee, or sudden rise of water level, etc. can be the causes of flash flood occurrences. It also can occur in normally dry areas without stream channels. The flash flood is a rapid-onset hydrologic event, which is hard to estimate. Rainfall and predicted runoff process are the main foundations that cause a flash flood, so it is essential to use these factors in the forecasting process. Higher rainfall intensity results in rapid runoff since the surface could not absorb the water speedily enough, so it causes flash floods.

2. Negative Effects of Flood

Flood produces damages through the immense power of the water moving. The affected factors by the flood are environmental impacts, loss of life and property, mass migration, and economy. Among all the countries worldwide, the flood occurred 1,280 times between 1900 and 2012, which were in Asia (41%) following by America (27%), Africa (17%), Europe (10%), and Oceania (4%). The floods killed 2.5 million people, and they affected 5.2 billion people (Ranke, 2016), as shown in **Figure 1**.

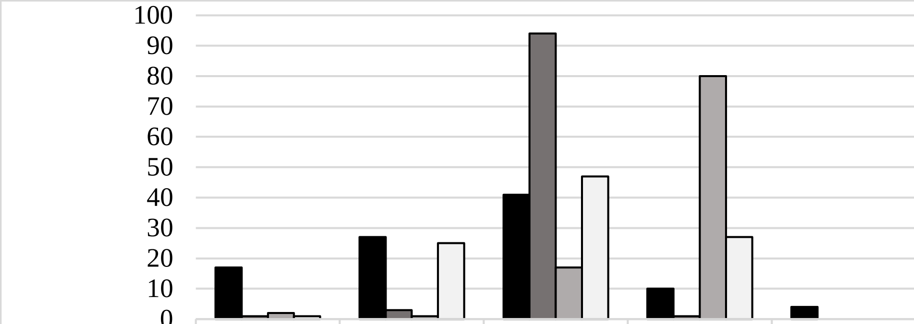

	Africa	Americas	Asia	Europe	Oceania
Events (%)	17	27	41	10	4
Killed (%)	1	3	94	1	0
Affected (%)	2	1	17	80	0
Damages (%)	1	25	47	27	0

Figure 1 Statistical evidence on worldwide flood risk

Droughts

Droughts are the result of water-related problems when their period is drier than the normal conduction. It occurs when rainfall is less than the usual condition for several weeks, months, as well as years. Moreover, it is related to the movement of the stream and river declines and the levels of the reservoirs descent and the deep of water in the good increase. Besides, the dry period will become to be a drought whether dry weather persists and water supply problems develop (Nagarajan, 2009). It is also related to timing, which focuses on the principle of season, delays the starting of the rainy season, and the relationship between rainfall and crop growth stage. Additionally, droughts are connected to the effectiveness of the number of rainfall events and rainfall intensity (Monacelli, 2005).

1. Types of Drought

Droughts are categorized into four classes such as meteorological, agricultural, hydrological, and socioeconomic droughts (Monacelli, 2005; Nagarajan, 2009).

1.1 Meteorological drought: It is defined by the regional-based by comparing the stages of rainfall and extent of aridness with the normal condition. It is related to the rainfall in that region. It is identified in terms of seasons, years, or decades of lacking rainfall. Moreover, the extent of droughts influences soil moisture, streamflow, water supply, and shallow groundwater tables.

1.2 Agricultural drought: Its impacts are based on the magnitude, duration, timing, and response of the regions' soil, plants, and animals to water stress. When there is an occurrence of droughts, it leads to a reduction of plant population and final yield. If the droughts occur in the later step of crop development, the crop will be destroyed. Typically, the damages of the crop are based on the crops' biological characteristics, growth stage, and physical and biological soil properties.

1.3 Hydrological drought: It focuses on the river basin scale. Additionally, it is measured by the effects of lacking rainfall on the surface or subsurface water supply (streamflow), reservoirs, lakes, and groundwater levels. Hydrological droughts refer to the lacking of water in the water supply due to not enough rainfall. It fails behind the meteorological drought and agricultural drought since it takes time for rainfall deficits to come.

1.4 Socioeconomic drought: It occurs when the water supply cannot meet the need of humans and the environment. It develops when meteorological, agricultural, and hydrological droughts affect the demand and supply of economic **goods.**

2. Negative Effects of Drought

Droughts affect directly or indirectly on social, economy, and environment throughout the world (Monacelli, 2005; Nagarajan, 2009).

2.1 Social impacts: is in the period of extreme and persistent droughts. It can affect human health and safety. In this case, emergency water is needed for public health.

2.2 Economic impacts: It is related to agriculture and other economic problems including forestry and fisheries, which depend on the surface water and groundwater supply. Droughts influence the crops' production as well as the increase of insects or diseases on the plants. \

2.3 Environmental impacts: in the long-term drought, landuse will be affected. For instance, land degradation such as soil erosion will occur. Soil moisture will be decreased due to the long time absence of rainfall.

Cambodia National Hazard and its Effects

Cambodia is a Southeast Asia country with an area of 181,035 km^2 and 46% covered by forest. The total population is 16.2 million which 78.1% live in rural areas by 2018. It is the developing countries, which vulnerable to climate change. It is listed in the rank of 19 to climate risk index and rank 54 to inform risk index, the risk of humanitarian crises and disaster. Most hazard is related to hydro-meteorological events including floods, droughts, storms, and tropical storms (UNDRR, 2019). There are several types of disasters that happened in Cambodia between 1993 and 2013 (NCDM, 2013), shown in **Figure 2**.

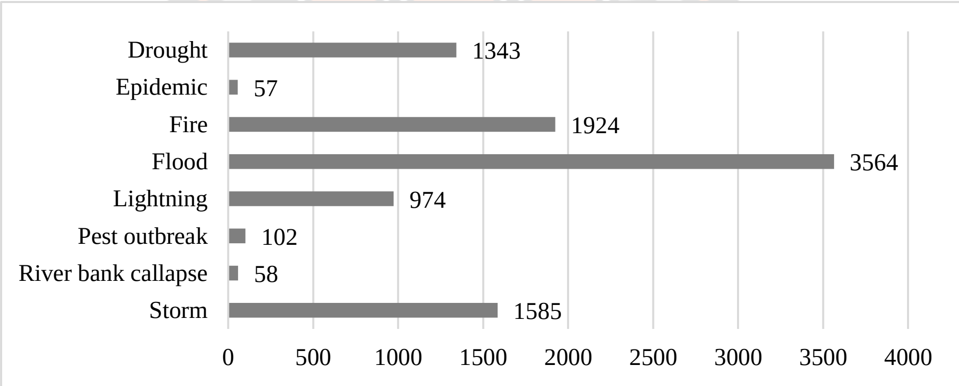

Figure 2 Disasters occurred in Cambodia 1993-2013

Cambodia: Droughts

Compare to floods, droughts are paid less attention. It is therefore hard to make national and international responses. The condition of drought is mainly a consequence of unpredictable rainfall. Additionally, the drought is worsened because of the limited irrigation system. Droughts are characterized due to their water source defeat, which is caused by abnormal seasonal rainfall. Besides, it severely distresses agricultural yield, particularly in rice-growing societies that depend only on rain and river-fed irrigation. The frequency of droughts varies from one province to one province. The most affected provinces are Kampong Speu, Takeo, and Battambang. El Nino in 2015-2016 produced less rainfall, high temperature, and delaying the rainy season, especially caused the shorter rainy season. According to the National Committee for Disaster Management (NCDM), 50% of districts in Cambodia were distressed by drought while 18 out of 25 provinces were severely affected by droughts. It is estimated that 2.5 million people were affected during that time. Moreover, there were crop damages because of low water supplies. Health centers also reported an increase in illnesses such as diarrhea, fever, and upper respiratory infections. In 2019, droughts affected 13 provinces. There was 57,965 ha of rice field damaged and 2,621 ha were destroyed. The droughts distressed 12 provinces and 14,103 ha of transplanted rice in 2010. In 2011, 3,804 ha of rice fields were affected and 53ha were destroyed. In 2012, droughts hit 11 provinces, affected 14,190 ha, and destroyed 3,151 ha of rice fields (CFE-DM, 2017).

Cambodia: Floods

Cambodia experiences flash floods usually after heavy rainfall during the rainy season. Battambang, Kampong Speu, Kampot, Kampong Thom, Kampong Chhnang, Pursat, Kandal, and Rattanakiri Provinces are frequently affected by flash floods. These provinces were also hit by the overspill of Tonle Sap River and Mekong arms, which inundated Kratie, Kandal, Stung Treng, Kampong Cham, Svay Rieng, Prey Veng, and Takeo Provinces. According to NCDM (2019) report data, Cambodia faced serious floods in 2000, 2011, and 2013. Floods affected over 3 million people and caused 388 death, 748 injured, two missing, 1,305 housed destroyed, 7,920 houses damaged, and 80,599 people evacuated from their houses in 2000. In 2011, floods affected 18 provinces, and four provinces along the Mekong River and Tonle Sap Lake had severe damage. The floods affected 350,000 households (over 1.5 million people). During that time, 52,000 households were evacuated. The death reached 250, and 23 people were injured from the flood in 2011. Approximately 431,000 ha of rice fields were affected and 267,000 ha were damaged. Moreover, the national and provincial roads 925 km and 360 km of urban roads were damaged. The total estimated loss of the 2011 floods is US$ 630 million (An, 2014). In 2013, there was an extreme flood event occurred that affected 20 provinces and 377,354 households. It forced 31,314 households to evacuate to safe places as well as took 168 people’s lives and (CFE-DM, 2017).

Table 1 Damage and loss data in each type of disaster

Event	Deaths	Injured	Missing	Houses Destroyed	Houses Damaged	Victims	Affected	Relocated	Evacuated
Drought	0	0	0	0	0	2,766,217	151,834	0	0
Epidemic	37	0	0	0	0	19	0	0	0
Fire	136	109	0	4,259	643	37970	9	0	69
Flood	1,150	792	0	2,393	31,312	1,226,6757	437	17,158	642,353
Lightning	1,031	542	1	38	176	2,252	36	0	1
Pest Outbreak	0	0	0	0	0	2,378	0	0	0
River Bank Collapse	3	2	0	101	526	1,222	0	292	46
Storm	114	523	2	11,762	26,428	113,417	1,716	0	3,111
TOTAL	**2,471**	**1,968**	**3**	**18,553**	**59,085**	**15,190,232**	**154,032**	**17,450**	**645,580**

Source: NCDM (2019)

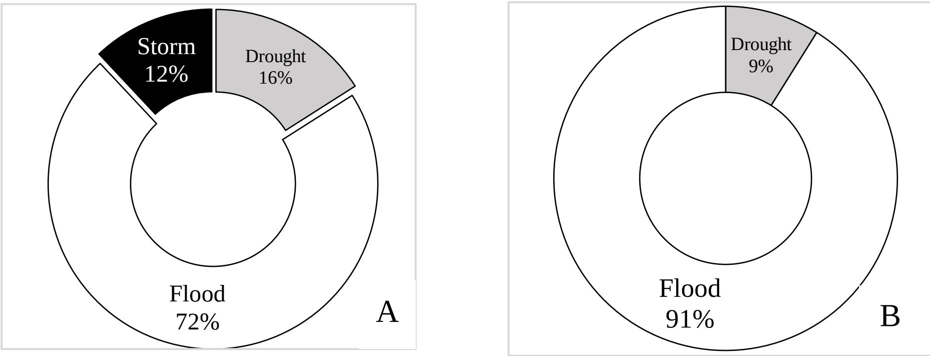

Figure 3 Disasters and risk profile: (A) Frequency of disasters, (B) Economic issues from each disaster

Source: CFE-DM, 2017

Floods and Droughts in Kampong Speu Province

Floods and Droughts are serious problems. Kampong Speu is one of the most vulnerable provinces that faces the problems of too much water throughout the rainy season and too little or no water throughout the dry season. The rainfall upstream (mountainous areas) is heavy throughout the rainy season. The water flows downstream to the Bassac River. It causes flash floods along the Stung Prek Thnot River (CFE-DM, 2017).

1. **Kampong Speu Floods**

According to NCDM, in 2000, 2001, 2002, 2003, 2005, 2006, and 2010, floods affected 140,644 people, 93,505 people, 60,355 people, 64,102 people, 65,924 people, 45,009 people, and 288 people respectively as shown in the **Table 2**. In 2016, floods affected at least 2,216 households (WorldVision, 2016). Provincial Committee for Disaster Management (PCDM) indicated that 230 households were evacuated, and 600 ha of rice fields were under the flood water (Walters, & Hun, 2018).

Table 2 Effects of flood in Kampong Speu province

Year	Deaths	Injured	Houses Destroyed	Houses Damaged	Victims	Evacuated
2000	3	2	34	2,466	140,644	0
2001	2	0	0	1,642	93,505	9,025
2002	0	0	0	0	60,355	0
2003	0	0	0	348	64,102	0
2005	0	0	2	504	65,924	0
2006	0	0	1	551	45,009	0
2010	0	0	0	60	288	0
TOTAL	**5**	**2**	**37**	**5,571**	**469,827**	**9,025**

Source: NCDM, 2019

2. **Kampong Speu Droughts**

Drought also affected Kampong Speu province. In 2002, 2004, 2005, 2006, and 2012, droughts affected 149,175 people, 308,225 people, 681,039 people, 100,592 people, and 1,925 people respectively as shown in **Table 3**. 2015-2016 was the year of serious drought because of El Nino. **Table 4** shows the effects of droughts on agriculture in Kampong Speu Province.

Table 3 Effects of drought in Kampong Speu Province

Year	Victims (person)
2002	149,175
2004	308,225
2005	681,039
2006	100,592
2012	1,925
TOTAL	**1,240,956**

Source: NCDM, 2019

Table 4 Effects of disaster on agriculture in Kampong Speu province

Year	Affect				Losses/damages		
	Droughts (Ha)	Pests (Ha)	Floods (Ha)	Livestock Diseases (Ha)	Droughts (Ha)	Floods (Ha)	Livestock Diseases (Ha)
2009	1,475	1,270	-	2,524	332	-	189
2010	1,929	-	1,766	2,845	223	227	125
2011	-	-	-	3,698	-	-	191
2012	10,715	-	-	1,574	320	-	144
2013	2,239	-	-	2,398	-	-	139
Total	**16,358**	**1,270**	**1,766**	**13,049**	**865**	**277**	**788**

Source: MAFF, 2013

Hazards Concept

According to Alexandar (2000), “a hazard is an extreme geophysical event that is capable of causing a disaster.” This means that hazards can become a disaster and sequential events. A hazard is a danger, but it is not a definite incident (Paul, 2011). A natural hazard is an event, which can threaten lives and belongings. Additionally, the process and events themselves are no hazards, but it is because of the human use of the land (Keller, & DeVecchio, 2012). According to ADPC (2015), “hazard is a dangerous phenomenon, substance, human activity or condition that may cause loss of life, injury or other health impacts, property damage, loss of livelihoods and services, social and economic disruption, or environmental damage.” Cambodia is a susceptible country impacted by climate change. The hazard to society, environment, and economy is strongly connected with the change of extreme events. Some areas do not only face one extreme event, but they can face two, three, or more such as floods, droughts, storms, lightning, etc. Multi-hazard assessment accounting for regional variations in frequency and magnitude of climate extremes is very important to find areas potentially more exposed to hazards in this perspective (Forzieri et al., 2016).

1. Types of Hazards

Hazards arise from various sources. The classification of hazards is essential for identifying similarities and generalizing hazardous events. The most hazard arises from interrelated causes, so the classification of hazard is based on the typology of hazard. However, it can be classified base on the origin. The hazard is divided into five categories as below (Paul, 2011).

1.1 Natural hazard: The natural events initiates from dangerous or common physical processes including earthquakes, volcanic eruptions, floods, droughts, tsunami, storms, landslides, etc.

1.2 Social hazard: It is caused by human activities including famine, warfare, acts of violence, public chaos, etc.

1.3 Biological hazard: It results from biological reasons such as epidemics. The sources of these hazards are viruses, bacteria, insects, medical wastes, plants, birds, animals, etc.

1.4 Technological hazard: It results after the interaction of civilization, machinery, and natural schemes. Examples of technological hazards are explosions, the release of toxic materials, oil spills, etc.

1.5 Chronic hazard: It is raised from lasting procedures including nonstop discharge exposure and work-related exposure. The hazards can affect health and the environment for a continuous and long time.

2. Importance of Hazard Assessment

Climate Change tends to increase the potential impact on humans because of human activities. Floods and droughts are the most dangerous and recurrent natural disasters. Moreover, they are closely connected to human activities and climate change. Floods and droughts influence the production and livelihood of society. In recent years, the incidence of natural hazards has amplified progressively such as heavy rainfall and severe droughts. Moreover, the spatial distribution of floods and droughts has widespread in many parts around the world especially their frequency and magnitude (Y. Liu et al., 2019). To minimize the disaster's loss, it is essential to convey the prevention, mitigation, preparedness, and response activities. Hazard assessment is important in disaster management. It can reduce the harm to society, the economy, and the environment. However, the exiting floods and droughts hazard assessment are still at a very early stage, so hazard assessment needs a more rigorous and formal approach. The information and data can support decision-makers, local, or national authorities to implement rescue campaigns and plan for mitigation, preparedness, and response on the time. It is also useful in planning better or appropriated floods and droughts risk-reduction strategies. Overall, hazard assessment contributes to lessen the adverse impacts of floods and droughts, save lives, reduce property and economic loss, reduce the hazards, and inform the public and relevant shareholders about floods and droughts hazards.

Multi-criteria evaluation (MCE)

Multi-criteria evaluation (MCE) is an approach used to develop hazard and vulnerability maps, especially for mapping floods and droughts hazard areas. The MCE plays an important part in determining the top substitute parameters for a detailed determination, and it can generate the rank of all parameters in conformity with their efficiencies. The MCE is based on several factors. Hence, the decision becomes more reliable and situational judgment between alternative solutions. The MCE can help users to make their decision based on multiple criteria more easily. Usually, the factors are physically persistent such as slope gradient, soil types, elevation, etc. and these influences could point to the comparative reliance of a certain region. The MCE combines both constraints and factors. The Analytical Hierarchy Process (AHP) is the best approach for multi criterial evaluation which developed in 1980 (T. L. Saaty, 1980).

Analytical Hierarchy Process (AHP)

The AHP is a dimension theory pairwise comparison based on the judgment of the experts and relative literature to obtain the important scales in the study (Thomas L. Saaty, 2008). AHP is used to handle the rational and the instinctive to choose the greatest as of the substitutes by evaluating with other criteria (Thomas L. Saaty, & Vargas, 2012). AHP licenses an ordered structure of the criteria that offers operators emphasis on detailed criteria and sub-criteria during assigning the weights. Moreover, it is significant since the other structure can prime a diverse last ranking. In theory, the AHP can advocate a precise decision, which helps decision-makers to figure out the best suit of the understanding problems. Thus, it means that AHP is an approach that depends on the genuine capability of persons to create a critical conclusion (Estoque, & Murayama, 2010). Its purpose is to judge the alternatives for a specific goal by emerging priorities for selected criteria. A pairwise comparison procedure is applied to obtain the significances of the criteria in terms of their significance. The significances are resulting in pairwise comparisons in terms of their performance in contradiction of each criterion. The three codes of AHP are therefore decomposition, comparative judgment, and synthesis of priorities (Thomas L. Saaty, 2008).

1. The structure of the decision problem

When conducting the AHP structure, sufficient related information to signify the problems is required. The important issues are the consideration of the location near the problem, identification of the matters or features that donate to the solution, and the contributors. The purpose of organizing the goals, qualities, matters, and participants includes providing an interpretation of complex interactions inherent in the solution or decision process and allowing the decision-makers to assess or compare the problems of the matching order of degree. Besides, the parameters being compared must be similar or comparable. The users can insert or omit levels or parameters to refine the emphasis of one or more parts of the system. Lastly, less significant parameters can be cut out from additional consideration since their relatively minor influence on the objective (Thomas L. Saaty, & Vargas, 2012).

2. The Fundamental Scale

AHP offers an essential numerical decision-making instrument to cope with unstructured problems. It also permits an improved, easier, and further capable structure for criteria identifying, the weight calculating and analyzing (Bojovic, & Milenkovic, 2008). AHP is applied to establish priorities for all criteria, and the information is drawn from the experts, participants, and mathematic. The fundamental scale of value represents the intensities of decisions is shown in **Table 5** and the pairwise comparison important scale is revealed in **Table 6**. The scale has been confirmed for efficiency by many applications and people through theoretical reasoning. Elements are equivalent or nearly equivalent in measurement, and the judgment is needed to be completed not to define how many times a criterion is larger than the other, but what portion it is greater than the other (Thomas L. Saaty, & Vargas, 2012). A scale of numbers that specifies how many times more significant is needed to make a comparison. Users can dominant one parameter over another parameter concerning the criterion to which they are compared.

Table 5 Fundamental scale of absolute numbers

Intensity of Important	Definition	Explanation
1	Equal importance	Two activities contribute equally to the objective
2	Weak or slight	
3	Moderate importance	Experience and judgment slightly favor one activity over another
4	Moderate plus	
5	Strong importance	Experience and judgment strongly favor one activity over another.
6	Strong plus	
7	Very strong or demonstrated importance	An activity is favored very strongly over another; its dominance demonstrated in practice
8	Very, very strong	
9	Extreme importance	The evidence favoring one activity over another is of the highest possible order of affirmation
Reciprocals of above	If activity i has one of the above non-zero numbers assigned to it when compared with activity j	A reasonable assumption
1.1-1.9	If the activities are very close	It may be difficult to assign the best value but when compared with other contrasting activities the size of the small numbers would not be too noticeable, yet they can still indicate the relative importance of the activities.

Source: Thomas L. Saaty, 2008

Table 6 Pairwise comparison important scale

Scale	Description	Reciprocals*
1	Element i and j have an equal importance	1
3	Element i is slightly important than element j	1/3
5	Element i is higher important than element j	1/5
7	Element i is strongly higher important than element j	1/7
9	Element i is very strongly higher important than element j	1/9

3. The Eigenvector Solution for Weights and Consistency

The AHP process can be defined in four steps as below:

3.1 Define the problems and decide what we want to find.

3.2 Structures the judgment order from the best with the goal of the judgment and purposes from a wide perception over the intermediate level to the last level.

3.3 Build a set of pairwise comparison matrices. Additionally, each parameter in a higher level is used to compare the parameters below in immediate level concerning it.

3.4 Use the significances acquired from the comparisons to weigh the significances in the immediate level below, and do it for all the parameters. Then each element in the level below add its weighted value and obtain its overall or global priority. Remain this method of evaluating and adding up until the last priorities of the alternatives at the bottom-most level are found.

The mathematically outlined AHP is shown below.

$C = (C_j \mid j = 1, 2, \ldots, n)$ is the set of criteria.

The consequence of the pairwise comparison on n criteria can be shortened in an (n_n) evaluation matrix A in which all element a_{ij} (I, j = 1, 2, .., n) is the quotient of weights of the criteria the **Equation 1**.

$$A = \begin{vmatrix} a_{11} & a_{12} & a_{1n} \\ a_{21} & a_{22} & a_{2n} \\ \vdots & \vdots & \vdots \\ a_{n1} & a_{n2} & a_{n3} \end{vmatrix}, \ a_{ij} = 1 \ , \ a_{ij} = 1/a_{ij}, \ a_{ij} \neq 0 \qquad (1)$$

In the final step of the AHP method, the mathematical procedure starts to normalize and find the comparative weights for each matrix. The relative weights are assumed by the right eigenvector (w) corresponding to the largest eigenvalue (λ_{max}) as in **Equation 2**.

$$A_w = \lambda_{max} .w \qquad (2)$$

Then the scores have been applied in the analysis of the relative significance of each parameter as a pairwise matrix comparison to developing the consistent weighting factor (w). The combined hazard is analyzed using **Equation 3**, which is presented by (Mohamed, 2019; S. A. Mohamed, & M. E. El-Raey, 2019; Soha A. Mohamed, & Mohamed E. El-Raey, 2019).

$$\text{Hazard} = \sum_{f=1}^{n} W_f \times S_f \qquad (3)$$

f is the hazard parameter

n is the total number of parameters

W_f is the relative weight assigned to each parameter

S_f is the parameter score.

If the pairwise comparisons are completely consistent, matrix A has rank 1 and λ_{max} =n. In this example, weights could be acquired by normalizing any of the rows or columns of A (Wang, & Yang, 2007). Furthermore, it should be remembered that the value of the AHP output is strictly connected to the reliability of the pairwise comparison judgments. The consistency is well-defined by the relation among the entries of A: a_{ij} x a_{jk} = a_{ik}. The measurement of reliability can be applied to assess the reliability of decision-makers along with the reliability of the whole hierarchy (Wang, & Yang, 2007).

The Consistency Ratio (CR) is the relation of the CI and the Random Index (RI) and expressed mathematically using **Equation 4** and the value of RI is given in **Table 7**. The CR is applied to check the reliability of pairwise. The maximum threshold of CR is 10% (CR must be < 0.1). In the example of exceedance, a three-step process is used including identifying the most unreliable decision in the judgment matrix, defining a variety of values the unreliable judgment can be improved to. It would therefore lessen the related inconsistency and request the decision-makers to review the judgment to a rational value.

$$CR = \frac{CI}{RI} \tag{4}$$

Equation 5 gives the Consistency Index (CI).

$$CI = \frac{(\lambda max - n)}{n-1} \tag{5}$$

CR is the consistency ratio

CI is the consistency index

n is the number of hazard parameters being compared

λ_{max} is the largest value of the eigenvector matrix

Table 7 Random consistency index according to the order of the pairwise matrix

N	**1**	**2**	**3**	**4**	**5**	**6**	**7**	**8**	**9**	**10**
RI	0	0	0.58	0.9	1.12	1.24	1.32	1.41	1.45	1.49

4. Philosophy and Practice of the AHP

AHP is a broad concept of measurement, and it is applied to obtain the relation scales from separate and continuous paired judgments in multilevel hierarchic structures. It is significant for using AHP (Thomas L. Saaty, & Vargas, 2012) as the following state:

4.1 It has a different concern with departure from reliability and the measurement of this departure and with dependence within and between the clusters of elements.

4.2 It is the broadest application in multi-criteria for decision-making.

4.3 It carries out both logical and inductive thinking without the use of syllogism.

4.4 It allows dependence and reaction and makes numerical tradeoffs to arrive at a synthesis or assumption.

4.5 It can apply to both physical and social domains.

The AHP method has been applied in some studies to map flood and drought hazard maps in different places. It is used combined with the Geographic Information System (GIS), which is an influential tool in flood and drought identification. These methods have been used by several pieces of research (Bukari et al., 2016; Danumah et al., 2016; Elkhrachy, 2015; Mohamed, 2019; Ouma, & Tateishi, 2014; Palchaudhuri, & Biswas, 2016; Rahmati et al., 2015; Stefanidis, & Stathis, 2013).

Flash Flood Hazard Index

Flood is divided into three kinds, and its causes are different. Flash flood hazard variables are the most important part of mapping flash flood hazards in the study areas. This section presents the elements and variables that contribute to the flash flood occurring. These parameters are needed in the development of flash flood hazard maps by applying the AHP combined with GIS and base on the experts' knowledge and another literature review. Normally, the types of floods have the main impact on the decision of variables for multi-criteria analysis. Thus, the parameters considered include rainfall, elevation, slope, soil types, geology, flow direction, stream order, Landuse, distance from drainage, and drainage density (Dano, 2020; Danumah et al., 2016; Mohamed, 2019; Ouma, & Tateishi, 2014; Radwan et al., 2018; Stefanidis, & Stathis, 2013).

1. Rainfall

Rainfall is commonly known as the main factor cause flood, and among the rainfall during a certain period over the area can be determined how fast the flood starts to occur. Heavy rainfall is the main cause of floods; most flooding happens because of heavy rainfall especially flash floods while the surface cannot absorb the water in a timely. When the water cannot immediately filtrate into the ground, it will cause runoff and flooding. Rainfall and runoff are related to each other. Thus, the level of water in lakes or rivers rise is connected to among of rainfall. Generally, there are two types of sources to collect rainfall data such as rain gauge networks and remote sensing systems, ground-based weather radar, and satellite. The rain gauges are the relatively simple equipment, which directly simples the rain by accumulating raindrops continuously over a fixed time interval at individual locations. It can be used to map rainfall over small areas, but it has some errors when it comes to large areas and remote land areas. Hence, rain gauge observation can be considered as a ground truth because of its fairly accurate and reliable measurement, but it still has a small error due to its limitation of spatial coverage. Likewise, satellite-based rainfall data add valuable information to the climate database due to its wide geographical coverage. It is the cost-effective input source for flood estimation in many conditions, and it is available on a global basis from the internet and uninterrupted during catastrophic situations (Mahendra et al., 2017).

2. Elevation and Slope

Elevation and slope are vital parts in governing the terrain's constancy. The slope affects the amount and the path of the surface water runoff and subsurface drainage getting to the site. Also, the slope in the specific areas affects the contribution of rainfall to streamflow. It also can control the duration of infiltration, subsurface flow, and overland flow. The slopes can aggravate or decrease the velocity of runoff water (Stefanidis, & Stathis, 2013). The water can flow quickly because of a smooth and flat surface. This slop will be the advantage of flooding. Flat topography is vulnerable to waterlogging when steeper slopes are more susceptible to surface runoff. The low slopes are highly susceptible to flood more than high slopes. The low slope usually causes rain or extreme water from the river to gather in a specific area. On the order hand, the high gradient slope areas do not permit the water to accumulate that can cause flooding. The difference level of elevation on the DEM cells can be considered if the core distress about the flood is a river. For instance, the elevation with the higher surrounding elevation would be more important, this means that the elevation is associated with the flood risk. Normally, slope and elevation maps are developed with the digital elevation model (DEM) from satellite images and using powerful approaches in GIS (Ouma, & Tateishi, 2014). The lower slope classes are assigned with the higher rank due to almost flat terrain while the higher slopes classes are in the lower rank due to its comparatively high runoff.

3. Soil Types

Soil types are the components and features of soils. The soil has a great influence on flooding because some types like sand can absorb water soon and few runoffs occur. In contrast, some soil types, especially clay soils hold water longer and less porous. This can create more runoff, so it may cause more flood. Moreover, soil moisture performances as a border between the atmosphere and the surface. It acts as a significant part in the dividing of rainfall into runoff and groundwater storage. There are plenty of rainfall losses to groundwater and streams when the levels of soil moisture rise. It is also essential for soil erosion, slope stability, and crop and plant growth. Consequently, the types of soil in the study areas are very important factors as they control the quantity of water infiltrate into the ground. Soil types have different capacities for absorbing water. The decrease of soil infiltrate capacity will give the chance of increasing flood hazards in the areas. The water moves downslope as runoff on sloping land when the water is supplied at the rate over the infiltration capacities of the soil (Ouma, & Tateishi, 2014).

4. Geology

Geology is the main affecting the vulnerability to flash floods (Soha A. Mohamed, & Mohamed E. El-Raey, 2019; Shamir et al., 2013). For example, some river terraces are relative to upstanding floodplain areas. In contrast, the higher parts may remain dry. Additionally, alluvium rends to be low-lying and get flood during the major rainfall event even in the small tributary valleys can prone to flash flood. The permeable rocks allow the water the pass through pores and cracks, but impermeable rocks do not. Hence, if the impermeable rocks make up a valley, it will increase the surface runoff that causes flooding.

5. Flow Direction

Flow direction defines which direction the water will flow. Flow direction is divided into two categories such as single and multiple flow direction. The single flow direction is all flow as of a cell that goes in one direction to a single adjacent cell. The multiple flow direction is the flow from a single cell to all nearby cells with minor values. It is determined by the slope and flows width. The direction of the water flows through flow direction. Several studies have been used flow direction for flood simulation (Mohamed, 2019; Soha A. Mohamed, & Mohamed E. El-Raey, 2019).

6. Stream Orders

A stream is commonly known as the movement of the water driven by gravity in the natural waterway. The stream flows down due to the gravity forces. The higher hill has more gravitational energy. Besides, the streams will be the most energetic that cause the fastest erosion rate where the slopes are steepest and the hills are highest. Normally, one stream can flow into another stream. The smaller of the two streams is a tributary of the larger streams in that area. The stream with no tributaries is called a first-order stream. Moreover, a stream with only first-order tributaries is a second-order stream. The third stream is a stream with many second-order tributaries and none higher. More and more branches joint in a drainage network is called the master stream. Hence, when the flood occurs, the higher-order streams take longer to shape up to the flood stage than the lower streams. Additionally, it takes slower for the flood to diminish (Dawes, 2013; Soha A. Mohamed, & Mohamed E. El-Raey, 2019).

7. Landuse

Landuse management is the primary concern in flood mapping since they are the factors that not only reflect the current uses of the land. Landuse is connected to the permeation ability and runoff coefficient (Rahmati et al., 2015). Landuse with the vegetation or grassland influences the capacities of soil acting as the water storage and better in infiltration. This is the disadvantage of the flood occurring. Furthermore, Landuse with crop cover is better than bare fields in terms of reducing the rainwater runoff. The existence of thick vegetation also reduces the speech of rainwater to the soil. However, the impermeable surface cover like concrete almost cannot absorb water at all. Landuse such as roads, slum areas, and buildings declines the capacity of soil to receive water, or no water is received. In brief, Landuse plays a crucial factor in the assessment of the probabilities of flood occurring (Ouma, & Tateishi, 2014; Stefanidis, & Stathis, 2013).

8. Distance from the drainage

The distance from the drainage network indicates the distance to the water channels or streams. Since the distribution of the drainage system is very significant to the beginning of the flooding, areas located near the drainage system are added probably to be flooded (Elkhrachy, 2015).

9. **Drainage density**

The drainage density is a basic idea in the hydrological inquiry that is defined as the relation of the length of the drainage network within a basin area. It is controlled by permeability, erodibility of the surface, vegetation, slope, and time. It is the reverse function of the infiltration; the greater drainage density specifies high runoff inside the basin area along with erodible geologic materials and less prone to flood. Hence, the rating for drainage density decreases with the increase in drainage density (Ogato et al., 2020).

Drought Hazard Index

Drought is a frequent hazard of weather. It is different from aridity, which is classified as a less rainfall region, and it is a permanent random event. Drought is related to continuous average conditions of the balance among evapotranspiration and rainfall. It is related to the principle of occurrence such as delays at the start of the wet season (Monacelli, 2005). Drought hazard variables are the most important part of mapping drought hazards in the study areas. This section presents the elements and variables that contribute to the drought occurring. These parameters are needed in developing drought hazard maps by applying the AHP combined with GIS. The drought hazard indicators include average monthly rainfall, monthly temperature, relative humidity, elevation, slope, soil types, Landuse, and drainage density.

1. **Rainfall**

Rainfall is the most important affected element in the occurring of drought (Gocic, & Trajkovic, 2013). The changes in rainfall affect the severity of the drought. The change in the rainfall impetuous different features of drought in the hazard-prone areas, especially on spatial distribution and temporal pattern (Zhai, & Feng, 2008). Several studies present the relationship between rainfall and drought (Dogan et al., 2012; Gocic, & Trajkovic, 2013; Piccarreta et al., 2004; SÖNmez et al., 2005).

2. **Relative Humidity**

The relative humidity is one of the main parameter influence meteorological droughts. The areas that received low relative humidity are more likely prone to droughts than the areas that received more humidity (Hoque et al., 2020). It has been used as a criterion to assess drought hazards and vulnerability (Hoque et al., 2020; Palchaudhuri, & Biswas, 2016).

3. Temperature

The temperature has a significant relation with the droughts, and it has been used to assess drought risk (Palchaudhuri, & Biswas, 2016). Heater temperatures can rise water stresses and evapotranspiration that make bigger stress on water supplies. Additionally, heater temperatures amplify the impacts of drought. Increasing the temperature can enhance the evaporation from soil and make periodic droughts worse than they would be under cooler conditions.

4. Slope

The exposure of slope to wind and sunshine impacts vegetation, soils, and rates of evaporation and transpiration. For instance, light increases the transpiration rates more than usual. East facing slopes, mainly those at the shoreline, so it has greater evapotranspiration rates than western facing slopes, where the afternoon sun has a greater effect on evapotranspiration rates than does exposure to winds. Slope also has been used in the study of assessing vulnerability and risk of drought (Hoque et al., 2020; Palchaudhuri, & Biswas, 2016).

5. Soil Types

Soil sorts and role influences on groundwater favorable to moisture retention, and with soils less susceptible to erosion, such areas are much less inclined to drought than areas of steep slopes and shallow soils. Shallow soils are noticeably greater inclined to drought and the existence of shallow soils is used as a criterion in mapping areas at the hazard of drought (Palchaudhuri, & Biswas, 2016). Most of the soil in the central plain is well-drained. There are however some areas of heavy clay and poor drainage. Heavy clays might maintain moisture longer which is beneficial in dry stages but hinder crop development in usual environments. Furthermore, soils in the limestone area are typically alkaline and light where there is an overlay of calcareous sandstones, heavy over calcareous grits, deep, and well-drained over calcareous marls. Well-drained soils lose moisture shortly so that plant life in such areas reaches the wilting factor quite quickly in dry periods.

6. Landuse

Landuse is one of the important factors for assessing drought hazard areas. Landuse can be divided into different categories such as bare soil, sand, water, river, tributary, forest, agriculture, building, etc. These categories have different effects on drought (Palchaudhuri, & Biswas, 2016).

7. Drainage density

The drainage density is the completed length of all the streams and rivers divided by the completed area of the drainage basin. Drainage density is viewed that an area with high drainage density has more water contact areas as compared to a location without drainage. Opposing the influence of different causes, it can be indicated that areas with high drainage density are much less susceptible to drought (Jose et al., 2016).

Geographic Information System (GIS) for Hazard Assessments

GIS technique provides an appropriate outline for integration and analyzing the diverse sorts of file sources essential for disaster assessment and observing. The GIS combined with Remote Sensing (RS) gives a proper method for flood and drought hazard analysis than order approaches. Multi-Criteria Decision Making (MCDM) is a complicated method, which geographic information is joint and distorted into a judgment. Spatial MCDM is extra difficult and hard than predictable MCDM. The massive numbers of factors need to identify and consider high correlated relationships among the factors. GIS plays an important part in significantly lessen the difficulty. Several data layers are needed to be handled, so it can be accomplished suitably using GIS (Palchaudhuri, & Biswas, 2016). The weighted overlap method assembled into ArcView Model Builder is applied for the combination of input data layers. The ranking of every parameter is multiplied by its weight. Additionally, the sum of the cumulative values of the parameter is used for the classification into different classes using Jenks National Break Classification.

1. Image Classification

Image classification is the task of extracting the information on landuse and landuse from many band raster images. The result of classification can use to develop the thematic maps. There are two types of classifications based on the interaction between the analyst and the computers (Verbyla, 2002).

1.1 Supervised Image classification: use the spectral signatures taken from the training samples to classify the image. Supervised classification is not better than unsupervised classification; it is just another strategy for image classification. However, supervised classification has some potential. The user can delineate training fields, which could be mixed spectral classes in unsupervised classification including shadow, water, and a burned area. However, supervised classification has some limitations compared to unsupervised classification. The user may not know some cover types, so it will lose the information about the class. The training field delineation could be an error, and classification sometimes is difficult to achieve due to the size of the training field (large ad homogeneous).

1.2 Unsupervised Image classification: find clusters or spectral classes in many band images without help from the analyst's intervention. Unsupervised classification can create clusters, analyze the quality of the clusters, and access the classification automatically (without training data).

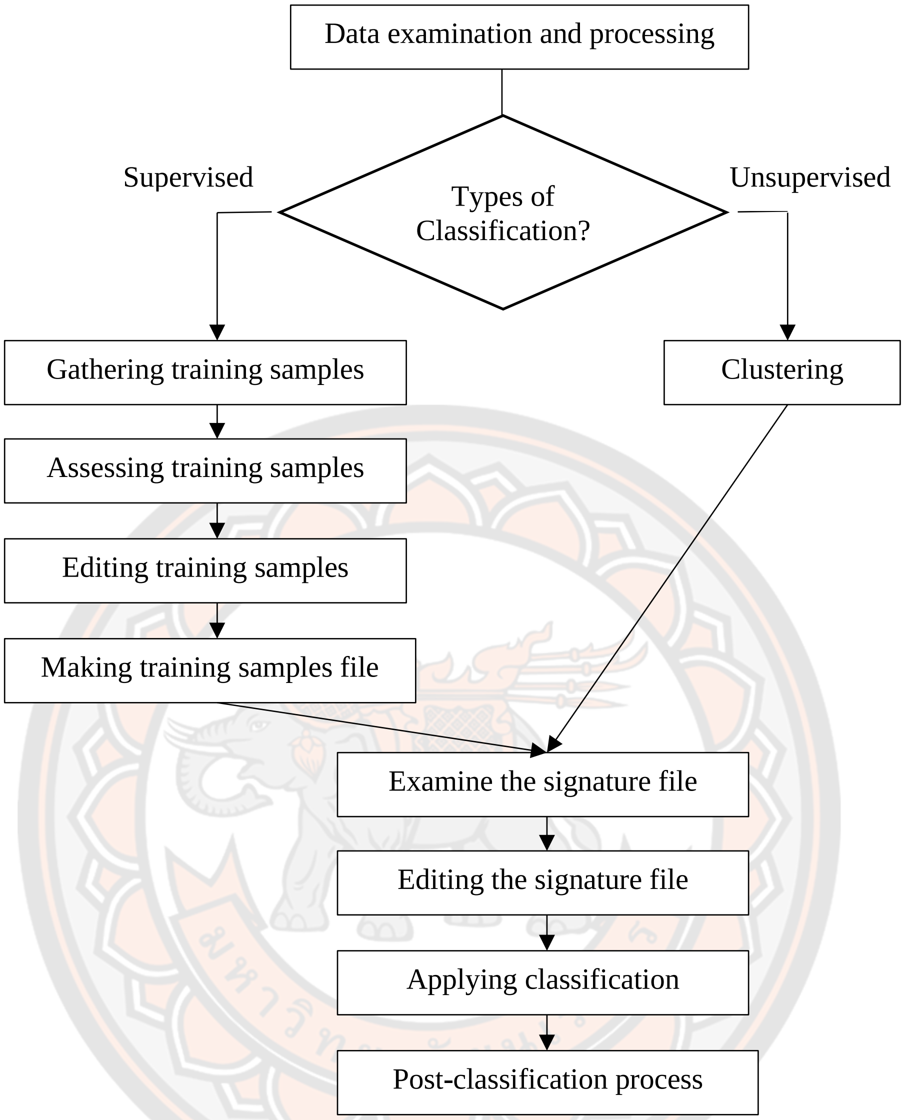

Figure 4 Image classification process

2. Overlay

An overlay is a tool developed in GIS for superimposing multiple data sets together to identify the relationship between each layer. There are several polygon overlay tools in GIS, which provide various purposes.

2.1 Intersection: the result includes the polygon that both overlay; others are excluded.

2.2 Union: all parts of the polygons even though it is not an intersection.

2.3 Subtract: its result includes the polygon, which occurs only in one layer.

Related studies

Table 8 Related studies

Author	Tittle	Aims	Methods	Finding
Mohamed (2019)	Application of satellite image processing and GIS-Spatial modeling for mapping urban areas prone to flash floods in Qena governorate, Egypt	To study flash floods vulnerability.	AHP and GIS	The vulnerability of flash floods
Palchaudhuri, & Biswas (2016)	Application of AHP with GIS in drought risk assessment for Puruliya District, India	To assess drought risk in Puruliya District of West Bengal with the help of AHP and GIS.	AHP and GIS	Drought risk maps
Radwan et al. (2018)	Flood risk assessment and mapping using AHP in arid and semiarid regions	Assesses and maps flood risk for arid and semiarid regions based on spatial AHP and GIS	AHP and GIS	Five classes of risk vulnerability flood maps
Danumah et al. (2016)	Flood risk assessment and mapping in Abidjan District using AHP model and geoformation techniques	To identify, and map areas of flood risk in Abidjan District.	AHP and GIS	Flood map

Author	Tittle	Aims	Methods	Finding
Elkhrachy (2015)	Flash flood hazard mapping using satellite images and GIS: A case study of Najran City	To generate a flash flood map for Najran city, Saudi Arabia, using satellite images and GIS tools.	AHP and GIS	Flash flood map
Seejata et al. (2018)	Assessment of flood hazard areas using AHP over the Lower Yom Basin, Sukhothai Province	To model a flood hazard area using the spatial multi-criteria index to understand the relative importance of the parameters used	AHP and GIS	Flood hazard areas
Skilodimou et al. (2019)	Multi-hazard assessment modeling via multi-criteria analysis and GIS: a case study	Implemented a multi-hazard approach considering landslide, flood, and seismic hazard.	AHP and GIS	Suitable for urban development
KARAMAN (2015)	Integrated Multi-Hazard Map Creation By using AHP and GIS	To get all possible hazard maps as raster maps, classify them into 7 classes, and merge them as a multi-hazard map using GIS.	AHP and GIS	Multi-hazard map of earthquake, landslide, flood, fire, and tsunami
(Rahmati et al., 2015)			AHP and GIS	Flood hazard maps from natural and anthropogenic factors

Author	Tittle	Aims	Methods	Finding
	Assessing the Accuracy of GIS-Based AHP for Watershed Prioritization; Gorganrood River Basin, Iran	To apply two flood hazard indices in terms of GIS-based AHP for dissolving the mentioned problem in the sub-watersheds prioritization field		
Dano (2020)	Flash Flood Impact Assessment in Jeddah City: An Analytic Hierarchy Process Approach	To apply the AHP model to explore the impacts of flash flood hazards and identify the most effective approaches to reducing the flash flood impacts in Jeddah using expert's opinions.	AHP and GIS	Flash flood hazard map with the expert's opinion

CHAPTER III

METHODOLOGY

Introduction

The purpose of the current study is to assess the seasonal special analysis in the determination of flash flood and drought hazard areas with the help of the AHP method and GIS techniques: A case study of Kampong Speu Province in Cambodia. This chapter explains the study design including the study area, data collection, and method for analyzing the data.

Study Area

Kampong Speu Province is located at 11.6155° N, 104.3792° E (**Figure 5**). The total area is 6,966 km^2 equal to 3.87% of the whole country's total area. It consists of seven districts (Odong, Aoral, Phnum Sruoch, Kong Pisei, Thpong, Samraong Tong, and Basedth Districts) and one municipality (Chbar Mon) with the total communes of 87. It is located 48 km to the west of Phnom Penh Capital City. It borders in the east with Takeo and Kandal Provinces, in the south with Takeo and Kampot Provinces, in the north with Kampong Chhnang and Pursat Provinces, and in the west with Koh Kong and Preach Sihanouk Provinces. The total population is 872,219 (NIS-MoP, 2019). The average annual rainfall is 1,562 mm, and the average monthly temperature is 27.5 $^{\circ}$C. The elevation is between 03 m to 1,814 m. Kampong Speu Province is selected for the study because it has a high incidence of flash floods and droughts (CFE-DM, 2017). Kampong Speu Province faces the difficulties of too much water throughout the rainy season and too little or no water throughout the dry season.

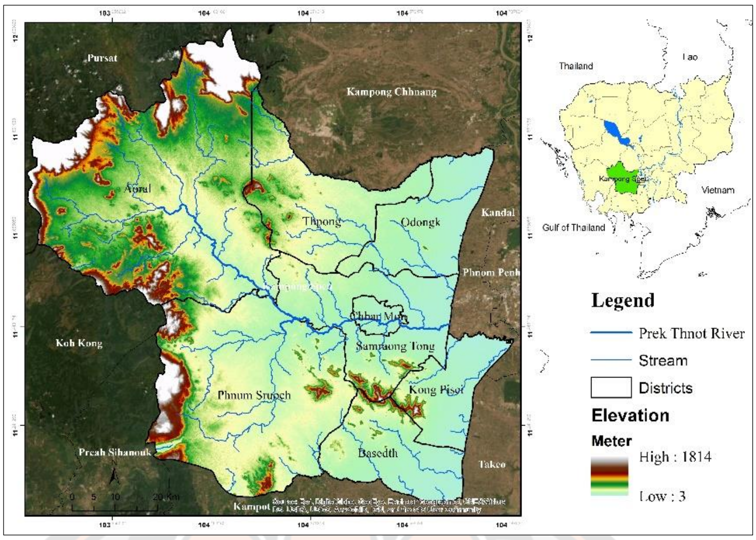

Figure 5 Map of Kampong Speu Province

There is a river called Steung Prek Thnot River located in a part of Chbar Mon Municipality, Samraong Tong District, and Kong Pisei District in Kampong Speu Province, and part of Ang Snuol and Kandal Strueng Districts in Kandal Province. It extends from the Roleang Chrey Regulator to the west of National Road No.3. The water flows from the mountainous area in the west of Kampong Speu Province to downstream crossed Kandal Province to the Bassac River. During the rainy season (May-October), the rainfall upstream causes the flash flood. The west of the province (upstream) is surrounded by mountainous and steep areas. The gravity of the steepness produces rapid runoff, which pushes rainwater downhill very fast at the same time. It is very dangerous. However, there is no rainfall or too little rainfall during the dry season (November-April), so it causes droughts.

Data Collection

To analyze the seasonal flash flood hazard, drought hazard, and bi-hazard of flash flood and drought, significant data are required as below.

1. Rainfall: Rainfall station density in Kampong Speu Province is very few. Moreover, the installed stations are poorly monitored and managed, which limits the availability of continuous monthly rainfall data from those stations. The rainfall dataset was therefore obtained from the Tropical Rainfall Measuring Mission (TRMM, 2011),

which accessible on a nearly global scale. It offers a high spatial and temporal resolution compared to the other satellite-derived rainfall products. The TRMM (3B43) data with the spatial resolution of 0.25° or 27-28 km are used for the generation of the rainfall map and extracted from the given study. The rainfall data were downloaded from 12 different points over Kampong Speu Province whining 20 years starting from 2000 to 2019.

2. Relative humidity and Temperature: Since the study area suffers from a shortage of meteorological data, the data from the satellite is considered one of the most important climatic data sources. NASA POWER dataset has been tested and verified by several studies, and it is an acceptable substitute (Aboelkhair et al., 2019; Bai et al., 2010). The monthly dataset of relative humidity, maximum temperature, and minimum temperature at the same spatiotemporal distribution to rainfall was therefore collected from NASA POWER with the resolution of 0.5° or 55 km, which available on NASA's website https://power.larc.nasa.gov. The single point technique (endpoint), which produces a time series of data based on the registered coordinate was applied to fit the selected sites.

3. Landuse: Landsat-8 images are freely downloaded from the USGS Website https://earthexplorer.usgs.gov. Two Landsat images (path 127 and row 052 and path 126 and raw 052) with a spatial resolution of 30 m were used for Landuse extraction in the study area. The satellite images should be clear without the cloud. Satellite images were acquired on 30 January 2019 and 25 March 2019, respectively.

4. Topography and Hydrology: ASTER DEM images were obtained from NASA Earthdata https://earthdata.nasa.gov. They were used for the generation of topographic maps (elevation and slope) and the hydrological maps (flow direction, stream orders, distance from drainage, and drainage density) of the study area.

5. Soil types and Geology: soil and geological information were derived from the Open Development Cambodia (ODC) https://opendevelopmentcambodia.net.

6. Administrative boundaries: The shapefile was obtained from Open Development Cambodia (ODC) https://opendevelopmentcambodia.net.

7. Cambodia Disaster Damage & Loss Information System (CamDi): The disaster damage and loss data were collected from the National Committee for

Disaster Management (NCDM) in Cambodia through their main website http://camdi.ncdm. gov.kh/DesInventar/profiletab.jsp?countrycode=kh2&continue=y.

Table 9 Data description

Data Types	Date	Format	Source	Derived Data
Climate data	2000-2019	NetCDF	TRMM	Rainfall
Climate data	2000-2019	csv	NASA POWER	Relative humidity, Maximum temperature, and Minimum temperature
Administrative	2016	shp	ODC	Administrative boundaries
Geological Map	2006	shp	ODC	Geology
Soil Map	2014	shp	ODC	Soil types
ASTER DEM	2020	GeoTIFF	NASA	Elevation, Slope, Flow direction, Stream orders, Distance from drainage, and Drainage density
Landsat-8 Images	2019	GeoTIFF	USGS	Landuse
CamDi	2000-2020	xlsx	NCDM	Historical disaster damage and loss information

Method

The study assesses the seasonal flash flood hazard, drought hazard, and bi-hazard of flash flood and drought areas. The qualitative method was used for preliminary hazard assessment in the study area. These assessments used Multi-Criteria Analysis, Analytical Hierarchy Process (AHP), joint with GIS. Likewise, analysis of the spatiotemporal variation of flash floods has provided important understandings of the principal flash flood generation mechanisms and their controlled factors (Ye et al., 2017). A central problem of flash flood prediction and application of inclusive safety procedures has been the absence of comprehensive information concerning seasonal variations (Bush, & Cerveny, 2013). Not different from flash floods, droughts are also considered. Both flash flood and drought hazard assessments were therefore examined based on seasonal periods, which are the dry season (November-April) and the rainy season (May-October), as shown in **Figure 6**. The maps of flash floods and drought hazards cannot be measured for the production of a reliable single map. It can be defensible that different hazards may occur with other intensity and significance compared to others as well as they can interact with each other (Skilodimou et al., 2019). To solve this problem, the AHP approach was applied to assess the relative significance of the two hazards.

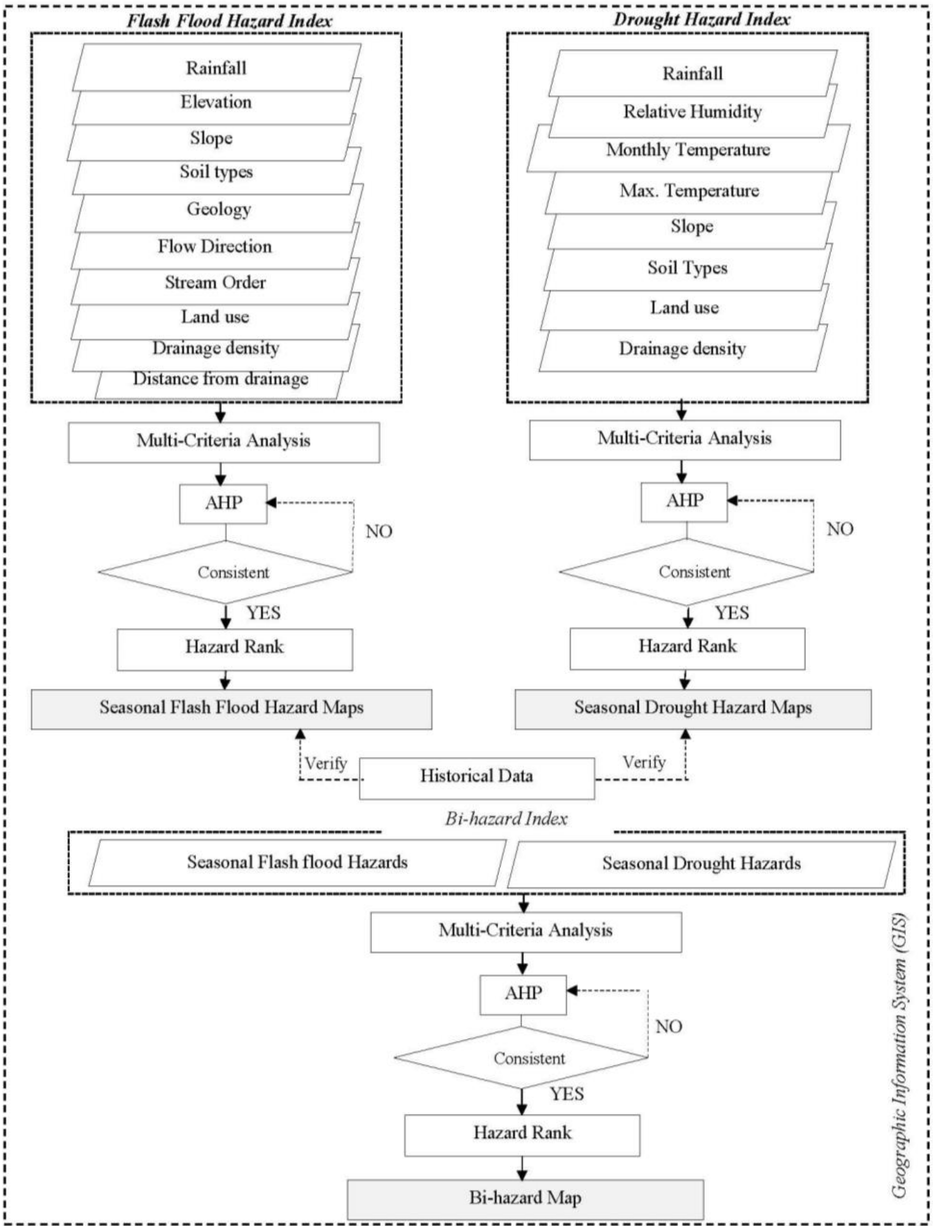

Figure 6 Conceptual framework of the study

Hazard Assessments

The integrated AHP-GIS analysis was used to develop the seasonal spatial distribution of flash flood and drought hazard maps and bi-hazard maps. The process of hazard assessment is demonstrated in **Figure 7**. First, the parameters that influence flash flood and drought hazards were identified. Second, the sensitivity score of each parameter was given based on the literature review. Each parameter was manipulated in GIS with the five hazard levels namely very low, low, moderate, high, and very high. Third, a pairwise comparison matrix was established to carry all the parameters in each hazard to weigh each parameter. In the AHP method, the consistency check was conducted to check the pairwise comparison matrix if it is reasonable and acceptable. Fourth, the value of the hazard was calculated by using Map Algebra in GIS toolboxes by following **Equation 3** (Mohamed, 2019; S. A. Mohamed, & M. E. El-Raey, 2019; Soha A. Mohamed, & Mohamed E. El-Raey, 2019). Finally, the hazard maps were developed in GIS by classifying them into five categories including very low, low, moderate, high, and very high hazard represented in different colors. The results were verified with the historical disaster loss data records obtained from the NCDM.

$$\text{Hazard} = \sum_{f=1}^{n} W_f \times S_f \qquad (3)$$

Where f is the hazard parameter,
n is the total number of parameters,
W_f is the relative weight assigned to each parameter, and
S_f is the parameter score.

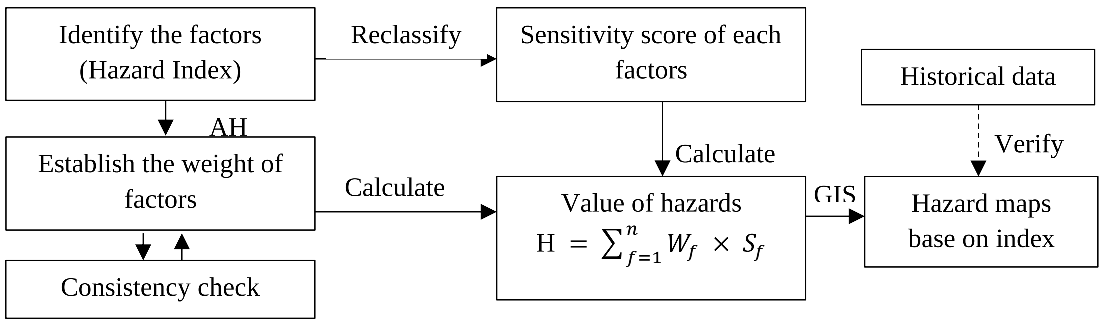

Figure 7 Hazard assessment processes

1. **Hazard Index**

Based on the local environmental characteristics, several influent indicators or indexes of flash floods, droughts, and bi-hazard assessments were selected based on the literature review as shown below.

1.1 Flash flood hazard index: rainfall, elevation, slope, soil types, geology, flow direction, stream order, landuse, distance from drainage, and drainage density.

1.2 Drought hazard index: rainfall, relative humidity, monthly temperature, maximum temperature, slope, soil types, landuse, and drainage density.

1.3 Bi-hazard index: dry seasonal flash flood hazard, rainy seasonal flash flood hazard, dry seasonal drought hazard, and rainy seasonal drought hazard.

2. **Hazard Indicators Analysis**

The entire parameters were obtained from diverse sources and used different methods to extract or derive. The parameters were assigned the scores or classes consistent to one of the five hazard levels based on the local features and the extent to which the risk classes pose potential threats as presented in the various literature. There are different five categories as very low, low, moderate, high, and very high impact, and they are represented by the value of 1, 2, 3, 4, and 5, respectively.

2.1 ***Rainfall:*** Rainfall impacts flash flood occurrences. Matingo et al. (2018), Tekeli and Fouli (2016), and Duan et al. (2017) evaluated satellite-based rainfall (Tropical Rainfall Measuring Mission-TRMM) for the flood assessment. TRMM information was therefore applied in the current study. TRMM data were imported into the GIS from NetCDF to raster layers using the Make NetCDF Raster Layer tool. Then the Extract Multi-Value to Point tool was applied to obtain the rainfall data in each station in the study area (12 stations). All the rainfall data were combined in an Excel file. Since the flash flood and drought hazard assessments were conducted based on the seasonal as mentioned above, the data were divided into two categories including the data for November-April and May-October. The climatic data analyzes consisted of five steps. First, the data were arranged due to the two periods (dry season and rainy season). Second, the data were converted to ArcGIS. Third, they were projected to UTM zone 48N. Fourth, the data were clipped to match the coundary of Kampong Speu Province. Lastly, the images were transformed to points for using in the Inverse Distance Weight (IDW) interpolation algorithm (Isohyet) over the study area.

2.2 ***Temperature and Relative humidity***: These data are very crucial in drought hazard studies. The data were downloaded in a CSV file then they were converted into an excel file. Since the drought hazard assessments were conducted based on the seasonal as mentioned above, the data were divided into two categories as the rainfall data. Moreover, the process of developing maps was following the rainfall maps by using Isohyet.

2.3 ***Soil types:*** The soil map derives from ODC was used to determine categories of soil over Kampong Speu Province. The shapefile was imported to GIS. Then it was clipped to match the boundaries of the study area.

2.4 ***Geology:*** The study used the geological map obtained from ODC in 2006. This map consists of very detailed information about geology in Cambodia. The data was imported into GIS. Then it was clipped to match the Kampong Speu Province boundary.

2.5 ***Elevation and Slope:*** Satellite images in the Geotiff file were downloaded free from the USGS website with a 30 m resolution. The images were projected into UTM zone 48N. Then it was clipped to match the boundaries of Kampong Speu Province. The projected and clipped files were transformed into points. It was then interpolated by the Inverse Distance Weight (IDM). The slope was obtained from the interpolated elevation raster grid to find the elevation changes of each raster cell.

2.6 ***Flow direction and Stream order:*** They were obtained from the ASTER DEM. To derive these parameters, the ASTER DEM images were imported into the GIS then followed some steps as shown in **Figure 8**. The hydrological analysis was accomplished in GIS with the hydrology tool in the GIS toolbox. Additionally, the hydrological analysis was used to extract several parameters such as flow direction, flow accumulation, and stream network. Flow direction defines which direction the water will flow in the cell. It was determined by finding the surrounding cells that have the lowest elevation value. It was the raster grid cells where water will flow of its eight adjacent cells, eight-direction (D8) flow model as presented in **Figure 9** (Jenson, & Domingue, 1988). The cell was given value one when the flow direction was east. Then when the flow goes to the southeast, the value was two. When the flow goes to the south, the value was four. Until the northeast, the value becomes 128. The stream orders were assigned from the source (headwaters) downstream as order number one then the confluence of two first-order streams was ordered number two. The meeting of two second-order streams was ordered number three, and at a meeting of two streams with the same order, the downstream segment got the next highest numbered order (Soha A. Mohamed, & Mohamed E. El-Raey, 2019; A. N. Strahler, 1952).

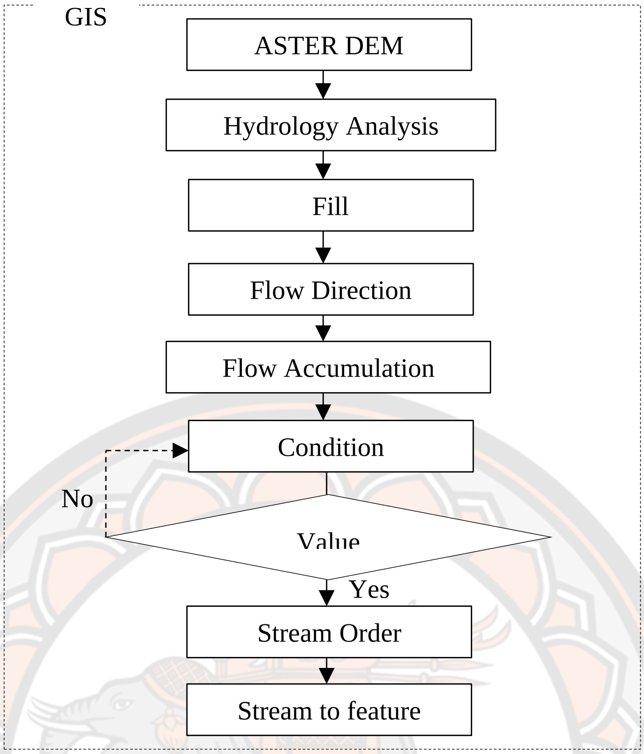

Figure 8 Delineation of hydrological parameters in GIS

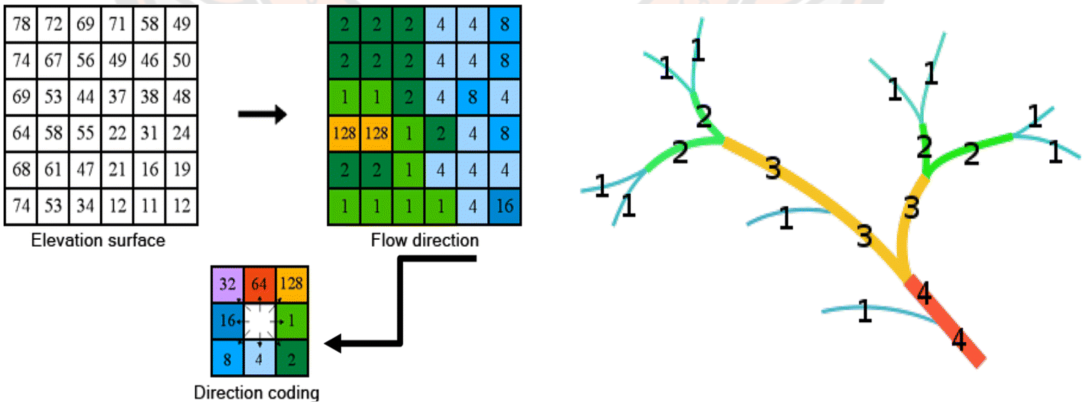

(a). Flow direction (b). Stream

Figure 9 Hydrologic parameter

2.7 ***Landuse:*** Landsat-8 images were used to extract Landuse over Kampong Speu Province. Landuse over Kampong Speu Province are urban, agriculture, built-up infrastructure, water, bare soil, etc. This analysis consisted of several steps. Image processing comprises layer stacking to combine two Landsat-8 images to get a single image by using the Mosaicked Image Processing algorithm in GIS. The two Landsat-8 were mosaicked to cover the entire province. Then Supervised Image Classification was applied to derive landuse types. Several polygons were used as training areas to extract landuse. Training areas were carried out for all landuse kinds using ground truth information and google earth. Many drill areas were used to represent every landuse type. The drill samples were saved as a supervised signature file. The Maximum Likelihood Classification (MLC) algorithm was used to assess the accuracy of landuse extraction as shown in **Figure 10**. Accuracy assessment was an important phase to confirm the method of image classification. It was therefore conducted.

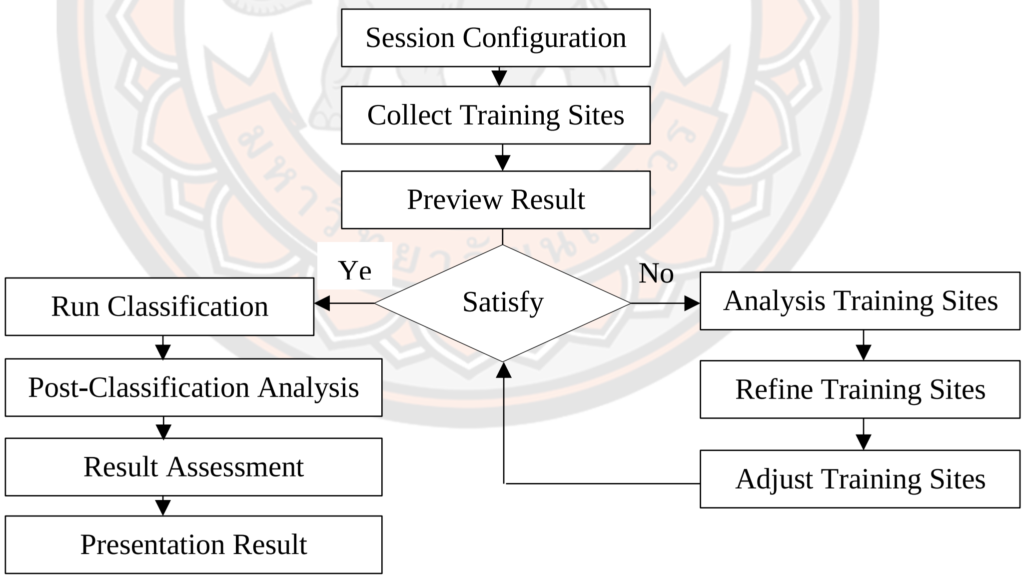

Figure 10 Supervised image classification process

2.8 ***Distance from the drainage***: It was obtained from the corresponding topographic and stream maps and classified based on (N. Strahler, 1957). The first-order and second-order streams could make a minor influence on flooding, so only the third-order and higher-order streams were considered. The stream order was buffer in GIS by using the Multi-Ring Buffer tool. The stream was buffered with a distance of 100, 300, 600, 1,000, and more than 1,000 m. The nearer the distance to the drainage network, the higher chances of the floods to occur (Bathrellos et al., 2016). The buffer zones that enclose the closest distances were allocated.

2.9 ***Drainage density:*** It was acquired from the ASTER DEM images. It is defined as a relation of the completed length of the streams (km) within a basin to the completed areas (km^2) of the basin. The higher value of the drainage density would show a rapid storm response. It is indicative of high flood hazard potential when the drainage density value is high. The map could be resulting from the drainage map. For instance, a drainage map is overlaid on the watershed map to find out the ratio of the total length of the streams in the watershed to the total area of the watershed and is categorized. Within the Spatial Analyst Tools in GIS, the Line density module was applied to compute the drainage density of the watershed. The Line density modules calculate a magnitude per unit location from polyline aspects that fall inside a radius around each cell. The density layer was labeled into five categories using Jenks Natural Break Classification. The drainage density was calculated by using **Equation 6** presented by Agarwal (1998).

$$Drainage\ density = \frac{\sum_{i=1}^{i=n} D_i}{A} (km^{-1}) \tag{6}$$

Where $\sum D$ is the completed length of all stream within the watershed (km)
A is the area of the watershed (km^2).

3. Hazard Index Map Classification

The parameters such as rainfall, relative humidity, temperature, elevation, slope, and drainage density were labeled into five classes by using Jenks Natural Breaks Classification in GIS. Elkhrachy (2015) and Hoque et al. (2019) used Jenks Natural Breaks to categorize flash flood hazard maps. This classification technique is more reliable and effective to present the spatial pattern of flash flood and drought hazard maps (Baeza et al., 2016; Tehrany et al., 2014). For soil types, Landuse, flow direction, stream orders, Landuse, and distance from drainage were classified base on the literature review. All the parameter maps had been rated the score depended on the literature review except the seasonal flash flood hazard and seasonal drought hazard (parameters) that were already classified. All the maps must be in the raster layer. However, if some of them are in the vector layer, they are transformed by using the Polygon to Raster Tool in GIS consisted of several steps. First, the vector layer was imported into GIS and applied Polygon to the Raster tool in the ArcToolbox. The map of each parameter was categorized into five levels including very low, low, moderate, high, and very high with the represented value of 1, 2, 3, 4, and 5, respectively.

4. Analytical Hierarchy Process (AHP)

Mapping the spatial distribution of flash floods hazard, drought hazard, and bi-hazard was accomplished due to the combining of several parameters. The AHP method was used to allocate comparative weight to all influent parameters to acquire the hazard maps. Besides, the final hazard maps were ranked into five classes including very low, low, moderate, high, and very high. The pairwise comparison matrix was constructed in AHP to find the comparative significance of related factors. The weights of all parameters were determined once they are rated according to their comparative significance. The significance of all parameters' value in scale from one to nine score represents less important to more important.

The given scores to flash flood and drought hazard were depended on previous research studies or literature. Furthermore, the given scores to bi-hazard indicators were based on the flash flood and drought disaster data loss from the National Committee for Disaster Management (NCDM) (CamDi, 2020). The criteria Weight Arithmetic Mean (WAM) was used to calculate the aggregate value of the disaster loss from 2000 to 2019. The given scores for each criterion were based on KOEM and TANTANEE (2021) and Shadmehri Toosi et al. (2019). **Equation 6** was used to calculate the WAM of floods and droughts loss in Kampong Speu. The higher value means the higher loss.

$$\text{WAM} = \frac{\sum \text{wx}}{\sum \text{w}} \qquad (6)$$

Where W is the weight given to each criterion, and
X is a type of disaster loss.

Then the score of each parameter was used to calculate the comparative significance of all criteria as a pairwise comparison matrix to get the weight of each parameter. Each row's value was compared with all columns to obtain the comparative importance to find a rating score for all parameters.

The process of AHP is presented below:

1. A pairwise comparison matrix of 10 x 10 cells (flash floods), 8 x 8 cells (droughts), and 4 x 4 cells (Bi-hazard) are created to hold hazard indicators as mentioned in **3.5.1**. Elements in column j and row i of the matrix are identified a_{ij}. The matrix has the property of reciprocity ($a_{ij} = 1/a_{ij}$).

2. The comparative significance of all parameters is found based on **Table 10**. This phase is called prioritizing.

3. The matrix is homogenous with the mathematical expression $a_{ij} / \sum_{ij=1}^{n} = a_{ij}$

4. The normalized comparison matrix is multiplied by the weighted values to acquire eigenvectors.

Table 10 Pairwise comparison important scale

Scale	Description	Reciprocals*
1	Element i and j have equal importance	1
3	Element i is slightly important than element j	1/3
5	Element i is higher important than element j	1/5
7	Element i is strongly higher important than element j	1/7
9	Element i is very strongly higher important than element j	1/9

5. **Consistency Check**

The study acknowledged that the weights of all influent parameters have the probability to make the outcome bias of every suitability assessment. They were therefore considered for consistent outcomes. The consistency of the matrix for analyzing the weight of each parameter in AHP was needed to be evaluated. The Consistency Ratio (CR) was used to evaluate the pairwise comparison matrix. The CR is the relation of the Consistency Index (CI) and the Random Index (RI). It was conveyed mathematically with **Equation 4**. The CI could be found by using **Equation 5**, and the RI value is given in **Table 11**. The acceptable CR must be < 0.1.

$$CR = \frac{CI}{RI} \quad (4)$$

$$CI = \frac{(\lambda max - n)}{n-1} \quad (5)$$

Where CR is the consistency ratio,
CI is the consistency index,
n is the number of all influences parameters, and
λ_{max} is the largest value of the eigenvector matrix.

Table 11 RI based on the order of pairwise comparison matrix

N	**1**	**2**	**3**	**4**	**5**	**6**	**7**	**8**	**9**	**10**
RI	0	0	0.58	0.9	1.12	1.24	1.32	1.41	1.45	1.49

6. **Hazard Mapping**

Raster Overlay analysis under the Spatial Analyst Tools in GIS was applied to develop a hazard map. It was consists of several steps as following. First, in the Spatial Analyst Tools, the Map Algebra was opened then choose Raster Calculator. The weight of all parameters acquired from the AHP method to create the flash flood hazard, drought hazard, and bi-hazard map. Additionally, the sensitive score of all parameters was calculated with **Equation 3**. Finally, the hazard map was categorized into five hazard levels such as very low, low, moderate, high, and very high hazard with a different color on the map. **Figure 11** illustrates the GIS techniques used to generate hazard maps.

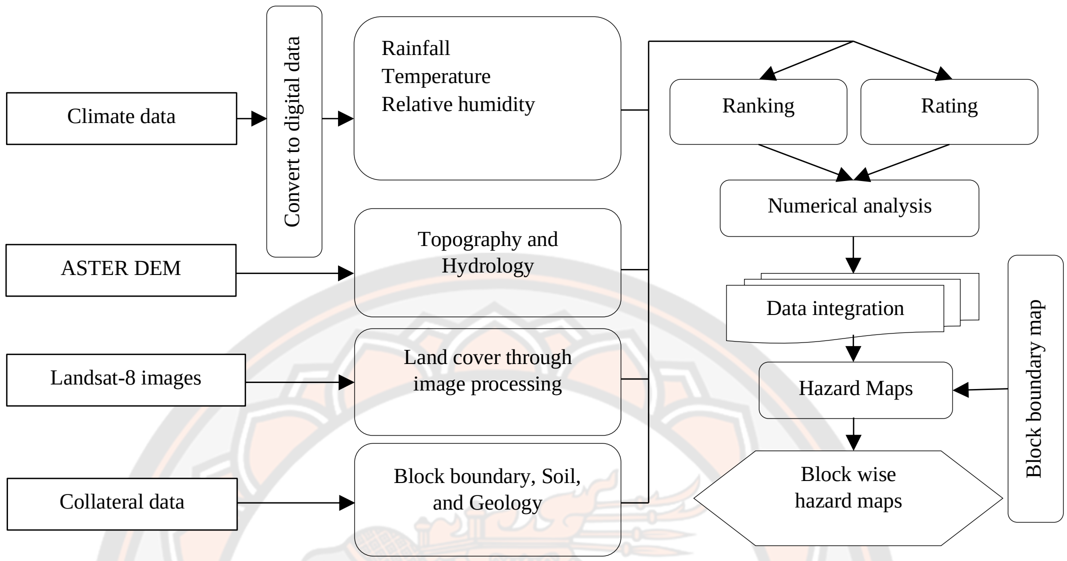

Figure 11 GIS model for hazard assessment

Result Verification

The record historical data of floods and droughts of the National Committee for Disaster Management (NCDM) was used to compare the hazard areas since the MODIS satellite flood map cannot capture the extension of the flash flood during the flood events. This information was obtained or downloaded from the NCDM Website http://www.ncdm.gov.kh/. The downloaded data consists of data loss from the disaster in each commune. The affected communes were therefore used to verify the simulated hazard maps of the study.

CHAPTER IV

RESULTS AND DISCUSSION

In this chapter, the results and discussion under the topic of seasonal spatial analysis in the determination of flash flood and drought hazard areas with the help of AHP and GIS: A case study of Kampong Speu Province in Cambodia, concerning the research objectives, set earlier in Chapter I is illustrated.

Results

1. Flash Flood and Drought Hazard Index

Several parameters were applied to develop flash flood and drought hazard maps in Kampong Speu Province, Cambodia. Rainfall, geology, soil types, flow direction, stream order, distance from drainage, drainage density, and landuse were used to identify both dry and rainy seasonal flash flood hazard over Kampong Speu Province. Besides, rainfall, average temperature, maximum temperature, relative humidity, soil types, slope, drainage density, and landuse were used to map both dry and rainy seasonal drought hazard areas over Kampong Speu Province.

1.1 Rainfall

As mentioned in Chapter III, rainfall data were divided into two parts, which are the dry season and the rainy season. The average monthly rainfall is between 44 mm and 57 mm in the dry season whereas the average rainfall in the rainy season is between 187 mm and 266 mm, as presented in **Table 12**. **Figure 12** shows the isohyet maps of average monthly rainfall in both dry seasons **(a)** and rainy season **(b)** over Kampong Speu Province.

1.2 Temperature

In the dry season, the lowest average monthly temperature is 27.5 ˚C while the maximum average monthly temperature is 29 ˚C. The temperature however decreases in the rainy season, which is between 26.7 ˚C and 27.6 ˚C. Moreover, the maximum temperature during the dry season is higher than in the rainy season. The maximum temperature in the dry season is between 32.3 ˚C and 34.3 ˚C. Besides, the maximum temperature is between 29.6 °C and 31 °C in the rainy season. **Figure 12 (c), (d), (e), and (f)** illustrates the iso-temperature maps of monthly average and maximum temperature in both dry and rainy season, respectively.

1.3 Relative Humidity

The relative humidity is relatively low in the dry season and a bit increase in the rainy season. The relative humidity is between 63% and 71% in the dry season then it increases to 83-87% in the rainy season. **Figure 13** illustrates the iso-humidity maps of the average relative humidity in both dry seasons **(a)** and rainy season **(b)** over Kampong Speu Province.

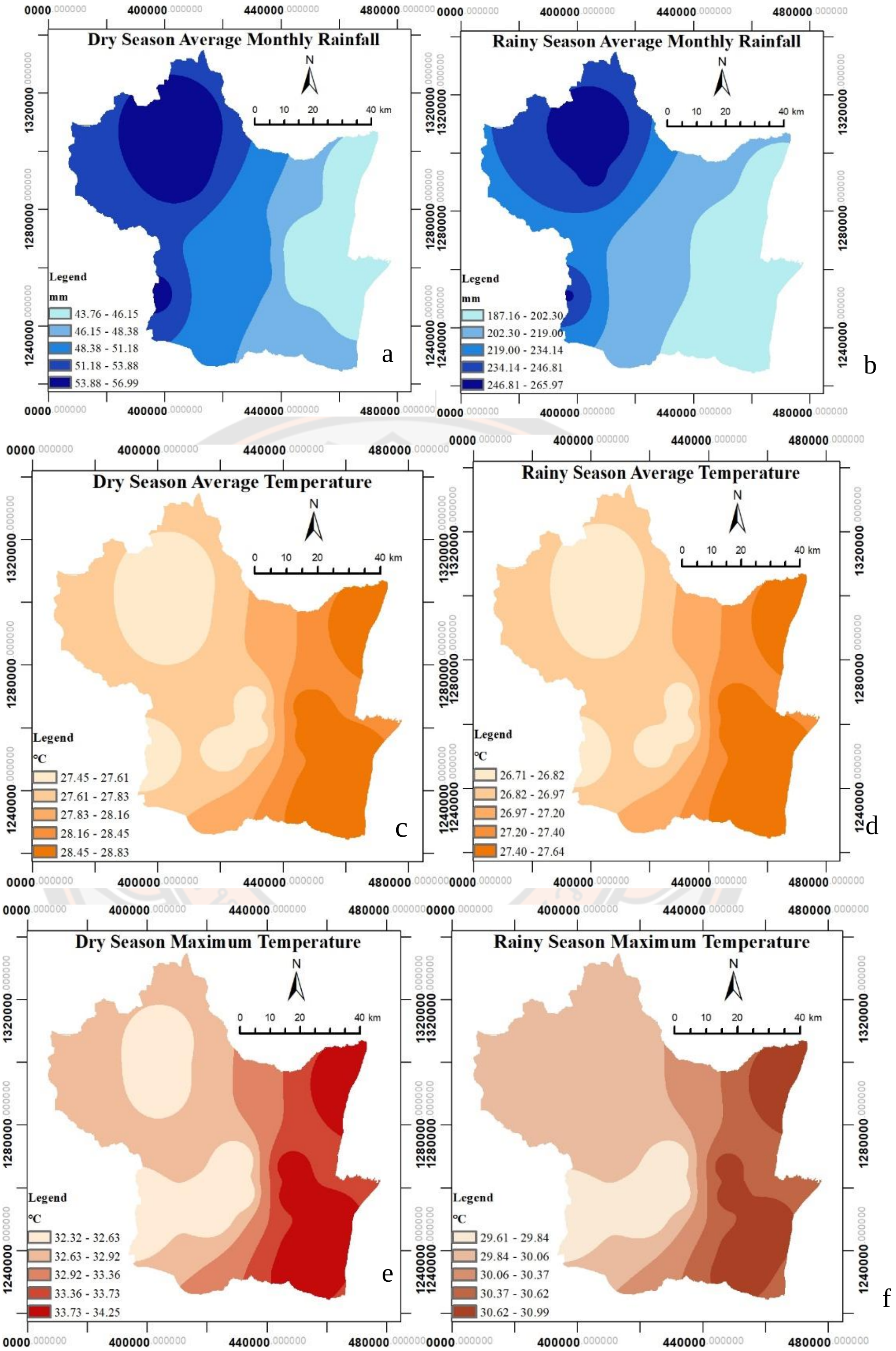

Figure 12 (a) dry season rainfall, (b) rainy season rainfall, (c) dry season average temperature, (d) rainy season average temperature, (e) dry season maximum temperature, and (f) rainy season maximum temperature over Kampong Speu

1.4 Geology

Geology in Kampong Speu Province composes of Old alluvium (43.70%), Young alluvium (21.30%), Diorite including late Cretaceous-Paleogene gabbro and gabroi (7.06%), Devono-Carboniferous sandstone and shale (6.70%), Granite (6.23%), Jurassic-Cretaceous sandstone (5.17%), Rhyolite and dactite (3.70%), Triassic sandstone (3.49%), Homfelse (2.17%), Cambrian-Silurian quartzite (0.42%), Permian: limestone (0.04%), and Andesite (0.01%), as shown in **Table 12**. **Figure 13 (c)** shows the map of geology over the study area.

1.5 Soil Types

The soil over Kampong Speu Province consists of eight different types including Red-yellow Podzols (27.69%), Acid Lithosols (26.28%), Planosols (18.62%), Cultual hydromorphics (12.49%), Grey hydromorphics (8.47%), Alluvial Lithosols (4.90%), Plinthite podzols (1.54%), and Lacustrine Alluvial Soils (0.01%), as presented in **Table 12**. **Figure 13 (d)** shows the map of soil types over Kampong Speu Province.

1.6 Elevation

The Digital Elevation Model (DEM) reveals the changes of elevation higher or lower the Mean Sea Level (MSL). Based on the DEM obtained from NASA, the elevation over Kampong Speu Province is located between 03 m to 1,814 m, as presented in **Table 12**. **Figure 13 (e)** illustrates the elevation map over the Kampong Speu Province.

1.7 Slope

The slope is the relation of the steepness of a specific place on a surface to the horizontal plane. The slope ranges between 0 degrees and 65.6 degrees over the study area, as revealed in **Table 12**. **Figure 13 (f)** demonstrates the slope map over Kampong Speu Province.

1.8 Flow Direction

Flow direction describes the direction of the water flow to a specified cell. Moreover, the flow direction is acquired by defining the minimum elevation value of the nearby eight adjacent cells. The cell was given the value 1 when the water flows in the eastward direction and the value 2 when the water flow to the southwest. The water flows to the south, southwest, west, northwest, north, and northeast when its value is 4, 8, 16, 32, 54, and 128, respectively. Water flows to the east about 18.45% and flows to the south 18.26%. Additionally, about 16.74% and 16.66% of the water flow to the west and north. The water also flows to the southeast, southwest, and northwest about 8.14%, 8.07%, 7.53%, and 6.15%, respectfully (**Table 12**). **Figure 14 (a)** presents the flow direction map over the study area.

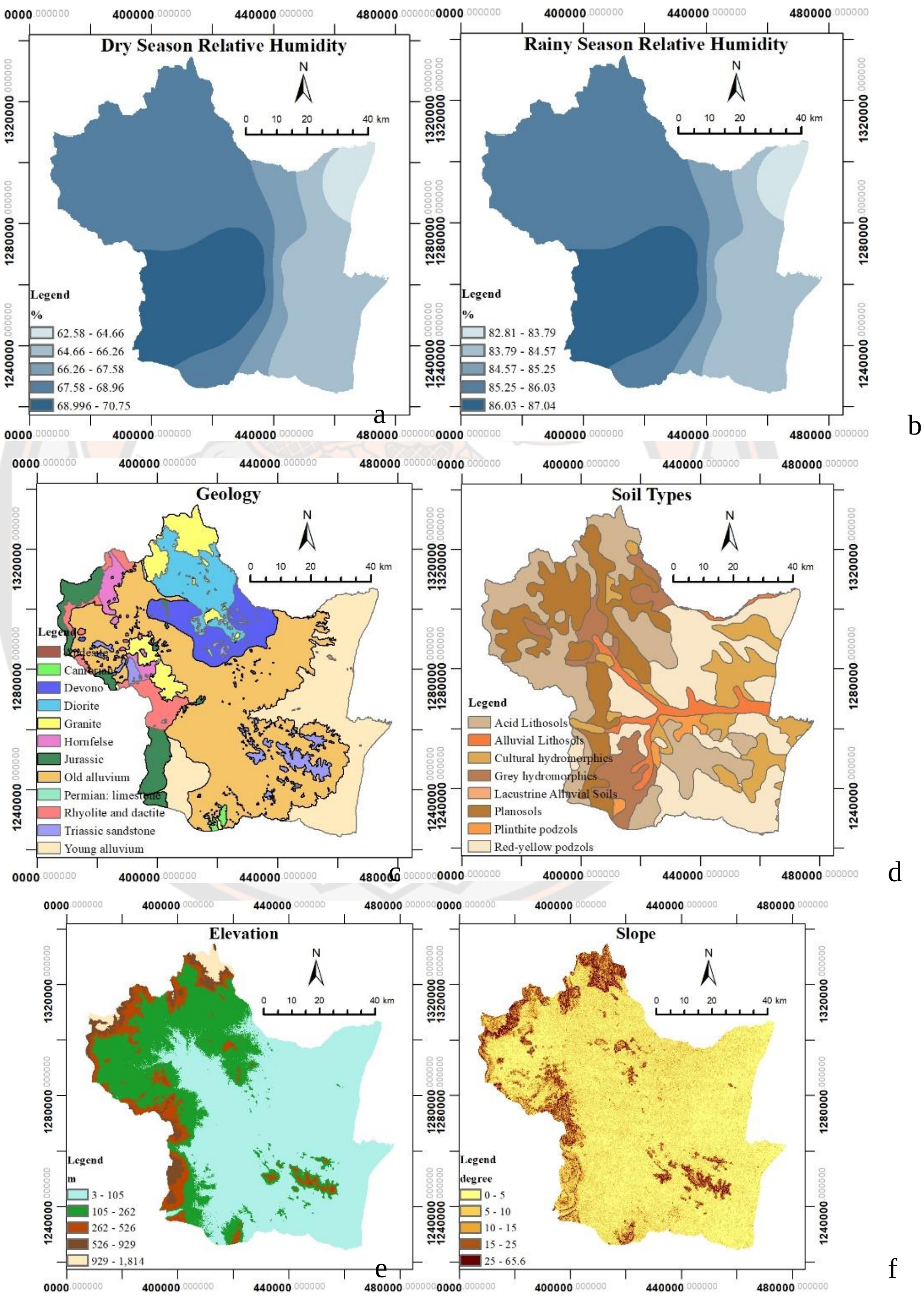

Figure 13 (a) dry season relative humidity, (b) rainy season relative humidity, (c) geology, (d) soil types, (e) elevation, and (f) slope over Kampong Speu Province

1.9 Stream Order

The stream order extracted technique was used to allocate the stream a numerical order with the hierarchy of streams (N. Strahler, 1957). The joint of the same-order will produce a higher stream order as the stream order increase if the same stream order intersect. The intersection of two-stream orders however maintains the value of the highest stream order. The detail of the stream order over Kampong Speu Province is presented in **Table 12**. The first stream order was found 49.15% while the second, third, fourth, five, six, and seven are 25.76%, 14.32%, 3%, 0.6%, and 0.47% of the total areas, respectively. **Figure 14 (b)** demonstrates the stream order map over Kampong Speu Province.

1.10 Distance from Drainage

The distance from the drainage network indicates the space to the water channels or streams. The third and higher stream orders were chosen for buffering since the first and second stream orders have a small contribution to flooding. The distance from the drainage network within 100 m is 7.22% whereas the distance within 300 m is 13.39%. Additionally, the distance within 600 m, 1,000 m, and more than 1,000 m are 18.03%, 20.66%, and 40.70%, respectively, as shown in **Table 12**. **Figure 14 (c)** shows the distance from the drainage network map over the study area.

1.11 Drainage Density

The drainage density is the completed length of all streams and rivers divided by the completed areas of the drainage basin. The drainage density over Kampong Speu Province was divided into five classes such as 0.35-1.74 km^{-1}, 1.74-2.42 km^{-1}, 2.42-2.99 km^{-1}, 2.99-3.62 km^{-1}, and 3.62-4.86 km^{-1} with the value of 8.90%, 22.71%, 30.92%, 24.71%, and 12.76% of the total area, respectively. The detailed information is illustrated in **Table 12**. **Figure 14 (d)** presents the drainage density map over Kampong Speu Province.

1.12 Landuse

Landuse was obtained with the Supervised Image Classification (SIC). The drill sample depended on google earth pro, topography map, and the digital globe was applied to train the classifier. Five particular classes of landuse were recognized from the Landsat-8 image with the Maximum Likelihood Classification (MLC). The area is covered by forest 36.82%, water 0.31%, built-up 16.25%, agriculture 42.16%, and bare soil 4.46% of the total areas, as shown in **Table 12**. The accuracy of landuse is 91.07%. **Figure 14 (e)** demonstrates the landuse map over Kampong Speu Province.

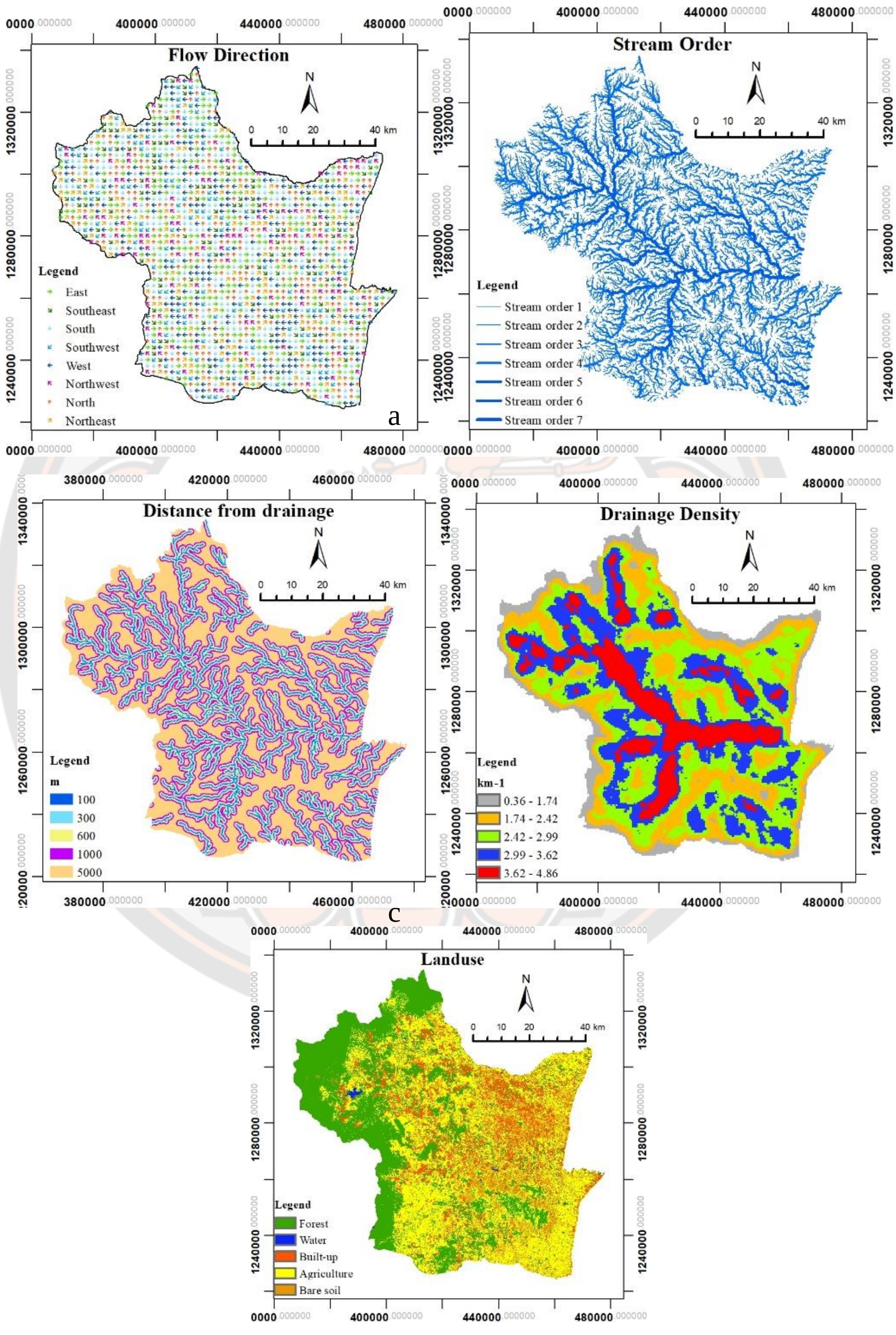

Figure 14 (a) Flow direction, (b) stream order, (c) distance from drainage, (d) drainage density, and (e) landuse over Kampong Speu Province

Table 12 Each parameter's categories and areas

Parameters	Classes	Areas (km^2)	Percentages (%)
Dry season average monthly rainfall (mm)	43.76 – 46.15	1,308.00	18.78
	46.15 – 48.38	1,137.00	16.32
	48.38 – 51.18	1,606.00	23.05
	51.18 – 53.88	1,6.93.00	24.30
	53.88 – 56.99	1,222.00	17.54
Rainy season average monthly rainfall (mm)	187.16 – 202.30	1,945.00	27.92
	202.30 – 219.00	1,868.00	26.81
	219.00 – 234.14	1,154.00	16.56
	234.14 – 246.81	1,313.00	18.84
	246.81 – 265.97	687.00	9.87
Dry season average temperature (˚C)	27.45 – 27.61	1,617.00	23.21
	27.61 – 27.83	2,508.00	36.00
	27.83 – 28.16	765.00	10.98
	28.16 – 28.45	749.00	10.75
	28.45 – 28.83	1,327.00	19.05
Rainy season average temperature (˚C)	26.71 – 26.82	1,542.00	22.14
	26.82 – 26.97	2,561.00	36.76
	26.97 – 27.20	775.00	11.13
	27.20 – 27.40	694.00	9.96
	27.40 – 27.64	1,394.00	20.01
Dry season maximum temperature (˚C)	32.32 – 32.63	1,629.00	23.39
	32.63 – 32.92	2,601.00	37.34
	32.92 – 33.36	721.00	10.35
	33.36 – 33.73	795.00	11.41
	33.73 – 34.25	1,220.00	17.51
Rainy season maximum temperature (˚C)	29.61 – 29.84	915.00	13.14
	29.84 – 30.06	3,368.00	48.35
	30.06 – 30.37	712.00	10.22
	30.37 – 30.62	923.00	13.25
	30.62 – 30.99	1,048.00	15.04
Dry season relative humidity (%)	62.58 – 64.66	274.00	3.93
	64.66 – 66.26	1,488.00	21.36
	66.26 – 67.58	526.00	7.55
	67.58 – 68.96	3,260.00	46.80
	68.99 – 70.75	1,418.00	20.36

Parameters	**Classes**	**Areas (km^2)**	**Percentages (%)**
Rainy season relative humidity (%)	82.81 – 83.79	259.00	3.72
	83.79 – 84.57	1,470.00	21.10
	84.57 – 85.25	508.00	7.29
	85.25 – 86.03	3,281.00	47.10
	86.03 – 87.04	1,448.00	20.79
Geology	Young alluvium	1,484.00	21.30
	Jurassic	360.00	5.17
	Triassic sandstone	243.00	3.49
	Devono	467.00	6.70
	Cambrian	29.00	0.42
	Homfelse	151.00	2.17
	Rhyolite and dactite	258.00	3.70
	Andesite	0.90	0.01
	Granite	434.00	6.23
	Permian: limestone	3.00	0.04
	Diorite	492.00	7.06
	Dolerites	0.10	0.00
	Old alluvium	3,044.00	43.70
Soil types	Acid Lithosols	1,831.00	26.28
	Alluvial Lithosols	341.00	4.90
	Cultual hydromorphics	870.00	12.49
	Grey hydromorphics	590.00	8.47
	Lacustrine Alluvial	1.00	0.01
	Planosols	1,297.00	18.62
	Plinthite podzols	108.00	1.54
	Red-yellow podzols	1,929.00	27.69
Elevation (m)	3 – 105	4,199.00	60.28
	105 – 262	1,898.00	27.25
	262 – 526	517.00	7.42
	526 – 929	241.00	3.46
	929 – 1,814	111.00	1.59
Slope (degree)	0 – 5	3,534.66	50.74
	5 – 10	2,185.00	31.36
	10 – 15	540.00	7.75
	15 – 25	479.00	6.88
	25 – 65.5	227.00	3.27

Parameters	Classes	Areas (km^2)	Percentages (%)
Flow direction	East	1,285.5	18.45
	Southeast	562.2	8.07
	South	1,271.7	18.26
	Southwest	524.2	7.53
	West	1,166.2	16.74
	Northwest	428.7	6.15
	North	1,160.7	16.66
	Northeast	566.8	8.14
Stream order (km)	Stream Order 1	5,082.10	49.15
	Stream Order 2	2,663.88	25.76
	Stream Order 3	1,479.86	14.31
	Stream Order 4	693.96	6.71
	Stream Order 5	309.77	3.00
	Stream Order 6	62.13	0.60
	Stream Order 7	48.11	0.47
Distance from drainage (m)	100	503.00	7.22
	300	933.00	13.39
	600	1,256.00	18.03
	1,000	1,439.00	20.66
	>1,000	2,835.00	40.70
Drainage density (km^{-1})	0.36 – 1.74	620.00	8.90
	1.74 – 2.42	1,582.00	22.71
	2.42 – 2.99	2,154.00	30.92
	2.99 – 3.62	1,721.00	24.71
	3.62 – 4.86	889.00	12.76
Landuse	Forest	2,564.80	36.82
	Water	21.50	0.31
	Built-up	1,132.10	16.25
	Agriculture	2,937.20	42.16
	Bare soil	310.40	4.46

2. Flash Flood Hazard

2.1 Sensitivity Score of Each Parameter

The flash flood hazard index was ranked into five categories including very low, low, moderate, high, and very high. Then they were allocated to the numerical ranks 1, 2, 3, 4, and 5, correspondingly. The rank or score of each category was based primarily on previous research studies or literature reviews. The flash flood hazard maps were obtained by converting all parameter layers to raster grids with equal cell sizes in GIS. Then all the parameters were given the score based on their rating, as shown in **Table 13.**

Rainfall is the core factor that causes a flash flood. Among the rainfall during a certain period over a specific area could be determined how fast the flash flood starts to occur. Additionally, heavy rainfall is one of the main causes of flash floods, and most flooding happens because of heavy rainfall, especially flash floods, which happen when the surface cannot absorb the water in a timely. When the water cannot immediately filtrate into the ground, it will cause runoff and flooding. Rainfall and runoff are related to each other (Mahendra et al., 2017). The higher average monthly rainfall constitutes a high level of flash flood hazard (Abu El-Magd et al., 2020; Mohamed, 2019). The highest rainfall was rated as 5, a very high hazard level. The following classes were given the value of 4, 3, 2, and 1, respectively. **Figure 15** presents the flash flood hazard level for **(a)** dry season rainfall **(b)** rainy season rainfall over Kampong Speu Province.

The soil has an influence on flooding since several types of soil cannot absorb water efficiently, which could cause runoff. The classification ranking of soil types was depended on the capacity of absorbing water of each type of soil over the study area. Mohamed (2019) divided the soil class into three classes including low, medium, and high. The first class includes soils containing rock and dissected limestone whereas the second class includes sandy, gravelly lithosols, and gravel soils. The third class consists of alluvium soils. Kampong Speu Province has eight different soil types provided by Crocker (1962). According to Scotland'sSoils (2013), Acid lithosols soils are restricted in-depth, coherent rock within the 10 cm of the surface, so it is a well-drained soil type. Alluvial lithosol has a wide range of draining conditions while Lacustrine Alluvial is a very well sorted soil type, devoid of coarse particles such as coarse sand or gravel. These soil types were therefore ranked as the lowest score, very low hazard level. Plinthite podzol is aerobic soil. The water can infiltrate freely through the upper part of the profile. Thus, these two types of soil were given a value of 2 (low hazard). Red-yellow podzol is zonal soil having leached and subsoil containing clay. It was therefore rated as the moderate hazard indicator with a value of 3. Grey hydromorphics and cultural hydromorphics are poor drainage of surface water

(Breemen, & Buurman, 1998); therefore, it was rated as a high hazard with a value of 4. Lastly, Planosols has more clay-rich, less permeable, and abruptly overlie dense, which slowly permeable subsoil with significantly more clay (Blake et al., 2008). This soil type was rated as the highest score (5) since the capacity to absorb water is not good. **Figure 15 (c)** presents the map of flash flood hazard levels for soil types over Kampong Speu Province.

Geology is a significant parameter as it amplifies and extenuates the greatness of flash flood events. Permeable rock favors water permeation. Impermeable rock however favors surface runoff. The alluvium is the sediments deposited by rivers. It is known as fertile soil because it is made up of sand, silt, rocks, clay, and other organic matter. The alluvium is not old enough to have been compacted into solid stone (Pariona, 2017). According to Kazakis et al. (2015), alluvial was assigned as the least hazard to flood compared to other geology types. Sandstone is moderately hard to let the water infiltrate from the upper parts. It is better to filter out pollutions from the surface than rocks with cracks and crevices like limestone. Quartzite is a sandstone that has been converted into a solid quartz rock (Tikkanen, 2019). Hornfels is platy or elongate crystals randomly oriented. Rhyolite and dacite called Rhyodacite are formed from granitic magma, a rock with two-grain sizes such as large crystals and small crystals. Andesite contains crystals composed primarily of plagioclases feldspar and minerals pyroxene and lesser amounts of hornblende (USGS, 2015). The impermeable rock like crystalline rock is significant in runoff (Bonacci et al., 2006). Based on Stefanidis and Stathis (2013) and Kazakis et al. (2015), crystalline rocks were assigned as the highest rank to flood hazard. Sandstone is contributed to flooding runoff greater than granite (Tanaka et al., 2004). Limestone is low permeability (Bradbury, & Rushton, 1998), but it is still better than sandstone. Limestone was ranked as the smallest flood hazard compared to crystal igneous (Stefanidis, & Stathis, 2013). In the current study, young alluvium was assigned as the least hazard to flash flood with the value of 1 while old alluvium was given the value of 2. Additionally, Permian limestone was assigned a value of 3 whereas granite was given the value of 4. Finally, Jurassic-Cretaceous sandstone, Triassic sandstone, Devono-Carboniferous sandstone and shale, Cambrian-Silurian quartzite, Hornfels, Rhyolite and dacite (Rhyodacite), Andesite, and Diorite: late Cretaceous-Paleogene gabbro were assigned as the highest hazard to flash flood hazard with the value of 5. **Figure 15 (d)** shows the map of flash flood hazard levels for geology over Kampong Speu Province.

Elevation influences the water movement from the upper to the lower elevation whereas the slope affects the volume of surface runoff and permeation. The plane area in low elevation could inundation quicker than the area in the higher elevation with a steeper slope (J. Liu et al., 2019). Typically, areas located in low elevation and slope will be flooded first as compared to the higher slope areas (Kazakis et al., 2015; Mishra, & Sinha, 2020). Thus, the lowest elevation and slope was given the value of 5, and the followed classes were given the value of 4, 3, 2, and 1, separately. The higher elevation appears in the northwest, west, and southwest parts of the study area with a steeper slope. The lowest elevation is commonly found in the middle, northeast, east, southeast, and parts of the north and south of Kampong Speu Province. **Figure 15** shows the flash flood hazard levels for **(e)** elevation and **(f)** slope.

Flow direction defines which direction the water will flow to in a specified area. Soha A. Mohamed and Mohamed E. El-Raey (2019) classified the flow direction into three particular classes, namely low, moderate, and high. The lowest score was assigned to the direction flows from the lower elevation to the higher elevation. The direction flows from a higher elevation to lower elevation were however assigned as the highest score whereas other flows were assigned as the medium score. The flow direction to the east and southeast were therefore assigned as the highest score with the value of 5 while other flow directions, northeast, south, north, southwest, west, and northwest were assigned the value of 4, 3, 3, 2, and 1, respectively. **Figure 15 (g)** illustrates the flash flood hazard level for flow direction over the study area.

Stream order can affect the occurring of flash floods. The higher stream order can take a longer time to build up the flood stage compared to the lower stream order, which takes a short time to fill in. The higher stream order also takes a long time for flood to decrease (Dawes, 2013; Soha A. Mohamed, & Mohamed E. El-Raey, 2019). Each stream order was rated differently based on the hazard levels. The study of Mohamed (2019) focusing on flash flood mapping, divided vulnerability ranks of each parameter into three classes. The first and second stream orders were rated in the low vulnerability parameter while the third stream order was ranked in the moderate class. The fourth, fifth, and sixth stream order were ranked in the high class of flood vulnerability. There are seven stream orders over Kampong Speu Province. The first stream order was given the value of 1 followed by the second and third stream order with the value of 2 and 3, respectively. The fourth and fifth stream orders were given the value of 4 while the sixth and seventh stream orders were given the value of 5. **Figure 15 (h)** presents the flash flood hazard level for stream order over Kampong Speu Province.

Nature and the amount of landuse control over the runoff features of the river and catchment. Landuse affects the infiltration rate, which is the interaction between the surface and groundwater along with a debris flow. Moreover, it influences the surface roughness, which controls the surface water movement features including depression storage capacity, velocity, etc. (Bahremand et al., 2006). While forest and lush vegetation favor infiltration, urban and pasture areas support the overland flow of water. Urbanization increases the probability of flash flood occurrences (Butler et al., 2006). Different characteristics of landuse such as forest and build-up areas differ hugely in their capacities to seize rainfall and prevent flooding (Duo et al., 2018; Rogger et al., 2017). The major parts of the study area comprise agriculture, forest, built-up, bare soil, and water. Built-up is more prone to flood hazards than the base lands and marshy areas (Ghosh, & Kar, 2018). According to Skilodimou et al. (2019) and Shadmehri Toosi et al. (2019), built-up and water were rated as the highest hazard score and followed by bare soil, agriculture, and forest. Abu El-Magd et al. (2020) and Rahmati et al. (2015) also rated built-up as the most hazard, bare soil as the second hazard, and agriculture as the third hazard area. The land covered by built-up and water was therefore given the value of 5, and bare soil, agriculture, and forest were given the value of 4, 3, and 1, individually. **Figure 15 (i)** presents the flash flood hazard level for landuse over Kampong Speu Province.

Distance from drainage network has a high weight from the AHP method since the inundation initiates from riverbeds and enlarges in the surroundings. The riverbed is reduced as the distance increases. River overflow is very essential for the start of a flash flood incident (Kazakis et al., 2015). The classes of this criterion were defined due to Bathrellos et al. (2016) and Skilodimou et al. (2019). It seems that the zone close to the stream is highly prone to flash flood hazard whereas the influence of this parameter decrease in distance. In order word, the flood hazard decrease as the distance from the active stream increases (Mishra, & Sinha, 2020). The nearest distance was given the value of 5, and the following classes were assumed the value of 4, 3, 2, and 1, respectively. **Figure 15 (j)** presents the flash flood hazard level for distance from the drainage network over Kampong Speu Province.

The distribution of the drainage density to a certain extent determines the varied extend to flood vulnerability. The greater the drainage density is the higher the flood occurrences (J. Liu et al., 2019). In other words, a high drainage density causes high runoff rates (Radwan et al., 2018). The highest drainage density was therefore given the value of 5 and followed by 4, 3, 2, and 1, respectively, for the following drainage density classes. **Figure 15 (k)** presents the flash flood hazard level for drainage density over Kampong Speu Province.

Table 13 Sensitivity score of flash flood hazard indicators

Parameter	**Class**	**Score**	**Weight**
Dry season monthly average rainfall (mm)	43.76 – 46.15	1	0.30
	46.15 – 48.38	2	
	48.38 – 51.18	3	
	51.18 – 53.88	4	
	53.88 – 56.99	5	
Rainy season monthly average rainfall (mm)	187.16 – 202.30	1	0.30
	202.30 – 219.00	2	
	219.00 – 234.14	3	
	234.14 – 246.81	4	
	246.81 – 265.97	5	
Soil types	Alluvial lithosols	1	0.02
	Lacustrine Alluvial	1	
	Acid lithosols	1	
	Plinthite podzols	2	
	Red-yellow podzols	3	
	Cultural hydromorphics	4	
	Grey hydromorphics	4	
	Planosols	5	
Geology	Young alluvium	1	0.04
	Old alluvium	2	

Parameter	Class	Score	Weight
	Permian: limestone	3	
	Granite	4	
	Jurassic-Cretaceous	5	
	Triassic sandstone	5	
	Devono-Carboniferous	5	
	Cambrian-Silurian	5	
	Homfelse	5	
	Rhyolite and dacite	5	
	Andesite	5	
	Diorite	5	
Elevation (m)	3 – 105	5	0.08
	105 – 262	4	
	262 – 526	3	
	526 – 929	2	
	929 – 1,814	1	
Slope (degree)	0 – 5	5	0.15
	5 – 10	4	
	10 – 15	3	
	15 – 25	2	
	25 – 65.5	1	
Flow direction	West	1	0.03
	Northwest	1	
	Southwest	2	
	South	3	
	North	3	
	Northeast	4	
	East	5	
	Southeast	5	
Stream order	Stream order 1	1	0.10
	Stream order 2	2	
	Stream order 3	3	
	Stream order 4	4	
	Stream order 5	4	
	Stream order 6	5	
	Stream order 7	5	
Distance from drainage (m)	100	5	0.07

Parameter	Class	Score	Weight
	300	4	
	600	3	
	1,000	2	
	>1,000	1	
Drainage density (km^{-1})	0.36 - 1.74	1	0.18
	1.74 - 2.42	2	
	2.42 - 2.99	3	
	2.99 - 3.62	4	
	3.62 - 4.86	5	
Landuse	Forest	1	0.03
	Water	5	
	Built-up	5	
	Agriculture	3	
	Bare soil	4	

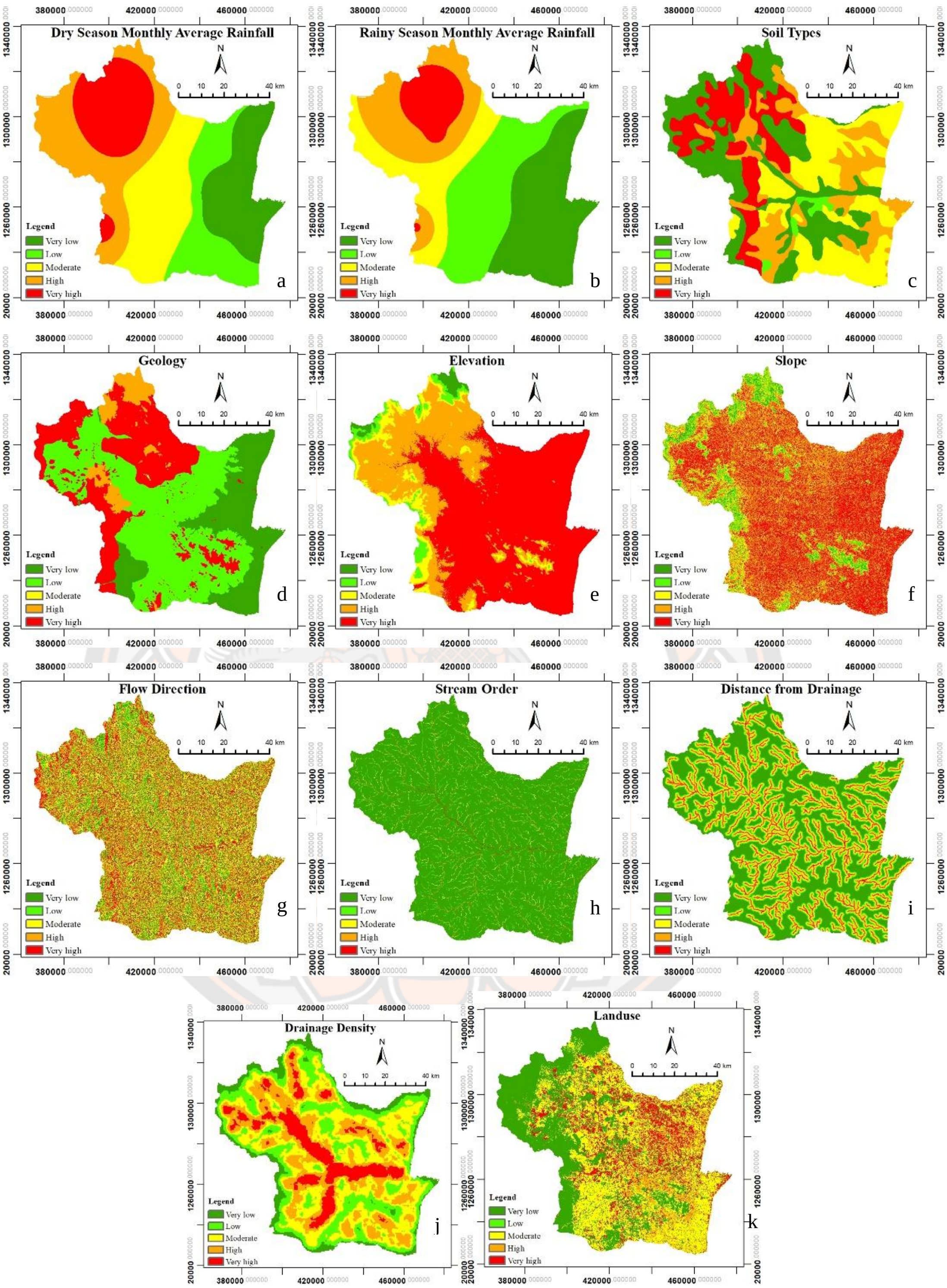

Figure 15 Flash flood hazard levels for each parameter (a) dry season rainfall, (b) rainy season rainfall, (c) soil types, (d) geology, (e) elevation, (f) slope, (g) flow direction, (h) stream order, (i) landuse, (j) distance from drainage, and (k) drainage density over Kampong Speu Province

2.2 Analytical Hierarchy Process for Flash Flood Hazard

The important scale of each criterion in the pairwise comparison matrix (**Table 14**) was assumed based on the previous studies or literature review (Abu El-Magd et al., 2020; Bathrellos et al., 2016; Danumah et al., 2016; Kazakis et al., 2015; Mishra, & Sinha, 2020; Mohamed, 2019; Rahmati et al., 2015; Seejata et al., 2018). Rainfall is the greatest significant factor that affects the flash flood hazard while soil types, flow direction, and landuse are the least important factors that influence flash flood hazard compared to other factors. Rainfall is moderated important than slope, stream order, and drainage density whereas it is strongly important than the elevation and distance from drainage. Rainfall is also demonstrated important than geology and extreme importance than soil types, flow direction, and landuse. Likewise, geology is moderated important than soil types, flow direction, and landuse whereas elevation is strongly important than soil types, flow direction, and landuse. The slope is extremely important than soil types, and it is strongly important than geology, flow direction, and landuse. It is also moderated important than elevation and distance from drainage. Flow direction is moderated important than soil types, and it is equally important to landuse. Moreover, stream order is strongly important than soil types, and it is moderated important than elevation, and distance from drainage. Landuse is moderated important than soil types. Distance from drainage is moderated important than soil types, elevation, flow direction, and landuse, and it is slightly important than geology. Lastly, drainage density is demonstrated important than soil types, flow direction, and landuse. Besides, it is strongly important than geology and moderated importance than slope, stream order, and distance from drainage.

Tables 14 and 15 show the pairwise and normalized pairwise comparison matrix for flash flood hazard assessment. **Table 15** demonstrates that rainfall has the highest weight with the value of 0.30, then drainage density of 0.18, and following by slope of 0.15. It means that rainfall is the most important factor that causes a flash flood. The stream order, elevation, distance from drainage, geology, flow direction, landuse, and soil weights with 0.10, 0.8, 0.7, 0.4, 0.3, 0.3, and 0.2, respectively.

2.3 Consistency Check

The CR is the relation of the Consistency Index (CI) and the Random Index (RI). The acceptable CR must be < 0.1. The λ_{max} is 10.83.

$$CI = \frac{(\lambda max - n)}{n-1} \quad (5)$$

CI = (10.83 - 10) / (10 - 1) = 0.09

$$CR = \frac{CI}{RI} \quad (4)$$

CR = 0.09 / 1.49 = 0.06 < 0.1

The pairwise comparison matrix of flash flood hazard is therefore consistent with the value of Consistency Ratio (CR) equal to 0.06, which is lower than 0.1.

Table 14 Pairwise comparison matrix for flash flood hazard assessment

Criteria	Rainfall	Soil	Geology	Slope	Elevation	Flow direction	Stream order	Landuse	Distance drainage	Drainage density
Rainfall	1.00	9.00	7.00	3.00	5.00	9.00	3.00	9.00	5.00	3.00
Soil	0.11	1.00	0.33	0.11	0.20	0.33	0.20	0.33	0.33	0.14
Geology	0.14	3.00	1.00	0.20	0.33	3.00	0.33	3.00	0.50	0.20
Slope	0.33	9.00	5.00	1.00	3.00	5.00	3.00	5.00	3.00	0.33
Elevation	0.20	5.00	3.00	0.33	1.00	5.00	0.33	5.00	0.33	0.33
Flow direction	0.11	3.00	0.33	0.20	0.20	1.00	0.33	1.00	0.33	0.14
Stream order	0.33	5.00	3.00	0.33	3.00	3.00	1.00	3.00	3.00	0.33
Landuse	0.11	3.00	0.33	0.20	0.20	1.00	0.33	1.00	0.33	0.14
Distance from drainage	0.20	3.00	2.00	0.33	3.00	3.00	0.33	3.00	1.00	0.33
Drainage density	0.33	7.00	5.00	3.00	0.33	7.00	3.00	7.00	3.00	1.00
Total	2.87	48.00	27.00	8.71	16.27	37.33	11.87	37.33	16.83	5.96

Table 15 Normalized pairwise comparison matrix for flash flood hazard assessment

Criteria	Rainfall	Soil	Geology	Slope	Elevation	Flow direction	Stream order	Landuse	Distance drainage	Drainage density	Weight
Rainfall	0.35	0.19	0.26	0.34	0.31	0.24	0.25	0.24	0.30	0.50	**0.30**
Soil	0.04	0.02	0.01	0.01	0.01	0.01	0.02	0.01	0.02	0.02	**0.02**
Geology	0.05	0.06	0.04	0.02	0.02	0.08	0.03	0.08	0.03	0.03	**0.04**
Slope	0.12	0.19	0.19	0.11	0.18	0.13	0.25	0.13	0.18	0.06	**0.15**

Criteria	Rainfall	Soil	Geology	Slope	Elevation	Flow direction	Stream order	Landuse	Distance drainage	Drainage density	Weight
Elevation	0.07	0.10	0.11	0.04	0.06	0.13	0.03	0.13	0.02	0.06	**0.08**
Flow direction	0.04	0.06	0.01	0.02	0.01	0.03	0.03	0.03	0.02	0.02	**0.03**
Stream order	0.12	0.10	0.11	0.04	0.18	0.08	0.08	0.08	0.18	0.06	**0.10**
Landuse	0.04	0.06	0.01	0.02	0.01	0.03	0.03	0.03	0.02	0.02	**0.03**
Distance drainage	0.07	0.06	0.07	0.04	0.18	0.08	0.03	0.08	0.06	0.06	**0.07**
Drainage density	0.12	0.15	0.19	0.34	0.02	0.19	0.25	0.19	0.18	0.17	**0.18**

2.4 Flash Flood Hazard Maps

Since the study was divided into two seasons, the flash flood maps were therefore separated into two different maps, which are rainy seasonal flash floods and dry seasonal flash flood hazard maps. **Figure 16** illustrates the rainy seasonal flash flood hazard over Kampong Speu Province. The results reveal that Kampong Speu Province is located in a very low, low, moderate, high, and very high rainy seasonal flash flood hazard levels with 15%, 31%, 26%, 18%, and 10% of the total areas, respectively, as presented in **Figure 17 (a)**.

Figure 17 (b) shows that the specific areas in Kampong Speu Province are more prone to rainy seasonal flash flood hazards, especially Aoral, Thpong, Phnum Srouch, and Samroang Tong Districts. These four districts are found in very high hazard rainy seasonal flash flood spatial distribution with approximately 9.29%, 0.61%, 0.28%, and 0.1% of the total areas, correspondingly. About 10.88% and 4.39% of Aoral and Phnum Srouch Districts respectively are identified in the high flash flood hazard. Basedth, Kong Pisei, Chbar Mon, and Odongk are not found located in very high hazard whereas Samroang Tong is found located in very high to rainy seasonal flash flood hazard only 0.01% of the total areas. Most parts of these early-motioned districts are identified in low and very low hazard levels (**Table 16**).

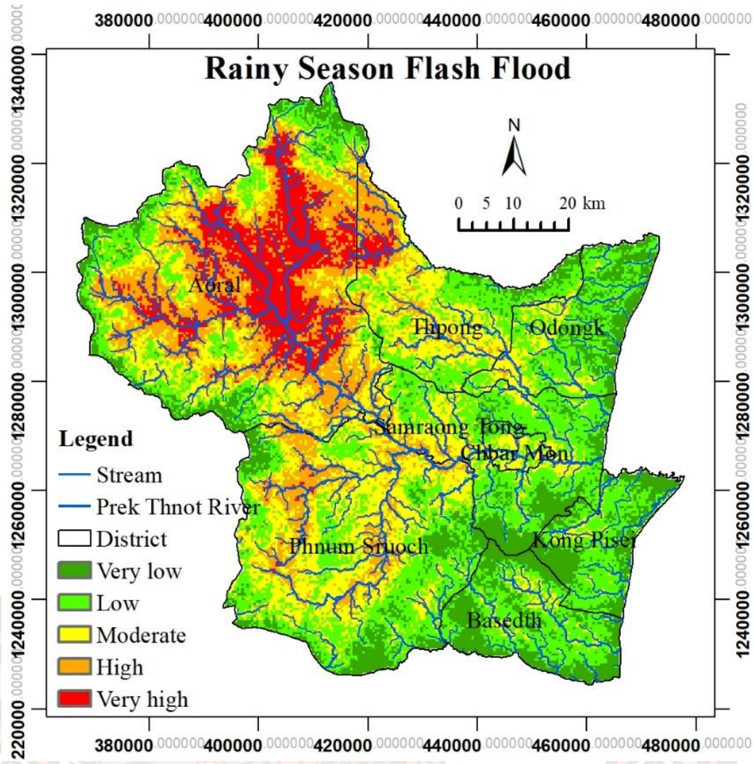

Figure 16 Rainy seasonal flash flood hazard over Kampong Speu Province

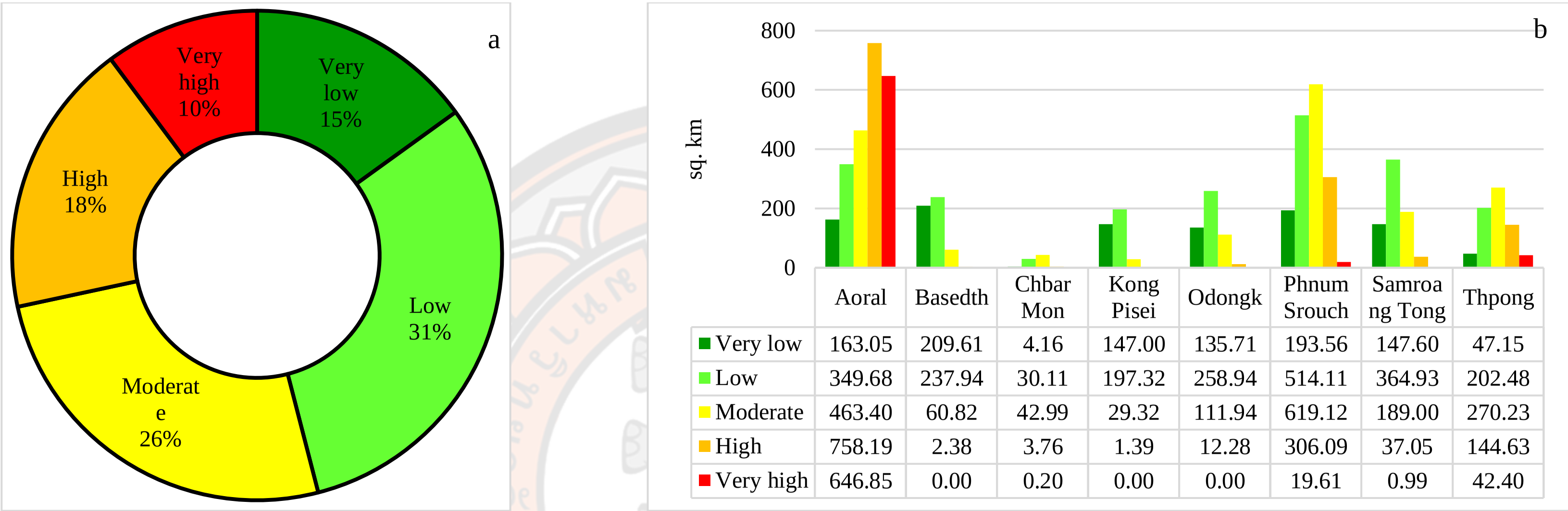

Figure 17 Rainy seasonal flash flood hazard (a) the percentage of hazard level and (b) flash flood hazard in each district

Table 16 Areas and percentages of rainy seasonal flash flood hazard over Kampong Speu Province

	Very low		**Low**		**Moderate**		**High**		**Very high**	
District	Area (km^2)	Area (%)	Area (km^2)	Area (%)	Area (km^2)	Area (%)	Area (km^2)	Area (%)	Area (km^2)	Area (%)
Aoral	163.05	2.34	349.68	5.02	463.40	6.65	758.19	10.88	646.85	9.29
Basedth	209.61	3.01	237.94	3.42	60.82	0.87	2.38	0.03	0.00	0.00
Chbar Mon	4.16	0.06	30.11	0.43	42.99	0.62	3.76	0.05	0.20	0.00

	Very low		Low		Moderate		High		Very high	
Kong Pisei	147.00	2.11	197.32	2.83	29.32	0.42	1.39	0.02	0.00	0.00
Odongk	135.71	1.95	258.94	3.72	111.94	1.61	12.28	0.18	0.00	0.00
Phnum Srouch	193.56	2.78	514.11	7.38	619.12	8.89	306.09	4.39	19.61	0.28
Samroang Tong	147.60	2.12	364.93	5.24	189.00	2.71	37.05	0.53	0.99	0.01
Thpong	47.15	0.68	202.48	2.91	270.23	3.88	144.63	2.08	42.40	0.61
Total	**1,047.84**	**15.04**	**2,155.52**	**30.94**	**1,786.82**	**25.65**	**1,265.77**	**18.17**	**710.05**	**10.19**

Figure 18 presents the dry seasonal flash flood hazard over Kampong Speu Province. Kampong Speu Province is located in the very low, low, moderate, high, and very high to dry seasonal flash flood hazard with 11%, 26%, 29%, 19%, and 15% of the total areas, respectively, as presented in **Figure 19 (a)**.

Figure 19 (b) shows that the specific areas in Kampong Speu Province are located at very high hazard to dry seasonal flash floods, especially Aoral, Phnum Srouch, Thpong, and Samraong Tong Districts. The four districts are found in the very high hazard areas with approximately 12.68%, 1.48%, 1.10%, and 0.04% of the total areas, respectively. Nearly 7.38%, 6.73%, and 2.41% of the total areas located in Aoral, Phnum Srouch, and Thpong Districts respectively are identified as high hazards to dry seasonal flash floods (**Table 17**). Chbar Mon, Kong Pisei, Odongk, and Basedth Districts are however not found in the very high dry seasonal flash flood hazard. These districts are mostly located in low and moderate hazard levels.

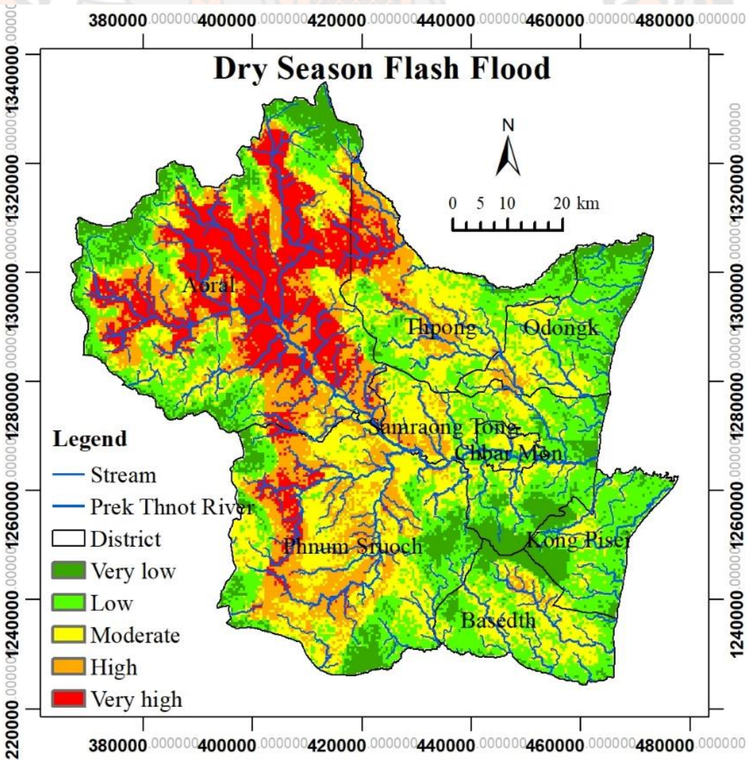

Figure 18 Dry seasonal flash flood hazard over Kampong Speu Province

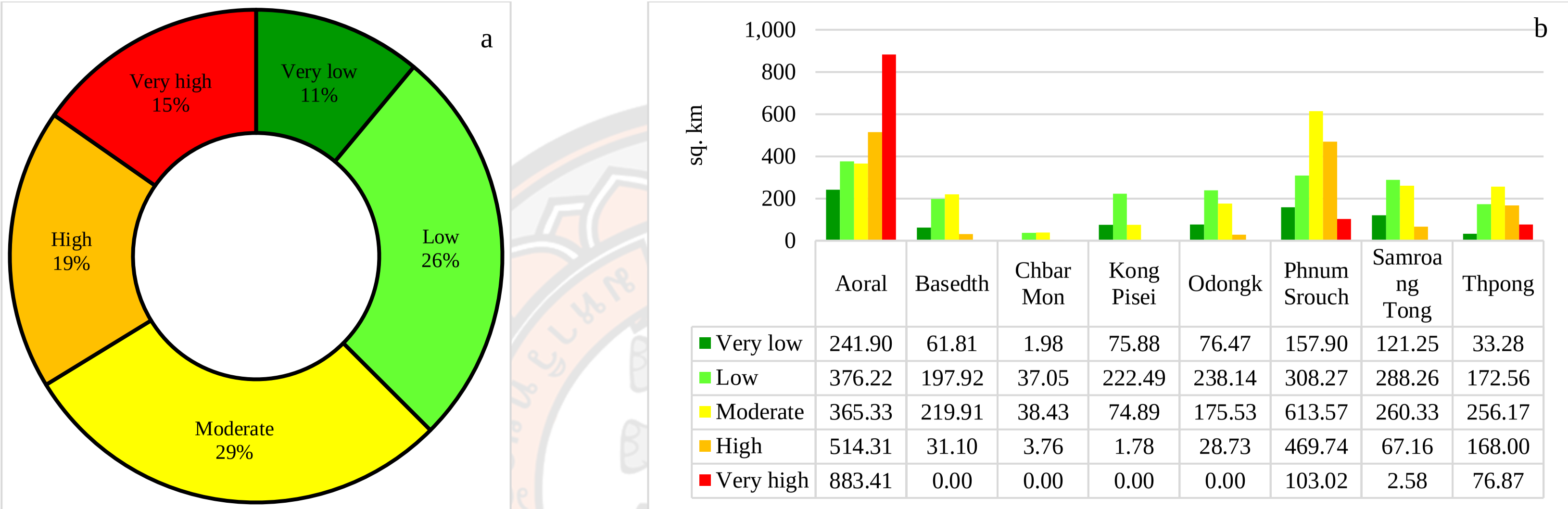

Figure 19 Dry seasonal flash flood hazard (a) the percentage of hazard level and (b) flash flood hazard in each district

Table 17 Areas and percentages of dry seasonal flash flood hazard over Kampong Speu Province

	Very low		**Low**		**Moderate**		**High**		**Very high**	
District	Area (km^2)	Area (%)	Area (km^2)	Area (%)	Area (km^2)	Area (%)	Area (km^2)	Area (%)	Area (km^2)	Area (%)
Aoral	241.90	3.47	376.22	5.40	365.33	5.24	514.31	7.38	883.41	12.68
Basedth	61.81	0.89	197.92	2.84	219.91	3.16	31.10	0.45	0.00	0.00
Chbar Mon	1.98	0.03	37.05	0.53	38.43	0.55	3.76	0.05	0.00	0.00

	Very low		Low		Moderate		High		Very high	
Kong Pisei	75.88	1.09	222.49	3.19	74.89	1.08	1.78	0.03	0.00	0.00
Odongk	76.47	1.10	238.14	3.42	175.53	2.52	28.73	0.41	0.00	0.00
Phnum Srouch	157.90	2.27	308.27	4.43	613.57	8.81	469.74	6.74	103.02	1.48
Samroang Tong	121.25	1.74	288.26	4.14	260.33	3.74	67.16	0.96	2.58	0.04
Thpong	33.28	0.48	172.56	2.48	256.17	3.68	168.00	2.41	76.87	1.10
Total	**770.48**	**11.06**	**1,840.91**	**26.43**	**2,004.16**	**28.77**	**1,284.59**	**18.44**	**1,065.87**	**15.30**

3. Drought Hazard

3.1 Sensitivity Score of Each Parameter

The drought hazard levels for each parameter were attained by converting all parameter layers to raster grids with equal cell size. Then all the parameters were assigned the score as shown in **Table 18.**

Rainfall is an influent factor in the drought occurring (Gocic, & Trajkovic, 2013). It is assumed that the region receiving minor rainfall generally is more prone to drought than the region receiving a greater volume of rainfall (Pandey et al., 2012). The area with the highest rainfall is therefore supposed to be a lower drought hazard than the areas receiving lower rainfall. The area receiving the lowest rainfall was given the value of 5 (very high hazard) whereas the lowest score of 1 was given to the area receiving the highest rainfall (very low hazard). **Figure 20** shows drought hazard levels maps for **(a)** dry season rainfall and **(b)** rainy season rainfall over the study area.

Relative humidity impacts drought events. The zones receiving low relative humidity are more prone to drought than the areas receiving more relative humidity (Hoque et al., 2020; Pandey et al., 2012). Thus, the highest score, 5 (very high hazard) was given to the areas with the lowest relative humidity. The map of relative humidity classified both in dry and rainy season is illustrated in **Figure 20 (c)** and **(d)**, respectively, over Kampong Speu Province.

Temperature is one of the climatic parameters that impact drought hazards. High-temperature increases evapotranspiration (Palchaudhuri, & Biswas, 2016). In other words, the higher temperature is reflected to be a higher hazard than the lower temperature (Hoque et al., 2020). The highest temperature was therefore rated the highest score then it was followed by the following classes. **Figure 20** shows the drought hazard levels maps for **(e)** dry season average temperature, **(f)** rainy season average temperature, **(g)** dry season maximum temperature, and **(h)** rainy season maximum temperature over Kampong Speu Province.

Figure 20 (i) shows the drought hazard levels maps for the slope parameter over the study area. The slope represents the topography of the study area. The larger slope could produce a larger amount of runoff, so less groundwater storage could be produced. The larger slope is considered to be more hazardous to drought (Jose et al., 2016). The highest slope was given the highest score compared to other classes.

Soil types were divided into five classes of hazards based on the physical properties of the soil over Kampong Speu Province. The lighter soil with the lesser water-bearing ability is more prone to drought hazard while the heavy soil with high water-bearing ability is reflected to be less prone to drought hazard (Ramkar, & Yadav, 2018). Accordingly, the clayed or heavy soil holding high water capacity are less prone to drought. The sandy shallow soil having minor water holding capacity is high susceptible (Thomas et al., 2016; Tsakiris et al., 2006). Bases on Scotland'sSoils (2013), Acid lithosols soil is restricted in-depth, coherent rock within the 10 cm of the surface. Alluvial lithosols soil has a wide range of draining conditions while Lacustrine Alluvial soil is very well sorted, devoid of coarse particles such as coarse sand or gravel. These soil types were therefore ranked as the highest score. Plinthite podzols are aerobic soil, and the water could infiltrate easily. Thus, these two types of soil were given a value of 4. Red-yellow podzols are zonal soil having a leached and a subsoil containing clay. It was rated as the moderate hazard indicator with a value of 3. Grey hydromorphics and cultural hydromorphics are poor drainages of surface water soils (Breemen, & Buurman, 1998). It was rated high hazard with a value of 2. Planosols soil has more clay-rich and less permeable and abruptly overlie dense, slowly permeable subsoil with significantly more clay (Blake et al., 2008). This soil type was rated as the lowest score since the capacity to absorb the water is not good. **Figure 20 (j)** demonstrates the drought hazard levels map for soil types over the study area.

Landuse has a direct impact on water resources, and it is reflected in the drought hazard analysis. According to Palchaudhuri and Biswas (2016), the bare soil was rated as the highest score to drought hazard and followed by forest, water, and agriculture as the least hazard. The study of Pandey et al. (2012) on drought hazard assessment however considered agriculture as the highest score for drought hazard assessment while forest, built-up, and water were following continuously. Jain et al. (2014) also mentioned landuse in the spatiotemporal drought assessment. Agriculture was given the highest score whereas built-up, forest, bare soil, and water were followed. Five different landuse types including forest, water, built-up, and agriculture cover the study area. Agriculture is therefore considered the highest hazard to drought with the given rate of 5 and followed by the built-up, forest, bare soil, and water with the score of 4, 3, 2, and 1, respectively. **Figure 20 (k)** displays the drought hazard levels map for landuse over Kampong Speu Province.

Figure 20 (l) illustrates the drought hazard levels map for drainage density parameter over the study area. The drainage density of an area substantially affects the hazard of drought. It was measured that a specific area with great drainage density has more water contact areas as compared to an area with no drainage. Thus, the region with great drainage density is less prone to drought hazards due to having increased water contact in comparison with areas with low drainage density (Hoque et al., 2020; Jose et al., 2016; Pandey et al., 2012). The highest drainage density was therefore assigned the value of 1 and followed by the following classes as the given value of 2, 3, 4, and 5, respectively.

Table 18 Sensitivity score of drought hazard indicators

Parameter	Class	Score	Weight
Dry season monthly average rainfall (mm)	43.76 - 46.15	5	0.33
	46.15 - 48.38	4	
	48.38 - 51.18	3	
	51.18 - 53.88	2	
	53.88 - 56.99	1	
Rainy season monthly average rainfall (mm)	187.16 - 202.30	5	0.33
	202.30 - 219.00	4	
	219.00 - 234.14	3	
	234.14 - 246.81	2	
	246.81 - 265.97	1	
Dry season average temperature (°C)	27.45 - 27.61	1	0.17
	27.61 - 27.83	2	
	27.83 - 28.16	3	
	28.16 - 28.45	4	
	28.45 - 28.83	5	
Rainy season average temperature (°C)	26.71 - 26.82	1	0.17
	26.82 - 26.97	2	
	26.97 - 27.20	3	
	27.20 - 27.40	4	
	27.40 - 27.64	5	
Dry season maximum temperature (°C)	32.32 - 32.63	1	0.07
	32.63 - 32.92	2	
	32.92 - 33.36	3	
	33.36 - 33.73	4	
	33.73 - 34.25	5	

Parameter	Class	Score	Weight
Rainy season maximum temperature (°C)	29.61 - 29.84	1	0.07
	29.84 - 30.06	2	
	30.06 - 30.37	3	
	30.37 - 30.62	4	
	30.62 - 30.99	5	
Dry season relative humidity (%)	62.58 - 64.66	5	0.09
	64.66 - 66.26	4	
	66.26 - 67.58	3	
	67.58 - 68.96	2	
	68.996 - 70.75	1	
Rainy season relative humidity (%)	82.81 - 83.79	5	0.09
	83.79 - 84.57	4	
	84.57 - 85.25	3	
	85.25 - 86.03	2	
	86.03 - 87.04	1	
Soil types	Acid lithosols	5	0.03
	Alluvial lithosols	5	
	Lacustrine alluvial	5	
	Plinthite podzols	4	
	Red-yellow podzols	3	
	Cultural hydromorphics	2	
	Grey hydromorphics	2	
	Planosols	1	
Slope (degree)	0 – 5	1	0.02
	5 – 10	2	
	10 – 15	3	
	15 – 25	4	
	25 – 65.5	5	
Drainage density (km^{-1})	0.36 - 1.74	5	0.24
	1.74 - 2.42	4	
	2.42 - 2.99	3	
	2.99 - 3.62	2	
	3.62 - 4.86	1	
Landuse	Agriculture	5	0.04
	Built-up	4	
	Forest	3	
	Bare soil	2	
	Water	1	

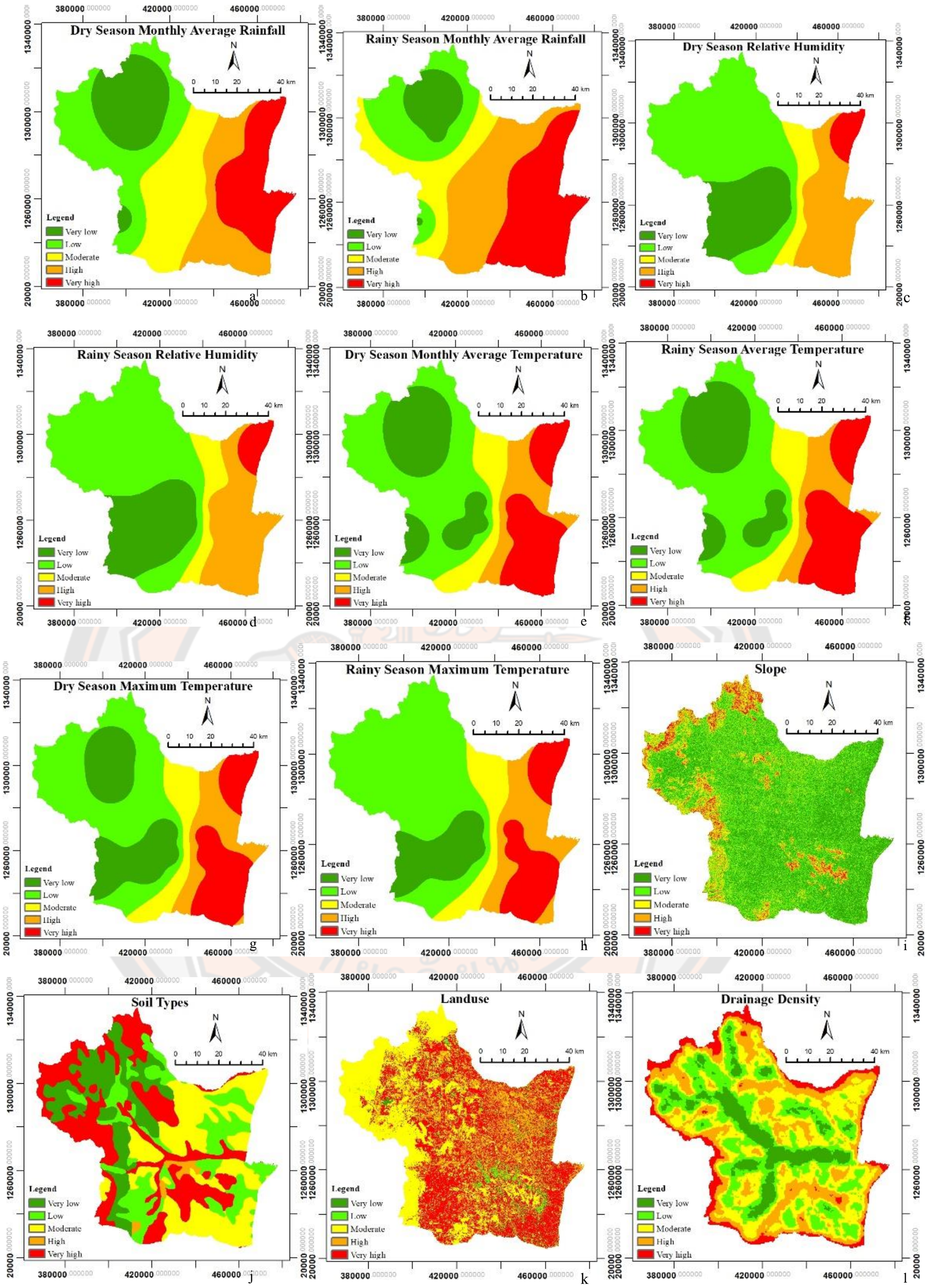

Figure 20 Drought hazard levels for each parameter (a) dry season rainfall, (b) rainy seasonal rainfall, (c) dry season humidity, (d) rainy season humidity, (e) dry season average temperature, (f) rainy season average temperature, (g) dry season maximum temperature, (h) rainy season maximum temperature, (i) slope, (j) soil types, (k) landuse, and (l) drainage density over Kampong Speu Province

3.2 Analytical Hierarchy Process for Drought Hazard

Tables 19 and 20 present the pairwise and normalized pairwise comparison matrix for drought hazard assessment. There are eight criteria of drought hazard assessment such as rainfall, relative humidity, average temperature, maximum temperature, slope, soil types, landuse, and drainage density. The important scale of each criterion (**Table 19**) was given based on the previous studies and literature review (Jain et al., 2014; Palchaudhuri, & Biswas, 2016; Pandey et al., 2012). Rainfall is the most affected parameter while the slope is the least affected parameter to drought hazard compared to other parameters. Rainfall is extremely important than slope and demonstrated important than maximum temperature, soil types, and landuse. It is also strongly important than relative humidity and moderated important than drainage density and slightly important than monthly temperature. Furthermore, relative humidity is strongly important than slope, and it is moderated important than maximum temperature, soil types, and landuse. Additionally, the average temperature is demonstrated important than slope and strongly important than soil type and landuse. It is also moderated plus important than maximum temperature and moderated important than relative humidity. Likewise, the maximum temperature is strongly important than slope whereas it is moderated important than soil type and landuse. Soil type is slightly important than slope. Landuse is slightly important than slope and soil types. Finally, drainage density is extremely important than slope, soil types, and landuse, and it is moderated important than relative humidity, average temperature, and maximum temperature.

Table 20 illustrates that rainfall has the maximum weight with the value of 0.33 whereas drainage density's weight is 0.24. It means that rainfall is the most significant parameter then following by drainage density. Then average temperature's weight is 0.17 and following by relative humidity, maximum temperature, landuse, soil types, and slope with the weights of 0.9, 0.7, 0.4, 0.3, and 0.2, respectively. The slope is the least important parameter in the drought hazard assessment.

3.2.1 Consistency Check

The CR is the relation of the Consistency Index (CI) and the Random Index (RI). It is conveyed mathematically using **Equation 4**. The CI can be found by using **Equation 5**. The acceptable CR must be < 0.1. The λ_{max} is 8.64.

$$CI = \frac{(\lambda max - n)}{n-1} \tag{5}$$

CI = (8.64 - 8) / (8 - 1) = 0.09

$$CR = \frac{CI}{RI} \tag{4}$$

CR = 0.09 / 1.41 = 0.06 < 0.1

The pairwise comparison matrix of drought hazard is therefore consistent with the value of the Consistency Ratio (CR) equal to 0.06, which is minor than 0.1.

Table 19 Pairwise comparison matrix for drought hazard assessment

Criteria	Rainfall	Relative humidity	Average temperature	Max. temperature	Slope	Soil types	Landuse	Drainage density
Rainfall	1.00	5.00	2.00	7.00	9.00	7.00	7.00	3.00
Relative humidity	0.20	1.00	0.33	3.00	5.00	3.00	3.00	0.33
Average temperature	0.50	3.00	1.00	4.00	7.00	5.00	5.00	0.33
Max. temperature	0.14	0.33	0.25	1.00	5.00	3.00	3.00	0.33
Slope	0.13	0.20	0.14	0.20	1.00	0.50	0.50	0.11
Soil types	0.17	0.33	0.20	0.33	2.00	1.00	0.50	0.11
Landuse	0.17	0.33	0.20	0.33	2.00	2.00	1.00	0.11
Drainage density	0.33	3.00	3.00	3.00	9.00	9.00	9.00	1.00
Total	2.63	13.20	7.13	18.87	40.00	30.50	29.00	5.33

Table 20 Normalized pairwise comparison matrix for drought hazard assessment

Criteria	Rainfall	Relative humidity	Average temperature	Max. temperature	Slope	Soil types	Landuse	Drainage density	Weight
Rainfall	0.38	0.38	0.28	0.37	0.23	0.23	0.24	0.56	**0.33**
Relative humidity	0.08	0.08	0.05	0.16	0.13	0.10	0.10	0.06	**0.09**
Aver. temperature	0.19	0.23	0.14	0.21	0.18	0.16	0.17	0.06	**0.17**
Max. temperature	0.05	0.03	0.04	0.05	0.13	0.10	0.10	0.06	**0.07**

Criteria	Rainfall	Relative humidity	Average temperature	Max. temperature	Slope	Soil types	Landuse	Drainage density	Weight
Slope	0.05	0.02	0.02	0.01	0.03	0.02	0.02	0.02	**0.02**
Soil types	0.06	0.03	0.03	0.02	0.05	0.03	0.02	0.02	**0.03**
Landuse	0.06	0.03	0.03	0.02	0.05	0.07	0.03	0.02	**0.04**
Drainage density	0.13	0.23	0.42	0.16	0.23	0.30	0.31	0.19	**0.24**

3.2.2 Drought Hazard Maps

Since the study was divided into two seasons, the drought hazard was separated into two parts, which are rainy and dry seasonal drought hazard. **Figure 21** presents the rainy seasonal drought hazard map over Kampong Speu Province. The results reveal that Kampong Speu Province is located in the very low, low, moderate, high, and very high rainy seasonal drought hazard spatial distribution with 16%, 30%, 20%, 18%, and 16% of the total areas, respectively, as presented in **Figure 22 (a)**.

Figure 22 (b) illustrates that the specific areas prone to very high rainy seasonal drought hazards are particularly located in Basedth, Kong Pisei, Odongk, and Samraong Tong Districts. The four earlier districts are found in very high hazard areas with 4.30%, 4.28%, 4.08%, and 2.62% of the total areas, respectively. Approximately 4.65%, 3.16%, 3.02%, 2.78%, 1.76%, 1.12%, and 1.10% of the total areas in Samraong Tong, Phnum Srouch, Basedth, Odongk, Thpong, Chbar Mon, and Kong Pisei Districts respectively are identified in high rainy seasonal drought hazard (**Table 21**). Aoral District is however not found in a very high and high rainy seasonal drought hazard. Most of Aoral District is situated in the very low and low drought hazard.

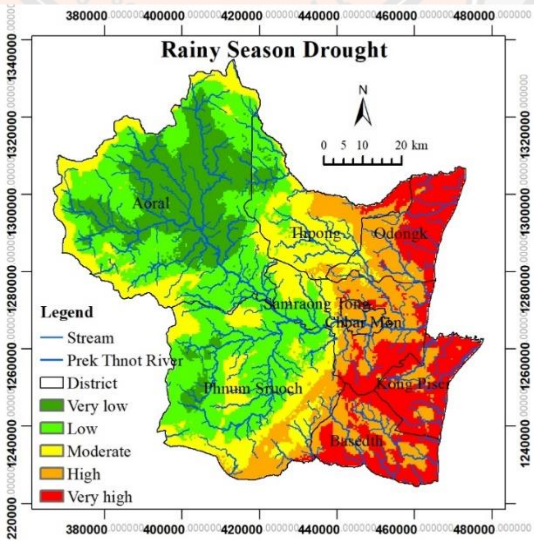

Figure 21 Rainy seasonal drought hazard map over Kampong Speu Province

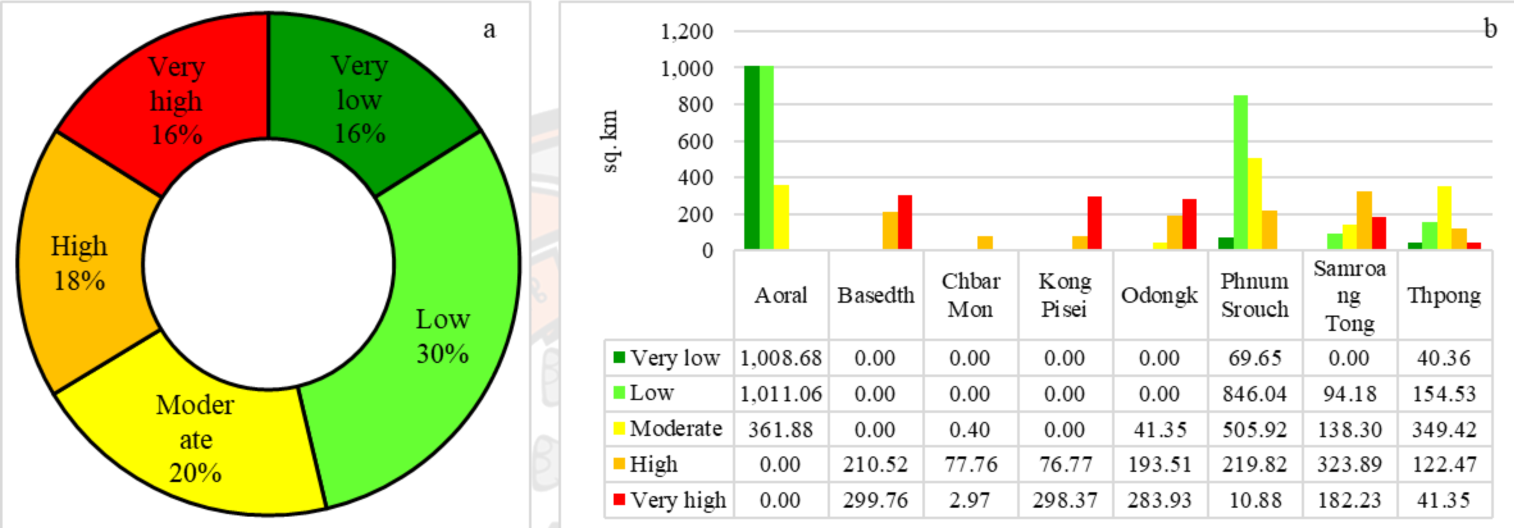

Figure 22 Rainy seasonal drought hazard (a) the percentage of hazard level and (b) drought hazard in each district

Table 21 Areas and percentages of rainy seasonal drought hazard over Kampong Speu Province

	Very low		**Low**		**Moderate**		**High**		**Very high**	
District	Area (km^2)	Area (%)	Area (km^2)	Area (%)	Area (km^2)	Area (%)	Area (km^2)	Area (%)	Area (km^2)	Area (%)
Aoral	1,008.68	14.48	1,011.06	14.51	361.88	5.19	0.00	0.00	0.00	0.00
Basedth	0.00	0.00	0.00	0.00	0.00	0.00	210.52	3.02	299.76	4.30
Chbar Mon	0.00	0.00	0.00	0.00	0.40	0.01	77.76	1.12	2.97	0.04

	Very low		Low		Moderate		High		Very high	
Kong Pisei	0.00	0.00	0.00	0.00	0.00	0.00	76.77	1.10	298.37	4.28
Odongk	0.00	0.00	0.00	0.00	41.35	0.59	193.51	2.78	283.93	4.08
Phnum Srouch	69.65	1.00	846.04	12.15	505.92	7.26	219.82	3.16	10.88	0.16
Samroang Tong	0.00	0.00	94.18	1.35	138.30	1.99	323.89	4.65	182.23	2.62
Thpong	40.36	0.58	154.53	2.22	349.42	5.02	122.47	1.76	41.35	0.59
Total	**1,118.69**	**16.06**	**2,105.81**	**30.23**	**1,397.28**	**20.06**	**1,224.74**	**17.58**	**1,119.48**	**16.07**

Kampong Speu Province is classified into five hazard classes, as presented in **Figure 23**. The results identify that Kampong Speu Province is located to very low, low, moderate, high, and very high with 17%, 28%, 22%, 19%, and 14% of the total areas, respectively, as presented in **Figure 24 (a)**.

Figure 24 (b) demonstrates that the specific areas in Kampong Speu Province are identified in very high hazard spatial distribution to dry seasonal drought, particularly Odongk, Kong Pisei, Samraong Tong, Basedth, and Thpong Districts. These seven districts are found in the very high hazard areas with approximately 4.26%, 4.21%, 2.72%, 1.76%, and 0.7% of the total areas, respectively. About 5.53%, 4.60%, 2.83%, 2.28%, 1.79%, 1.18%, and 1.12 of the total areas located in Basedth, Samraong Tong, Odongk, Phnum Srouch, Thpong, Kong Pisei, and Chbar Mon Districts respectively are found in high drought hazard (**Table 24**). Moreover, Aoral District is not found in a very high and high drought hazard whereas Phnum Srouch District is not situated in a very high dry seasonal drought hazard. The hazard zones are therefore found in the southeast, east, and northeast parts of the province.

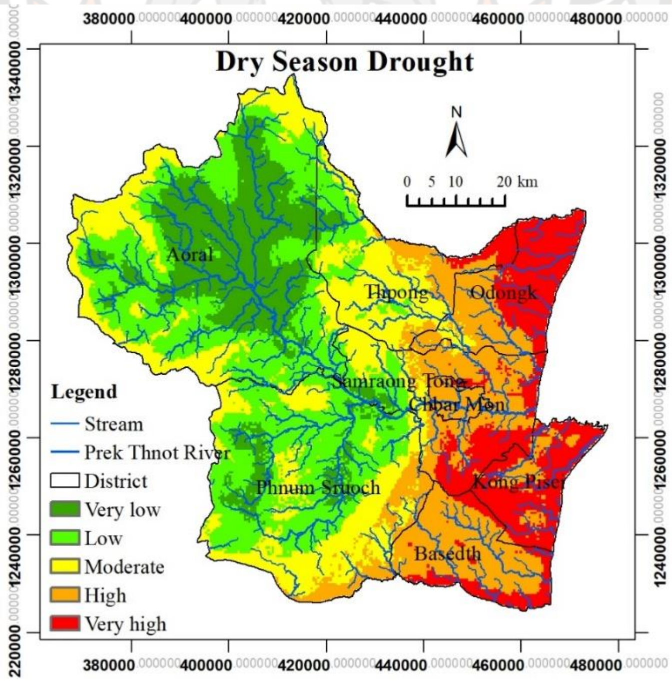

Figure 23 Dry seasonal drought hazard map over Kampong Speu Province

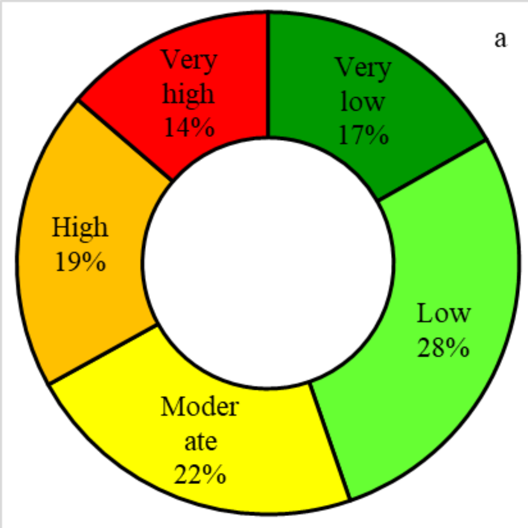

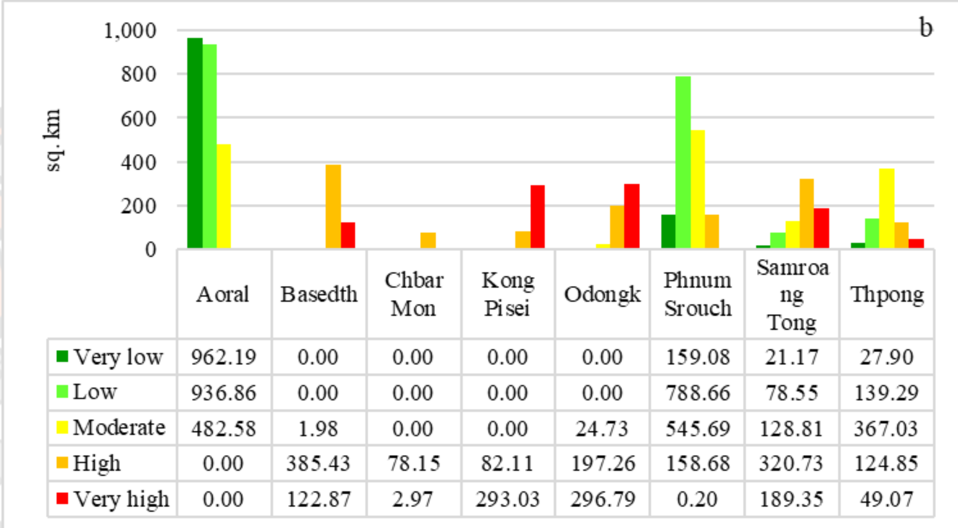

Figure 24 Dry seasonal drought hazard (a) the percentage of hazard level and (b) drought hazard in each district

Table 22 Areas and percentages of dry seasonal drought hazard over Kampong Speu Province

	Very low		**Low**		**Moderate**		**High**		**Very high**	
District	Area (km^2)	Area (%)	Area (km^2)	Area (%)	Area (km^2)	Area (%)	Area (km^2)	Area (%)	Area (km^2)	Area (%)
Aoral	962.19	13.81	936.86	13.45	482.58	6.93	0.00	0.00	0.00	0.00
Basedth	0.00	0.00	0.00	0.00	1.98	0.03	385.43	5.53	122.87	1.76
Chbar Mon	0.00	0.00	0.00	0.00	0.00	0.00	78.15	1.12	2.97	0.04

	Very low		Low		Moderate		High		Very high	
Kong Pisei	0.00	0.00	0.00	0.00	0.00	0.00	82.11	1.18	293.03	4.21
Odongk	0.00	0.00	0.00	0.00	24.73	0.36	197.26	2.83	296.79	4.26
Phnum Srouch	159.08	2.28	788.66	11.32	545.69	7.83	158.68	2.28	0.20	0.00
Samroang Tong	21.17	0.30	78.55	1.13	128.81	1.85	320.73	4.60	189.35	2.72
Thpong	27.90	0.40	139.29	2.00	367.03	5.27	124.85	1.79	49.07	0.70
Total	**1,170.33**	**16.80**	**1,943.37**	**27.90**	**1,550.81**	**22.26**	**1,347.22**	**19.34**	**954.27**	**13.70**

4. Bi-Hazard

4.1 Sensitivity Score of Each Parameter

The bi-hazard indicators were ranked into five different classes as flash flood and drought hazard. The score of each category was depended on the flash flood and drought data loss from the National Committee for Disaster Management (NCDM) (CamDi, 2020). The criteria Weight Arithmetic Mean (WAM) was used to calculate the aggregate value of the disaster loss from 2000 to 2019. The higher value means the higher loss. **Figure 25** shows the weighted arithmetic mean of the disaster loss to floods and droughts in Kampong Speu Province from 2000 to 2019. The floods occurred more frequently than droughts, and their effects contributed to greater loss.

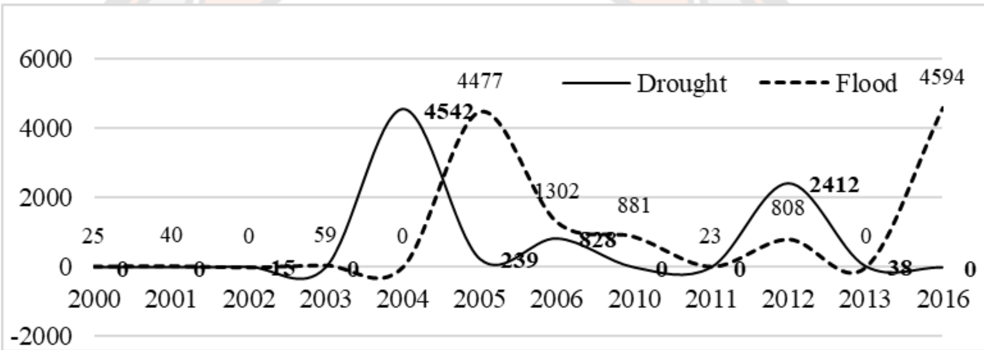

Figure 25 WAM of disaster loss in Kampong Speu Province

According to CamDi (2013), both flash flood and river flood normally starts from August to November whereas drought occurs in July and August. However, the disaster data loss (CamDi, 2020) in Kampong Speu Province obtained from the NCDM (2000-2019) illustrates that damages of floods started from July to December while droughts took place in February, June-August, November, and December (**Figure 26**). It means that floods mostly happened in the rainy season (May-November), and it sometimes took place in the early dry season (December). Likewise, droughts came in both rainy season (June-August and November) and dry season (February and December).

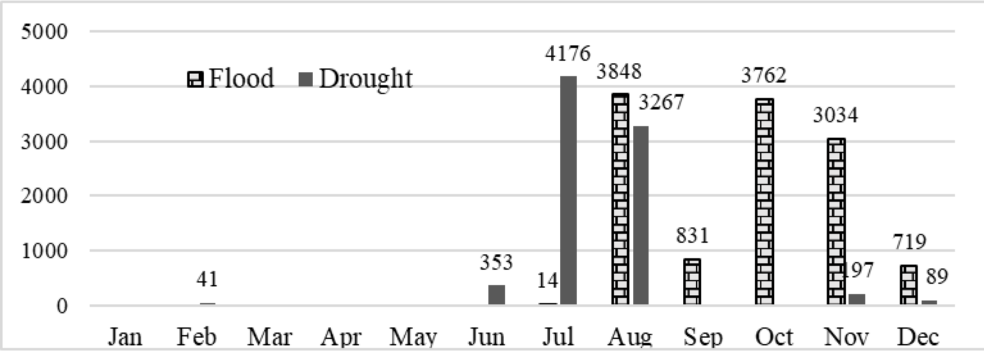

Figure 26 Temporal occurrence and WAM scores of floods and drought in Kampong Speu Province

4.2 Analytical Hierarchy Process for Bi-hazard Assessment

The weight of each criterion was described once they were ranked according to their comparative significance. A pairwise comparison matrix holding all criteria was therefore created to enable a significant comparison. **Tables 25 and 26** show the pairwise and normalized comparison matrix for bi-hazard assessment, respectively. The important scale of each criterion was given in the pairwise comparison matrix (**Table 25)**.

Rainy seasonal flash flood hazard is the most significant hazard in Kampong Speu Province compared to other hazards. It is much-demonstrated importance than dry seasonal flash flood hazard, moderated plus important than dry seasonal drought hazard, and moderated important than rainy seasonal drought hazard. Dry seasonal drought hazard is moderated important than dry seasonal flash flood hazard. Moreover, rainy seasonal drought hazard is strongly plus important than dry seasonal flash flood hazard and moderated important than dry seasonal drought hazard. **Table 26** shows that rainfall seasonal flash flood is the most significant hazard in Kampong Speu Province with a weight of 0.54. Furthermore, the rainy seasonal drought hazard also has an essential effect on bi-hazard with the value of 0.28 while dry seasonal drought hazard and dry seasonal flash flood hazard have the weighted value of 0.12 and 0.06, correspondingly.

Table 23 Pairwise comparison matrix for bi-hazard assessment

Criteria	Dry season flash floods	Rainy season flash floods	Dry season droughts	Rainy season droughts
Dry season flash floods	1.00	0.14	0.33	0.17
Rainy season flash floods	7.00	1.00	4.00	3.00
Dry season droughts	3.00	0.20	1.00	0.33
Rainy season droughts	6.00	0.33	3.00	1.00
Total	**17.00**	**1.68**	**8.33**	**4.50**

Table 24 Normalized pairwise comparison matrix for bi-hazard assessment

Criteria	Dry season flash floods	Rainy season flash floods	Dry season droughts	Rainy season droughts	Weight
Dry season flash floods	0.06	0.09	0.04	0.04	0.06
Rainy season flash floods	0.41	0.60	0.48	0.67	0.54
Dry season droughts	0.18	0.12	0.12	0.07	0.12
Rainy season droughts	0.35	0.20	0.36	0.22	0.28

4.3 Consistency Check

The CR is the relation of the Consistency Index (CI) and the Random Index (RI). It is expressed mathematically using **Equation 4**. The CI can be found by using **Equation 5**. The acceptable CR must be < 0.1. The λ_{max} is 4.07.

$$CI = (4.07 - 4) / (4 - 1) = 0.2$$

$$CR = 0.02 / 0.9 = 0.02 < 0.1$$

The pairwise comparison matrix of bi-hazard is accordingly consistent with the value of Consistency Ratio (CR) equal to 0.02, which is minor than 0.1.

4.4 Bi-Hazard Maps

The statistical distribution analysis was used to categorize the final map into five different classes, namely very low, low, moderate, high, and very high to show the bi-hazard of the study area clearly (**Figure 27**). Kampong Speu Province is located in the very low, low, moderate, high, and very high to bi-hazard with 12%, 31%, 24%, 30%, and 3% of the total areas, respectively, as presented in **Figure 28 (a)**. The specific areas in Kampong Speu Province located in the very high spatial distribution of bi-hazard predominantly are in all districts. Thpong and Aoral Districts however are found in very high hazard more than other districts with approximately 0.93% and 0.78% of the total areas, respectively, as shown in **Figure 28 (b)**.

About 13.80%, 3.39%, 3.32%, 2.56%, 2.34%, 2.31%, 2.30%, 2.04%, and 0.65% of Aoral, Phnum Srouch, Odongk, Samroang Tong, Thpong, Kong Pisei, Basedth Districts, and Chbar Mon Municipality respectively are identified in high bi-hazard areas (**Table 27**). Furthermore, Phnum Srouch and Aoral Districts are located in the very low bi-hazard area with 5.46% and 3.75% of the total areas, respectively.

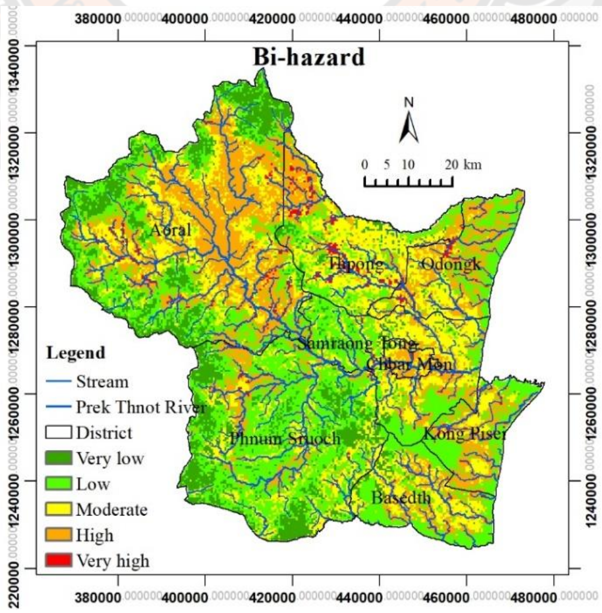

Figure 27 Bi-hazard map over Kampong Province

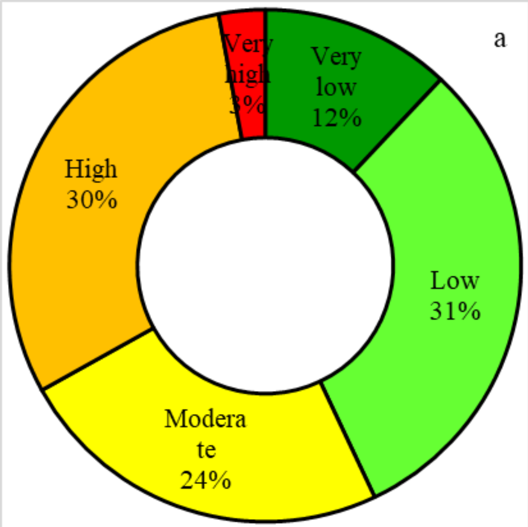

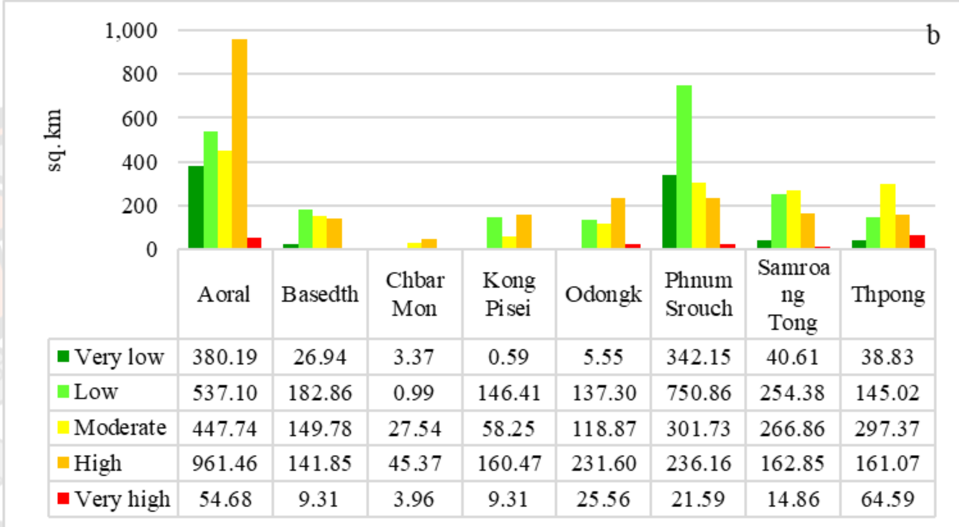

Figure 28 Bi-hazard (a) the percentage of Bi-hazard level and (b) Bi-hazard in each district

Table 25 Areas and percentages of Bi-hazard over Kampong Speu Province

	Very low		**Low**		**Moderate**		**High**		**Very high**	
District	Area (km^2)	Area (%)	Area (km^2)	Area (%)	Area (km^2)	Area (%)	Area (km^2)	Area (%)	Area (km^2)	Area (%)
Aoral	380.19	5.46	537.10	7.71	447.74	6.43	961.46	13.80	54.68	0.78
Basedth	26.94	0.39	182.86	2.63	149.78	2.15	141.85	2.04	9.31	0.13
Chbar Mon	3.37	0.05	0.99	0.01	27.54	0.40	45.37	0.65	3.96	0.06

	Very low		Low		Moderate		High		Very high	
Kong Pisei	0.59	0.01	146.41	2.10	58.25	0.84	160.47	2.30	9.31	0.13
Odongk	5.55	0.08	137.30	1.97	118.87	1.71	231.60	3.32	25.56	0.37
Phnum Srouch	342.15	4.91	750.86	10.78	301.73	4.33	236.16	3.39	21.59	0.31
Samroang Tong	40.61	0.58	254.38	3.65	266.86	3.83	162.85	2.34	14.86	0.21
Thpong	38.83	0.56	145.02	2.08	297.37	4.27	161.07	2.31	64.59	0.93
Total	**838.23**	**12.03**	**2,154.92**	**30.93**	**1,668.15**	**23.95**	**2,100.84**	**30.16**	**203.86**	**2.93**

Discussion

The integrated AHP-GIS analysis was used to estimate the spatial distribution of flash flood hazard, drought hazard, and bi-hazard in Kampong Speu Province. Ten influent parameters were taken into account for mapping flash flood hazard areas whereas eight factors were used for identifying drought hazards. The AHP approach was applied to obtain all parameters' weights. The outcomes are the potential seasonal flash flood hazard, drought hazard, and bi-hazard (Combination of flash flood and drought hazard).

The study reveals that rainfall is the most common parameter that contributes to flash flood occurrences with a weight of 0.30 whereas drainage density and slope are following with the weight of 0.18 and 0.15, respectively. Similarly, rainfall is recognized as the most affected hazard parameter to flash floods in the study (Mohamed, 2019). Drainage density and slope are also considered as the main contributors to flood after the rainfall as seen in the study of Seejata et al. (2018). It illustrates that the areas that receive higher rainfall might be located in high flash flood hazard levels. The areas located close to drainage density and have a lower slope could be more prone to flash flood hazards. The most significant reasons that are accountable for flash flood incidences at the lower reaches are the geomorphic topography of the drainage network. Besides, heavy rainfall, on steeply and bare cultivated land, impacts the water runoff volume and increases the flash flood hazard downstream (Woodward, 2009). Several flash floods occurrences are triggered by heavy rainfall upstream of the study areas (CFE-DM, 2017). The very high flash flood hazard areas in the rainy season and dry season are found in Aoral District (Northwest part) and the areas along the Stung Prek Thnot River, which is located in Phnum Srouch, Thpong, and Samroang Tong Districts, as shown in **Figures 16 and 18**. Those areas considerably receive more rainfall compared to other regions and located near the drainage density and flat in slope. During the heavy rainfall, the water flows from the mountainous areas located in the west to downstream crossed Kandal Province to Bassac River. The flash floods are caused along the river. Moreover, the water flows from the upstream rapidly fast and at high velocity since the gravity of the steepness produces rapid runoff. Thus, the rating scores over the northwest part and along the river are increasingly contributing to the weighting factor in the flood hazard index. It could be seen from **Tables 16 and 17** that approximately 710.05 km^2 or 10.19% of the total areas are identified in very high hazard to rainy seasonal flash flood (May to October) and 1,065.87 km^2 or 15.30% of the total areas are found in very high hazard to dry seasonal flash flood (November to April). The location of a very high hazard level to dry seasonal flash floods in Phnum Srouch District increases from 0.28% to 1.48% of the total areas due to high rainfall in that area compared to other areas during the dry season. Generally, the flash flood occurs during the rainy season. However, the flash flood could occur in the abnormal condition of rainfall during the dry season.

Kampong Speu Province was hit by floods many times (CamDi 2020). Samraong Tong, Basedth, Kong Pisei, and Aoral Districts are frequently affected by floods. For example, Aoral District was the most affected district, which directly affected 3,325 people during the floods in 2005. A person was dead, and 17 cattle were lost during the floods. Chbar Mon Municipality located in the high and moderate levels of flash flood hazard was however not seriously affected by the floods. During the floods in 2016, only 60 ha of crops were damaged by the floods. The adaptation capacity of Chbar Mon Municipality is, therefore, better than other districts. Although the flash flood hazard map developed here presents the same districts as the historical flood loss data, the flash flood hazard levels compared to the historical data are found to some difference due to several reasons. Firstly, the inappropriate data used might affect the flash flood hazard assessment. The adding and crossing of various data used in GIS is one of the reasons that caused the bias throughout the estimation of flash flood hazard (Danumah et al. 2016). The resolution of Landsat and DEM could not be well presented the physical characteristics of the flash flood hazard areas. Moreover, the rainfall distribution in the current study might be bias due to the use of satellite-based rainfall instead of observed rainfall. Secondly, the efficiency of the AHP analysis is one of the factors that influenced the hazard assessment. The weighting process could be unappropriated through the pairwise comparison to define each parameter's weight (Seejata et al. 2018). Accordingly, the weighting process might need to subordinate with the experts' opinions in the field of hydrology and disaster management rather than focusing on the literature only (Koem, & Tantanee, 2020). Lastly, flash flood risk assessment is associated with the various aspects of hazard, vulnerability, and coping capacity (Danumah et al. 2016; Skilodimou et al. 2019). Flash flood risk assessment is therefore required to take into account. The integrated AHP-GIS analysis over Kampong Speu Province could solve the complex problems of multi-criteria and produce a significant flash flood hazard map classified into five classes. AHP and GIS analysis have been used in many countries, particularly in neighboring countries like Thailand (Seejata et al. 2018) and Vietnam (Luu et al. 2017). The integrated AHP-GIS analysis simplifies a multi-criteria combination, which provides the actual benefits of an understanding of each parameter contributed to the flash flood, assessment crossing among parameters, and an efficient approach to develop the flash flood hazard map. However, the pairwise comparisons could present some failures due to the subjective judgment of the weighting. The normalization is therefore significant for minimizing the uncertainty of the weights. This uncertainty can be lessened by checking the Consistency Ratio (CR) of the decision.

The drought hazard is affected by rainfall with the represented weighted value of 0.33. Then it is followed by the drainage density and average monthly temperature with a weight of 0.24 and 0.17, respectively. The areas receive less rainfall than usual; there is more chance of drought occurrences (Pandey et al., 2012). The areas located far from the drainage density have more chance to experience droughts (Jose et al., 2016). Likewise, the monthly average temperature is one of the most influential parameters of the drought hazard assessment. The higher average temperature could cause a drought (Hoque et al., 2020). The study found that Kampong Speu Province was particularly covered by moderate, high, and very high hazards in both rainy and dry seasonal droughts. According to CFE-DM (2017), Kampong Speu Province was hit by droughts several times and caused diverse impacts. Based on the estimated result, most drought hazard zones are in the northeast, north, and southeast parts, which are located in the drown streams, as presented in **Figures 21 and 23**. **Tables 18 and 19** show that about 1,119.48 km^2 (16.07% of the total areas) are found in the very hazard to rainy seasonal drought (May to October) and 954.27 km^2 (13.70% of the total areas) are identified in very hazard to dry seasonal drought (November to April). The areas of very high hazard are located in the northeast, east, and southeast parts of Kampong Speu Province. The very high drought hazard areas during the dry season seem to decrease in Basedth District compared with the rainy seasonal drought hazard areas

(4.3% to 1.76% of the total areas). During the dry season, the rainfall in Basedth District is increasing compared with the other areas.

According to CFE-DM (2017), Kampong Speu Province was affected by droughts several times, particularly during El Niño in 2015-2016, which caused a severe impact. The northeast, east, and southeast parts of Kampong Speu are mostly covered by built-up and agriculture. These areas as well receive less rainfall and high temperature; therefore, these areas fell in the very high drought hazard zones. The result reveals that Chbar Mon Municipality is located in the high drought hazard zones; however, the historical data (CamDi, 2020) demonstrates that Chbar Mon municipality was unaffected by droughts. It could be due to the facilities existing there better than others do. Nguyen et al. (2009) mentioned that the high vulnerability of drought in Cambodia depends on the high poverty level and high dependency on agriculture level. The lack of food security, power supply, irrigation facilities, and low productivities add more vulnerability to drought. Moreover, the level of drought hazard spatial distribution compare to the drought historical data loss is a bit different although the areas prone to drought in both AHP and historical data are found in the same districts. This might be biased due to the weighted values of each parameter (Seejata et al., 2018), which could have huge effects on the developed hazard map. Additionally, the satellite-based climatological data might be bias (Bhart, & Singh, 2015) since the ground observed data were not used. The drought hazard study is just one component of the drought risk assessment. The further study, therefore, should take into account the drought risk assessment by using the AHP method, which as well as associate with the experts' opinions rather than focusing on literature review only. Besides, the use of observed climatological data should be considered.

Even though the single hazard map is significant in the initial stage of disaster management, they might ultimately complicate the people working in the analysis if they need to deal with a great amount of hazard maps with various data and diverse area covering and resolution (Skilodimou et al., 2019). The bi-hazard map however reinforces the disaster managers or stakeholders to the application of sustainable development by offering standardized data about the various hazards for a precise location. The current study develops a bi-hazard map that contributes to the recognition of appropriate locations for sustainable development by assessing the comparative significance between two single hazards by using the integrated AHP-GIS analysis. The study highlights the possible hazard by allocating Kampong Speu Province into five different classes starting from very low to very high hazard. The study found that 203.86 km^2 or 2.93% of the total areas are found as very high to bi-hazard, as shown in **Table 27**. The hazard patch is situated in the northwest, northeast, east, and southeast parts of Kampong Speu Province (**Figure 27**). In the bi-hazard map, most of the study areas are located in high hazard zones (30% of the total areas). A Bi-hazard map cannot express the level of every single hazard, but it can express which areas are prone to both flash floods and droughts during the rainy and dry seasons.

This study therefore could be beneficial for mitigation of the negative influence of flash floods and drought hazards. Likewise, the practical confirmation methods, which also consider historical data can lead to the calculation of the modified flood and drought hazard index and support the analysis. If the flash flood and drought hazards have shown the significance of tributaries and rivulets in the flash flood and drought events, it is necessary demonstrated to be comprised of flash flood and drought mitigation plans. From the consequential results, it illustrates that the suggested methodology differentiates the comparative degree of hazard to flash flood hazard, drought hazard, and bi-hazard over Kampong Speu Province.

CHAPTER V

CONCLUSION

Conclusion

The purpose of the current study is to assess the seasonal spatial distribution of flash flood and drought hazard areas using the AHP approach and GIS techniques in Kampong Speu Province, Cambodia. The AHP approach was applied to evaluate the weights of each influence parameter then they were categorized into five classes such as very low, low, moderate, high, and very high. GIS techniques provided an appropriate outline for incorporating and examining the ten parameters of flash flood hazard, eight parameters of drought hazard, and four parameters of bi-hazard. It finally helped to produce the flash flood hazard, drought hazard, and bi-hazard maps by integrating the weights and ratings for the study area.

The first objective is to assess and map the spatial distribution of seasonal flash flood hazard areas. The very high and high levels of flash flood hazard are found in the northwest part (Aoral District) and areas along Stung Prek Thnot River and the stream located Thpong, Phnum Srouch, and Samroang Tong Districts. The areas prone to very high and high rainy seasonal flash floods are 710.05 km^2 (10.19% of the total areas) and 1,265.77 km^2 (18.17% of the total areas), respectively. Furthermore, the areas situated in very high and high hazard to dry seasonal flash flood are 1,065.87 km^2 (15.30% of the total areas) and 1,284.59 km^2 (18.44% of the total areas), individually. Very high hazard areas are located in Aoral, Phnum Srouch, Thpong, and Samraong Tong Districts. These districts receive heavy rainfall and are located in the steepness areas, which affect the water runoff. Moreover, the very high areas are found along the river due to the great effects of drainage density. Very high flash flood hazard in the dry season seems to increase in Phnum Srouch District because this district receives more rainfall in the dry season comparing to other areas.

The second objective is to assess and map the spatial distribution of seasonal drought hazard areas. The very high hazard to droughts is mostly located in the northeast, north, and southeast parts of Kampong Speu Province, which are in the drown streams. These areas prone to very high rainy seasonal drought hazards and dry seasonal drought hazards are 1,119.48 km^2 or (16.07% of the total areas) and 954.27 km^2 (13.70% of the total areas), respectively. The study found that Samraong Tong, Phnum Srouch, Basedth, Odongk, Thpong, Chbar Mon, and Kong Pisei Districts are located in a very high drought hazard. Based on the historical data, Chbar Mon was not seriously affected by the droughts. This can be explained that Chbar Mon is a town, so the land is typically covered by the build-up. Moreover, the clean water system is better than in other districts. Furthermore, areas located in the very high hazard to bi-hazard are 203.86 km^2 (2.93% of the total areas). The districts located in the very high hazard more than others are Thpong and Aoral with the area of 64.59 km^2 (0.93% of the total areas) and 54.68 km^2 (0.78% of the total areas), respectively. These districts receive less rainfall, high temperature, located far from drainage density, and covered by built-up and agriculture. The very high rainfall in the dry seasonal drought hazard map decreases compared to the rainy seasonal drought hazard map in Basedth district in which this area receives more rainfall compared to others.

The last objective is to generate a bi-hazard map of flash floods and droughts. The areas prone to the very high hazard are mostly located in Thpong and Aoral district with areas of 64.59 km^2 (0.93% of the total areas) and 54.68 km^2 (0.78% of the total areas). The particular areas located at the high bi-hazard level are Aoral 961.46 km^2 (13.80% of the total areas), Phnum Srouch 236.16 km^2 (3.39% of the total areas), and Odongk Districts 231.60 km^2 (3.32% of the total areas). A Bi-hazard map can be used to provide the fair-based for distributing the disaster planning resources; encourage the practice of more effective, combined emergency preparedness, response, and recovery measures; and stimulate the establishment of cooperative agreement to comprise all interest and relevant groups or agency.

The consistency check was applied to assess the consistency of each matrix in the AHP method. The calculation shows the significance of the statistical distribution. Even the satellite information can be access through the internet, the MODIS satellite flood map cannot capture specific flash flood areas like Kampong Speu Province. Additionally, the comparison of the historical data and estimated hazard areas are satisfactory agreement even there are small gaps.

The integrated AHP-GIS analysis provides an overall idea of flash flood hazard, drought hazard, and bi-hazard associated with the province. The model is appropriate and valuable to identify flash flood and drought hazards. The proposed methodology therefore should be considered by the local authorities to implement strategies and policies for disaster mitigation and disaster risk reduction. The maps of flash flood hazard, drought hazard, and bi-hazard created a diversity of data and aid as an indicator of location deserving comprehensive disaster hazards and risk evaluation. The hazard maps can help decision-makers to visualize the flash flood and drought hazard and its levels to support stakeholders involved in agriculture and related fields with appropriate flash flood and drought mitigation measures. It also benefits in a flash flood and drought controlling to reduce the damages in extreme events. Furthermore, these consequential maps could assist as a guide for potential defensive measures, enhanced landuse development, as well as disaster risk management in climate change's impacts.

The disasters are the result of the complex relationship between natural systems and human activities. Several reasons and limitations therefore should be discussed in the study.

1. The current study only focused on the hazard analysis rather than risk assessment while the risk is the function of hazard, vulnerability, and coping capacity.

2. The weighting process of the AHP method may need hydrological experts rather than only reviewing the previous studies.

3. The DEM resolution adopted in the current study might not be well-presented with the physical features of the hazard areas.

4. Since the meteorological locations are poorly monitored and observed, which could limit the obtainability of various and continuous climatic data, satellite-based data were used. It therefore might cause some gaps.

Recommendation

The following recommendations indicate some perspective in further study:

1. Further studies should address the vulnerability, mitigation, and coping capacity at the local scale to support the disaster risk assessment since the risk is the consequence of the combination of hazard, vulnerability, and coping capacity.

2. The weighting process should be considered about the experts' opinion rather than focusing on the literature review only.

3. The very high hazard areas to both flash flood and drought hazard are required more detailed mapping by using high resolution of satellite images.

4. The updated observed climatic data at the stations should be used to enhance the accuracy of the assessment.

5. Similar factor weighting mechanisms such as the fuzzy method should be applied to develop a reliable model for comparison.

6. Due to the effectiveness and efficiency of the AHP method and GIS technique, it could be applied in other disaster assessments including landslide, wildfire, earthquake, etc.

The study also specifies some concepts for relevant stakeholder in the disaster management and disaster risk reduction agency as follows:

1. These presented methods should be used as the preliminary disaster assessment for National Committee for Disaster Management to use properly.

2. The bi-hazard map should be used to build and reinforce government organization settings composed of related stakeholders and stimulate funds in long-term innovation and technology development.

3. The authorities should consider constructing monitoring network stations for rainfall, flash flood, and drought.

4. Kampong Speu authorities should utilize the finding of the presented study as a contribution for enhanced planning in the purposed Community-based Early Warning System (CBEWS) to consequently lessen the losses and minimize the harms.

REFERENCES

REFERENCES

Aboelkhair, H., Morsy, M., & El Afandi, G. (2019). Assessment of agroclimatology NASA POWER reanalysis datasets for temperature types and relative humidity at 2 m against ground observations over Egypt. *Advances in Space Research*, *64*(1), 129-142. doi: https://doi.org/10.1016/j.asr.2019.03.032

Abu El-Magd, S. A., Amer, R. A., & Embaby, A. (2020). Multi-criteria decision-making for the analysis of flash floods: A case study of Awlad Toq-Sherq, Southeast Sohag, Egypt. *Journal of African Earth Sciences, 162,* 103709. doi: https://doi.org/10.1016/j.jafrearsci.2019.103709

ADPC. (2015). *Mainstreaming DRR & CCA into Development process at local level.* Bangkok, Thailand: Asian Disaster Preparedness Center.

Agarwal, C. S. (1998). Study of Drainage Pattern Through Aerial Data in Naugarh Area of Varanasi District, U.P. *Journal of the Indian Society of Remote Sensing*, *26*(4), 169-175.

An, L. H. (2014). *Country Report of Cambodia Disaster Management.* N.P.: n.p.

Baeza, C., Lantada, N., & Amorim, S. (2016). Statistical and spatial analysis of landslide susceptibility maps with different classification systems. *Environmental Earth Sciences, 75*(19). doi: https://doi.org/10.1007/s12665-016-6124-1

Bahremand, A., De Smedt, F., Corluy, J., Liu, Y. B., Poorova, J., Velcicka, L., & Kunikova, E. (2006). WetSpa Model Application for Assessing Reforestation Impacts on Floods in Margecany–Hornad Watershed, Slovakia. *Water Resources Management, 21*(8), 1373-1391. doi: https://doi.org/10.1007/s11269-006-9089-0

Bai, J., Chen, X., Dobermann, A., Yang, H., Cassman, K. G., & Zhang, F. (2010). Evaluation of NASA Satellite- and Model-Derived Weather Data for Simulation of Maize Yield Potential in China. *Agronomy Journal, 102*(1), 9-16. doi: https://doi.org/10.2134/agronj2009.0085

Bathrellos, G. D., Karymbalis, E., Skilodimou, H. D., Gaki-Papanastassiou, K., & Baltas, E. A. (2016). Urban flood hazard assessment in the basin of Athens Metropolitan city, Greece. *Environmental Earth Sciences, 75*(4). doi: https://doi.org/10.1007/s12665-015-5157-1

Blake, G. R., Steinhardt, G. C., Pombal, X. P., Muñoz, J. C. N., Cortizas, A. M., Arnold, R. W., Schaetzl, R. J., Stagnitti, F., Parlange, J. Y., Steenhuis, T. S., Chesworth, W., Mualem, Y., Morel-Seytoux, H. J., Spaargaren, O., Chesworth, W., Soon, Y. K., Orlov, D. S., & Spaargaren, O. (2008). Planosols. In W. Chesworth (Ed.). *Encyclopedia of Soil Science* (pp. 559-560). Dordrecht: Springer Netherlands.

Bojovic, N., & Milenkovic, M. (2008). The best rail fleet mix problem. *Operational Research*, *8*(1), 77-87. doi: https://doi.org/10.1007/s12351-008-0012-8

Bonacci, O., Ljubenkov, I., & Roje-Bonacci, T. (2006). Karst flash floods: an example from the Dinaric karst (Croatia). *Natural Hazards and Earth System Science, 6*(2), 195-203. doi: https://doi.org/10.5194/nhess-6-195-2006

Bradbury, C. G., & Rushton, K. R. (1998). Estimating runoff–recharge in the Southern Lincolnshire Limestone catchment, UK. *Journal of Hydrology, 211*, 86–99.

Breemen, N. V., & Buurman, P. (1998). *Hydromorphic Soils Soil Formation* (pp. 151-181). Dordrecht: Springer Netherlands.

Budimir, M., Atkinson, P., & Lewis, H. (2014). Earthquake-and-landslide events are associated with more fatalities than earthquakes alone. *Natural Hazards*, *72*(2), 895-914. doi: https://doi.org/10.1007/s11069-014-1044-4

Bukari, S. M., Ahmad, M. A., Wai, T. L., Kaamin, M., & Alimin, N. (2016). Spatial Analysis in Determination Of Flood Prone Areas Using Geographic Information System and Analytical Hierarchy Process at Sungai Sembrong's Catchment. *IOP Conference Series: Materials Science and Engineering*, *136,* 012039. doi: https://doi.org/10.1088/1757-899x/136/1/012039

Bush, C. E., & Cerveny, R. S. (2013). Diurnal and Seasonal Variations in Flash Floods Across the Western United States. *Journal of the Arizona-Nevada Academy of Science*, *44*(2), 143-152. doi: https://doi.org/49.231.30.229

Butler, D., Kokkalidou, A., & Makropoulos, C. K. (2006). *Supporting the Siting of New Urban Developments for Integrated Urban Water Resource Management* (pp. 19-34). N.P.: n.p. doi: https://doi.org/10.1007/1-4020-4685-53

CamDi. (2013). *Cambodia disaster loss and damage analysis report 1999-2013.* Phnon Penh: National Committee for Disaster Management and United Nation Development Programme.

CamDi. (2020). *Cambodia disaster damage & loss information system. from National Committee for Disaster Management (NCDM)*. Retrieved January 5, 2020, from http://camdi.ncdm.gov.kh/DesInventar/profiletab.jsp?countrycode=kh2&continue=y

CFE-DM. (2017). *Cambodia Disaster Management Handbook.* Phnom Penh: Center for Excellence in Disaster Management, & Humanitarian Assistance.

Dano, U. L. (2020). Flash Flood Impact Assessment in Jeddah City: An Analytic Hierarchy Process Approach. *Hydrology, 7*(1), 10. doi: https://doi.org/10.3390/hydrology7010010

Danumah, J. H., Odai, S. N., Saley, B. M., Szarzynski, J., Thiel, M., Kwaku, A., Kouame, F. K., & Akpa, L. Y. (2016). Flood risk assessment and mapping in Abidjan district using multi-criteria analysis (AHP) model and geoinformation techniques, (cote d'ivoire). *Geoenvironmental Disasters, 3*(1). doi: https://doi.org/10.1186/s40677-016-0044-y

Dawes, R. L. (2013). *Introduction to Physical Geology*. Washington, D.C.: Washington State Colleges.

Dogan, S., Berktay, A., & Singh, V. P. (2012). Comparison of multi-monthly rainfall-based drought severity indices, with application to semi-arid Konya closed basin, Turkey. *Journal of Hydrology, 470-471*, 255-268. doi: https://doi.org/10.1016/j.jhydrol.2012.09.003

Doswell, C. A. (2003). *Flooding.* United States of America: Elsevier Science

Duan, Z., Gao, H., & Tan, M. (2017). Extreme Precipitation and Floods: Monitoring, Modelling, and Forecasting. *Advances in Meteorology, 2017,* 1-3. doi:10.1155/2017/9350369

Duo, E., Trembanis, A. C., Dohner, S., Grottoli, E., & Ciavola, P. (2018). Local-scale post-event assessments with GPS and UAV-based quick-response surveys: a pilot case from the Emilia–Romagna (Italy) coast. *Natural Hazards and Earth System Sciences, 18*(11), 2969-2989. doi: https://doi.org/10.5194/nhess-18-2969-2018

El Morjani Zel, A., Ebener, S., Boos, J., Abdel Ghaffar, E., & Musani, A. (2007). Modelling the spatial distribution of five natural hazards in the context of the WHO/EMRO Atlas of Disaster Risk as a step towards the reduction of the health impact related to disasters. *Int J Health Geogr, 6,* 8. doi: https://doi.org/10.1186/1476-072X-6-8

Elkhrachy, I. (2015). Flash Flood Hazard Mapping Using Satellite Images and GIS Tools: A case study of Najran City, Kingdom of Saudi Arabia (KSA). *The Egyptian Journal of Remote Sensing and Space Science, 18*(2), 261-278. doi: https://doi.org/10.1016/j.ejrs.2015.06.007

Estoque, R. C., & Murayama, Y. (2010). Suitability Analysis for Beekeeping Sites in La Union, Philippines, Using GIS and Multi-Criteria Evaluation Techniques. *Research Journal of Applied Sciences, 5*(3), 242-253. doi: https://doi.org/10.3923/rjasci.2010.242.253

Forzieri, G., Feyen, L., Russo, S., Vousdoukas, M., Alfieri, L., Outten, S., Migliavacca, M., Bianchi, A., Rojas, R., & Cid, A. (2016). Multi-hazard assessment in Europe under climate change. *Climatic Change, 137*(1-2), 105-119. doi: https://doi.org/10.1007/s10584-016-1661-x

Ghosh, A., & Kar, S. K. (2018). Application of analytical hierarchy process (AHP) for flood risk assessment: A case study in Malda district of West Bengal, India. *Natural Hazards, 94*(1), 349-368. doi: https://doi.org/10.1007/s11069-018-3392-y

Gill, J. C., & Malamud, B. D. (2016). Hazard interactions and interaction networks (cascades) within multi-hazard methodologies. *Earth System Dynamics, 7*(3), 659-679. doi: https://doi.org/10.5194/esd-7-659-2016

Gocic, M., & Trajkovic, S. (2013). Analysis of precipitation and drought data in Serbia over the period 1980–2010. *Journal of Hydrology, 494,* 32-42. doi:https://doi.org/10.1016/j.jhydrol.2013.04.044

Hazarika, M. K., & Bormudoi, A. (2007). Flood Hazard Mapping in Four Provinces of Cambodia Under the Mekong River Basin. In *5th AMFF - Improving Inputs towards Medium Term Flood Forecasting and Warning in the Mekong Basin*. N.P.: n.p. doi: https://www.researchgate.net/publication/262270027

Hoque, M. A., Pradhan, B., & Ahmed, N. (2020). Assessing drought vulnerability using geospatial techniques in northwestern part of Bangladesh. *Sci Total Environ*, *705,* 135957. doi: https://doi.org/10.1016/j.scitotenv.2019.135957

Hoque, M. A., Tasfia, S., Ahmed, N., & Pradhan, B. (2019). Assessing Spatial Flood Vulnerability at Kalapara Upazila in Bangladesh Using an Analytic Hierarchy Process. *Sensors (Basel), 19*(6). doi: https://doi.org/10.3390/s19061302

IPCC. (2014). *Climate Change 2014: Impacts, Adaptation, and Vulnerability Part A: Global and Sectoral Aspects Working Group II Contribution to the Fifth Assessment Report of the IPCC*. Cambridge: Cambridge University Press.

Jain, V. K., Pandey, R. P., & Jain, M. K. (2014). Spatio-temporal assessment of vulnerability to drought. *Natural Hazards, 76*(1), 443-469. doi: https://doi.org/10.1007/s11069-014-1502-z

Jenson, S. K., & Domingue, J. O. (1988). Extracting Topographic Structure from Digital Elevation Data for Geographic Information System Analysis. *Photogramm Eng Remote Sens, 54*(11), 1593–1600.

Jha, A. K., Bloch, R., & Lamond, J. (2012). *Cities and Flooding: A guide to integrated urban flood risk management for the 21st Century*. Washington, D.C.: The World Bank.

Jose, S. K., Jayakumar, M., & N, S. (2016). Drought Vulnerability Detection and Mapping in Attapadi, A Part of Southern Western Ghats, India - Using Geoinformation Science and Technology. *International Journal of Science and Research (IJSR), 5*(11), 1430-1434.

Kappes, M., Keiler, M., & Glade, T. (2010). *From single-to multi-hazard risk analyses: A concept addressing emerging challenges.* N.P.: n.p.

Kappes, M., Papathoma-Köhle, M., & Keiler, M. (2011). Assessing physical vulnerability for multi-hazards using an indicator-based methodology. *Applied Geography*, *32*(2), 577-590.

KARAMAN, H. (2015). Integrated Multi-Hazard Map Creation By using AHP and GIS. In *7th International Conference on NATURAL HAZARDS* (pp. 101-110). N.P.: n.p. doi: https://doi.org/978-1-61804-332-0

Kazakis, N., Kougias, I., & Patsialis, T. (2015). Assessment of flood hazard areas at a regional scale using an index-based approach and Analytical Hierarchy Process: Application in Rhodope-Evros region, Greece. *Sci Total Environ, 538*, 555-563. doi: https://doi.org/10.1016/j.scitotenv.2015.08.055

Keller, E. A., & DeVecchio, D. E. (2012). *Natural Hazards: Earth's Processes as Hazards, Disasters, and Catastrophes* (3rd ed.). USA: Prentice Hall.

Koem, C., & Tantanee, S. (2020). Flash flood hazard mapping based on AHP with GIS and satellite information in Kampong Speu Province, Cambodia. *International Journal of Disaster Resilience in the Built Environment*, *ahead-of-print(ahead-of-print).* doi:10.1108/IJDRBE-09-2020-0099

Koem, C., & Tantanee, S. (2021). Flood disaster studies: A review of remote sensing perspective in Cambodia. *Geographia Technica, 16*(1), 13-24. doi:10.21163/GT_2021.161.02

Li, G.-F., Xiang, X.-Y., Tong, Y.-Y., & Wang, H.-M. (2013). Impact assessment of urbanization on flood risk in the Yangtze River Delta. *Stochastic Environmental Research and Risk Assessment, 27*(7), 1683-1693. doi: https://doi.org/10.1007/s00477-013-0706-1

Liu, J., Xu, Z., Chen, F., Chen, F., & Zhang, L. (2019). Flood Hazard Mapping and Assessment on the Angkor World Heritage Site, Cambodia. *Remote Sensing, 11*(1), 98. doi: https://doi.org/10.3390/rs11010098

Liu, Y., You, M., Zhu, J., Wang, F., & Ran, R. (2019). Integrated risk assessment for agricultural drought and flood disasters based on entropy information diffusion theory in the middle and lower reaches of the Yangtze River, China. *International Journal of Disaster Risk Reduction, 38*, 101194. doi: https://doi.org/10.1016/j.ijdrr.2019.101194

Ly, S., Kim, L., Demerre, S., & Heng, S. (2018). Flood Mapping along the Lower Mekong River in Cambodia. *Engineering Journal, 22*(1), 269-278. doi: https://doi.org/10.4186/ej.2018.22.1.269

MAFF. (2013). *Plan of Action For Disaster Risk Reduction in Agriculture in Kampong Speu Province 2014-2018*. Phnom Penh: Ministry of Agriculture, Forestry, and Fisheries.

Mahendra, M. S., Tanaka, T., Ogawara, K., & Sugiartha, N. (2017). Application of GSMaP Product and Rain Gauge Data for Monitoring Rainfall Condition of Flood Events in Indonesia. *International Journal of Environment and Geosciences*, *1*(1). doi: https://doi.org/10.24843/ijeg.2017.v01.i01.p05

Matingo, T., Gumindoga, W., & Makurira, H. (2018). Evaluation of sub daily satellite rainfall estimates through flash flood modeling in the Lower Middle Zambezi Basin. *Proceedings of the International Association of Hydrological Sciences*, *378*, 59-65. doi: https://doi.org/10.5194/piahs-378-59-2018

Mishra, K., & Sinha, R. (2020). Flood risk assessment in the Kosi megafan using multi-criteria decision analysis: A hydro-geomorphic approach. *Geomorphology*, *350*, 106861. doi: https://doi.org/10.1016/j.geomorph.2019.106861

Mohamed, S. A. (2019). Application of satellite image processing and GIS-Spatial modeling for mapping urban areas prone to flash floods in Qena governorate, Egypt. *Journal of African Earth Sciences*, *158*, 103507. doi: https://doi.org/10.1016/j.jafrearsci.2019.05.015

Mohamed, S. A., & El-Raey, M. E. (2019). Land cover classification and change detection analysis of Qaroun and Wadi El-Rayyan lakes using multi-temporal remotely sensed imagery. *Environ Monit Assess*, *191*(4), 229. doi: https://doi.org/10.1007/s10661-019-7339-x

Mohamed, S. A., & El-Raey, M. E. (2019). *Vulnerability assessment for flash floods using GIS spatial modeling and remotely sensed data in El-Arish City, North Sinai*. Egypt: Natural Hazards. doi: https://doi.org/10.1007/s11069-019-03571-x

Monacelli, G. (2005). *Drought Assessment and Forecasting*. Czech Repiblic: World Meteorological Organization Weather, Climate and Water.

Nagarajan, R. (2009). *Drought assessment*. New Delhi, India: Springer.

Nasiri, H., Mohd Yusof, M. J., & Mohammad Ali, T. A. (2016). An overview to flood vulnerability assessment methods. *Sustainable Water Resources Management, 2*(3), 331-336. doi: https://doi.org/10.1007/s40899-016-0051-x

NCDM. (2013). *National Action Plan for Disaster Risk Reduction (NAP-DRR) 2014-2018.* Phnom Penh: The Royal Government of Cambodia.

NCDM. (2019). *Disaster Loss Databases: Temporal Behaviour.* Retrieved January 12, 2020, from http://camdi.ncdm.gov.kh/DesInventar/profiletab.jsp

NIS-MoP. (2019). *General Population Census of Cambodia 2019.* Phnom Penh, Cambodia: National Institute of Statistics, Ministry of Planning.

Ogato, G. S., Bantider, A., Abebe, K., & Geneletti, D. (2020). Geographic information system (GIS)-Based multicriteria analysis of flooding hazard and risk in Ambo Town and its watershed, West shoa zone, oromia regional State, Ethiopia. *Journal of Hydrology: Regional Studies, 27*, 100659. doi: https://doi.org/10.1016/j.ejrh.2019.100659

Ouma, Y., & Tateishi, R. (2014). Urban Flood Vulnerability and Risk Mapping Using Integrated Multi-Parametric AHP and GIS: Methodological Overview and Case Study Assessment. *Water, 6*(6), 1515-1545. doi: https://doi.org/10.3390/w6061515

Palchaudhuri, M., & Biswas, S. (2016). Application of AHP with GIS in drought risk assessment for Puruliya district, India. *Natural Hazards, 84*(3), 1905-1920. doi: https://doi.org/10.1007/s11069-016-2526-3

Pandey, S., Pandey, A. C., Nathawat, M. S., Kumar, M., & Mahanti, N. C. (2012). Drought hazard assessment using geoinformatics over parts of Chotanagpur plateau region, Jharkhand, India. *Natural Hazards, 63*(2), 279-303. doi: https://doi.org/10.1007/s11069-012-0093-9

Pariona, A. (2017). *What Is Alluvium?* Retrieved January 12, 2020, from https://www.worldatlas.com/articles/what-is-alluvium.html

Paul, B. K. (2011). *Environmental Hazards and Disasters: Contexts, Perspectives and Management.* New Delhi, India: Wiley-Blackwell.

Perry, R. W., & Lindell, M. K. (2008). Volcanic Risk Perception and Adjustment in a Multi-Hazard Environment. *Journal of Volcanology and Geothermal Research, 172*, 170-178.

Piccarreta, M., Capolongo, D., & Boenzi, F. (2004). Trend analysis of precipitation and drought in Basilicata from 1923 to 2000 within a southern Italy context. *International Journal of Climatology, 24*(7), 907-922. doi: https://doi.org/10.1002/joc.1038

Radwan, F., Alazba, A. A., & Mossad, A. (2018). Flood risk assessment and mapping using AHP in arid and semiarid regions. *Acta Geophysica, 67*(1), 215-229. doi: https://doi.org/10.1007/s11600-018-0233-z

Rahmati, O., Haghizadeh, A., & Stefanidis, S. (2015). Assessing the Accuracy of GIS-Based Analytical Hierarchy Process for Watershed Prioritization; Gorganrood River Basin, Iran. *Water Resources Management, 30*(3), 1131-1150. doi: https://doi.org/10.1007/s11269-015-1215-4

Ramkar, P., & Yadav, S. M. (2018). Spatiotemporal drought assessment of a semi-arid part of middle Tapi River Basin, India. *International Journal of Disaster Risk Reduction, 28,* 414-426. doi: https://doi.org/10.1016/j.ijdrr.2018.03.025

Ranke, U. (2016). *Natural Disaster Risk Management: Geosciences and Social Responsibility*. New York: Springer.

Rogger, M., Agnoletti, M., Alaoui, A., Bathurst, J. C., Bodner, G., Borga, M., … & Bloschl, G. (2017). Land use change impacts on floods at the catchment scale: Challenges and opportunities for future research. *Water Resour Res, 53*(7), 5209-5219. doi: https://doi.org/10.1002/2017WR020723

Saaty, T. L. (1980). *The analytical hierarchy process: planning, priority setting, resource allocation.* Pittsburg: RWS publication.

Saaty, T. L. (2008). Decision making with the analytic hierarchy process. *Int. J. Services Sciences, 1*(1), 83-98.

Saaty, T. L., & Vargas, L. G. (2012). *Models, Methods, Concepts & Applications of the Analytic Hierarchy Process* (2nd ed., Vol. 175). New York, USA: Springer.

Saowanee, W. (2018). Fuzzy AHP for drought risk assessment in Lam Ta Kong watershed, the north-eastern region of Thailand. *Soil and Water Research, 13*(4), 218-225. doi: https://doi.org/10.17221/158/2017-swr

Schmidt, J., Matcham, I., Reese, S., King, A., Bell, R., Henderson, R., Smart, G., Cousins, J., Smith, W., & Heron, D. (2011). Quantitative multi-risk analysis for natural hazards: A framework for multi-risk modelling. *Natural Hazards, 58*(3), 1169-1192. doi: https://doi.org/10.1007/s11069-011-9721-z

Scotland'sSoils. (2013). Guide to soil types. Scottish soil classification. Retrieved from https://soils.environment.gov.scot/soils-in-scotland/guide-to-soil-types/

Seejata, K., Yodying, A., Wongthadam, T., Mahavik, N., & Tantanee, S. (2018). Assessment of flood hazard areas using Analytical Hierarchy Process over the Lower Yom Basin, Sukhothai Province. *Procedia Engineering, 2012,* 340-347. doi: https://doi.org/10.1016/j.proeng.2018.01.044

Shadmehri Toosi, A., Calbimonte, G. H., Nouri, H., & Alaghmand, S. (2019). River basin-scale flood hazard assessment using a modified multi-criteria decision analysis approach: A case study. *Journal of Hydrology, 574,* 660-671. doi: https://doi.org/10.1016/j.jhydrol.2019.04.072

Shamir, E., Ben-Moshe, L., Ronen, A., Grodek, T., Enzel, Y., Georgakakos, K. P., & Morin, E. (2013). Geomorphology-based index for detecting minimal flood stages in arid alluvial streams. *Hydrology and Earth System Sciences*, *17*(3), 1021-1034. doi: https://doi.org/10.5194/hess-17-1021-2013

Shi, P., Yang, X., Liu, F., Li, M., Pan, H., Yang, …, & Meng, Y. (2015). *Mapping Multi-hazard Risk of the World* (pp. 287-306). N.P.: n.p.

Siddayao, G. P., Valdez, S. E., & Fernandez, P. L. (2014). Analytic Hierarchy Process (AHP) in Spatial Modeling for Floodplain Risk Assessment. International *Journal of Machine Learning and Computing, 4*(5), 450-457. doi: https://doi.org/10.7763/ijmlc.2014.v4.453

Skilodimou, H. D., Bathrellos, G. D., Chousianitis, K., Youssef, A. M., & Pradhan, B. (2019). Multi-hazard assessment modeling via multi-criteria analysis and GIS: a case study. *Environmental Earth Sciences, 78*(2). doi: https://doi.org/10.1007/s12665-018-8003-4

Smith, K., & Petley, D. N. (2009). *Environmental Hazards: Assessing Risk and Reducing Disaster* (5th ed.). Great Britain: Routledge.

SÖNmez, F. K., KÖMÜScÜ, A. L. I. Ü., Erkan, A., & Turgu, E. (2005). An Analysis of Spatial and Temporal Dimension of Drought Vulnerability in Turkey Using the Standardized Precipitation Index. *Natural Hazards, 35*(2), 243-264. doi: https://doi.org/10.1007/s11069-004-5704-7

Stefanidis, S., & Stathis, D. (2013). Assessment of flood hazard based on natural and anthropogenic factors using analytic hierarchy process (AHP). *Natural Hazards, 68*(2), 569-585. doi: https://doi.org/10.1007/s11069-013-0639-5

Strahler, A. N. (1952). Hypsometric (area-altitude) analysis of erosional topology. *Geol Soc Am Bull, 63*(11), 1117–1142.

Strahler, N. (1957). Quantitative Analysis of Watershed Geomorphology. *Transactions, American Geophysical Union, 38*(6).

Tanaka, Y., Matsukura, Y., Batnasan, N., & Tuvshinjargal, D. (2004). Distinct runoff processes in granite and sandstone drainage basins near Ulaanbaatar, Mongolia. *Environmental Geology, 47*(5), 640-646. doi:https://doi.org/10.1007/s00254-004-1189-7

Tehrany, M. S., Pradhan, B., & Jebur, M. N. (2014). Flood susceptibility mapping using a novel ensemble weights-of-evidence and support vector machine models in GIS. *Journal of Hydrology, 512*, 332-343. doi: https://doi.org/10.1016/j.jhydrol.2014.03.008

Tehrany, M. S., Pradhan, B., & Jebur, M. N. (2015). Flood susceptibility analysis and its verification using a novel ensemble support vector machine and frequency ratio method. *Stochastic Environmental Research and Risk Assessment, 29*(4), 1149-1165. doi: https://doi.org/10.1007/s00477-015-1021-9

Tekeli, A. E., & Fouli, H. (2016). Evaluation of TRMM satellite-based precipitation indexes for flood forecasting over Riyadh City, Saudi Arabia. *Journal of Hydrology, 541*, 471-479. doi: https://doi.org/10.1016/j.jhydrol.2016.01.014

Thomas, T., Jaiswal, R. K., Galkate, R., Nayak, P. C., & Ghosh, N. C. (2016). Drought indicators-based integrated assessment of drought vulnerability: a case study of Bundelkhand droughts in central India. *Natural Hazards, 81*(3), 1627-1652. doi: https://doi.org/10.1007/s11069-016-2149-8

Tikkanen, A. (2019). *Quartzite.* Retrieved January 5, 2020, from https://www.britannica.com/science/quartzite

TRMM. (2011). *TRMM (TMPA/3B43) Rainfall Estimate L3 1 month 0.25 degree x 0.25 degree V7 [NetCDF]*. N.P.: n.p.

Try, S., Lee, G., Yu, W., & Oeurng, C. (2019). Delineation of flood-prone areas using geomorphological approach in the Mekong River Basin. *Quaternary International, 503,* 79-86. doi: https://doi.org/10.1016/j.quaint.2018.06.026

Tsakiris, G., Pangalou, D., & Vangelis, H. (2006). Regional Drought Assessment Based on the Reconnaissance Drought Index (RDI). *Water Resources Management, 21*(5), 821-833. doi: https://doi.org/10.1007/s11269-006-9105-4.

UNDRR. (2019). *Disaster Risk Reduction in Cambodia: Status Report 2019.* Retrieved January 5, 2020, from https://reliefweb.int/sites/reliefweb.int/files/resources/68230_1cambodiaupdaed16oct2019.pdf

UNISDR. (2015). *Sendai Framework for Disaster Risk Reduction 2015 - 2030: UNISDR (United Nations International Strategy for Disaster Reduction).* Retrieved January 5, 2020, from https://www.undrr.org/publication/sendai-framework-disaster-risk-reduction-2015-2030

USGS. (2015). *Andesite.* Retrieved January 5, 2020, from https://volcanoes.usgs.gov/vsc/glossary/andesite.html

Verbyla, D. L. (2002). *Practical GIS Analysis.* London: Taylor & Francis.

Walters, N., & Hun, B. (2018). *Cambodia Flood 2018.* Retrieved January 5, 2020, from https://www.humanitarianresponse.info/sites/www.humanitarianresponse.info/files/documents/files/cambodia_hrf_sitrep_flood_2018-_23072018_.docx

Wang, J.-J., & Yang, D.-L. (2007). Using a hybrid multi-criteria decision aid method for information systems outsourcing. *Computers & Operations Research, 34*(12), 3691-3700.

Woodward, J. (2009). *The Physical Geography of the Mediterranean (Oxford Regional Environments)* (Vol. 8). New York, United States: Oxford University Press.

WorldVision. (2016). *3,409 Households Affected by Flooding in Kampong Speu and South Phnom Penh.* Retrieved January 5, 2020, from https://www.wvi.org/cambodia/pressrelease/3409-households-affected-flooding-kampong-speu-and-south-phnom-penh

Ye, S., Li, H.-Y., Leung, L. R., Guo, J., Ran, Q., Demissie, Y., & Sivapalan, M. (2017). Understanding Flood Seasonality and Its Temporal Shifts within the Contiguous United States. *Journal of Hydrometeorology, 18*(7), 1997-2009. doi: https://doi.org/10.1175/jhm-d-16-0207.1

Yu, Qin, X. S., & Larsen, O. (2012). Joint Monte Carlo and possibilistic simulation for flood damage assessment. *Stochastic Environmental Research and Risk Assessment*, *27*(3), 725-735. doi: https://doi.org/10.1007/s00477-012-0635-4

Zhai, L., & Feng, Q. (2008). Spatial and temporal pattern of precipitation and drought in Gansu Province, Northwest China. *Natural Hazards*, *49*(1), 1-24. doi: https://doi.org/10.1007/s11069-008-9274-y

APPENDIX

APPENDIX A FLOOD DISASTER STUDIES: A REVIEW OF REMOTE SENSING PERSPECTIVE IN CAMBODIA

Link: http://technicalgeography.org/index.php/on-line-first/362-02_koem?fbclid=IwAR11exjsF2B1Cm-xMqHFakaQlm_m9rz1-sGOseOWtnfNcYvcJ4ZecpmMXsk

APPENDIX B FLASH FLOOD HAZARD MAPPING BASED ON AHP WITH GIS AND SATELLITE INFORMATION IN KAMPONG SPEU PROVINCE, CAMBODIA

Link:https://www.emerald.com/insight/content/doi/10.1108/IJDRBE-09-2020-0099/full/html?skipTracking=true

APPENDIX C SPATIAL DISTRIBUTION OF DROUGHT HAZARD MAPPING BASED ON AHP AND GIS IN KAMPONG SPEU PROVINCE

APPENDIX D CLIMATIC DATA AND DISASTER LOSS DATA

- Rainfall data
- Relative humidity
- Average temperature
- Maximum temperature
- Flood loss data
- Drought loss data

Link:https://drive.google.com/drive/folders/1r8BsUoEpolGHyzJ33ZanS82j3H3OTcu6?usp=sharing

BIOGRAPHY

BIOGRAPHY

Name-Surname	CHHUONVUOCH KOEM
Date of Birth	18 October 1996
Address	Pak Klang commune, Mondol Seima District, Koh Kong province, Cambodia
Current Position	Master Student in Disaster Management, Faculty of Engineering, Naresuan University.
Work Experience	Internship in the Thai Meteorological Department (TMD), Thailand Technical Assistant at RTM Green Consultancy Co., Ltd Volunteer as a facilitator in the Action for Earth-Global Youth Summit 2017 (Winter) Member and peer educator dedicated service to the environment about recycling, reduce, and reuse Community educator of Child Rights
Education Background	Bachelor Degree of Science in Environmental Science at Royal University of Phnom Penh Communication Action and Leadership in Singapore (TFI-SCALE 2017) Biodiversity and Renovation in Japan (ASEP 2017) English Diploma program at PUC The Special Premier English Laboratory (SPEL)
Publication	Flood disaster studies: A review of remote sensing perspective in Cambodia Flash flood hazard mapping based on AHP with GIS and satellite information in Kampong Speu Province, Cambodia Spatial Distribution of Drought Hazard Mapping Based on AHP and GIS in Kampong Speu Province (GMSARN Conference)
Awards	Thesis and Innovation Award 2020 for Graduate Students of Naresuan University Royal Scholarship under Her Royal Highness Princess Maha Chakri Sirindhorn Education Project to the Kingdom of Cambodia for 2019 Scholarship for Majoring Environmental Science in Royal University of Phnom Penh, Cambodia Leadership award of being a president in a large class at PUC